Minkowski space Bethe-Salpeter equation within Nakanishi representation

Cristian Leonardo Gutiérrez Gómez

Orientador:

Lauro Tomio

Co-orientador:

Tobias Frederico

Outubro de 2016

To the love of my life,
Carmencita, and my family by
their unconditional support.

Acknowledgments

I would like to start by expressing my thank to IFT in São Paulo for the great opportunity to make part from this optimal institute as PhD student. I express my gratitude toward my supervisor Prof. Lauro Tomio for the guidance during the PhD studies, his aid to developed this project and his great personal values. I acknowledge to my colleagues of the IFT by their stimulating academic discussions and in general to all members of the institute.

I want to express my gratefulness to Profs Tobias Federico and Giovanni Salmè by allowing me to participate of their interesting project research, where I have taken very valuable knowledge to my formation. To the Prof. Gianni by the warm hospitality during the period in the INFN "Sezione di Roma". His advices to understand the physics even when it is difficult have contributed in a remarkably way for the developing of this thesis. Additionally for the opportunity of knowing that fantastic city: Rome. To Prof. Tobias for accepting me in his research group in the "Instituto Tecnológico de Aeronáutica" in São José dos Campos during the finalization of my studies, and his valuable suggestions always in sake of improving the research results.

I acknowledge to my colleague Vitor Gigante for his expertise and helpful aid to take the first steps at the beginning of this project. I also thank to the other colleagues Jorge Nogueira and Emanuel Ydrefors by the beneficial discussions and tough work during the last year of my studies. To my colleague Fernando Serna by the helpful academic discussions in the IFT and to my colleague Damaso Colasante by his friendship and nice academic conversations during the period in Italy.

It is very important to me to send the most tender expression of gratitude to my wife Carmencita for encouraging me to pursue my goals even leaving so many moments together. To my family, my parents José, Ana and my siblings Felipe and Alejandra for supporting me through the long distance, their words of encouragement and push for tenacity always rang in my mind.

Finally, I would like to thank to the Brazilian funding agency CAPES by the financial support provided to develop this project.

.

Resumo

O trabalho apresentado nessa tese foi dedicado em explorar soluções de estado ligado para a equação de Bethe-Salpeter, obtidas diretamente no espaço de Minkowski. Para isso, consideramos um procedimento que combina a representação integral de Nakanishi para a amplitude Bethe-Salpeter, desenvolvido por N. Nakanishi na década de sessenta, em conjunto com a projeção da amplitude de Bethe-Salpeter no plano nulo, também conhecida como a projeção na frente de luz. Este método, além de permitir calcular as energias de ligação, que são acessíveis a partir de cálculos bem conhecidos no espaço Euclidiano, permite que se obtenha a amplitude Bethe-Salpeter no espaço de Minkowski e a função de onda de valência na frente de luz. A verificação da validade desse procedimento foi confirmada através de comparação da amplitude de Bethe-Salpeter obtida directamente no espaço Euclidiano com a amplitude correspondente derivada da equação de Bethe-Salpeter, usando a representação integral de Nakanishi, uma vez a rotação de Wick é realizada. O sucesso dessa abordagem, quando aplicado ao problema do estado ligado de duas partículas escalares trocando uma outra partícula escalar no estado fundamental, assim como o estudo correspondente no limite de energia zero, nos motivou a ampliar a aplicação do procedimento para o estudo de outros problemas de interesse. Em particular, o método foi estendido para o estudo de sistemas com duas dimensões espaciais e uma temporal (2+1), considerando o interesse crescente que surgiu em Física da matéria condensada, onde podemos destacar o caso de elétrons de Dirac no grafeno. Nessa análise preliminar, nos restringimos ao modelo escalar que nos permitiu acessar as principais dificuldades que deverão ser enfrentadas ao estudar o problema do estado ligado entre dois férmions. Dessa forma, este tratamento pode ser considerado como um primeiro passo para a implementação de um método mais realístico em um problema fermiônico. Os cálculos anteriores que consideramos em nossos estudos foram realizados através da aproximação de escada para o kernel de interação irredutível para os estados de onda-s. Portanto, uma das extensões que exploramos nesta tese foi o efeito de se introduzir a contribuição de ordem seguinte no kernel de interação, conhecida como a contribuição de escada-cruzada (*cross-ladder*). Os efeitos nas energias de ligação e na função de onda na frente de luz é foram analisados de forma detalhada, através dos resultados

apresentados. Um estudo particularmente interessante, que foi extensivamente estudado nesta tese, se refere ao problema do espectro da equação Bethe-Salpeter para o estado ligado escalar-escalar. O espectro de estados excitados foi obtido com a abordagem da representação integral Nakanishi, sendo comparado com o obtido no espaço Euclidiano. Além disso, as raçoes excitado/fundamental do espectro relativístico foram reduzidas para às não-relativístico através da escolha de energias de ligação pequenas e considerando a massa do bóson trocado sendo próxima de zero. A função de onda de valência na frente de luz e a função de onda no parâmetro de impacto são apresentadas mostrando as principais características dos estados excitados conhecidos da estrutura não relativística. Na análise do espectro, também são estudadas as amplitudes de momentum-transverso para o estado fundamental e o primeiro estado excitado, que podem ser obtidos, de forma equivalente, no espaço de Minkowski assim como no espaço Euclidiano. Finalmente, focamos o estudo nos fatores de forma eletromagnéticos elásticos na abordagem da Bethe-Salpeter. Consciente de que o cálculo correto dos fatores de forma deve ser feito no espaço de Minkowski, o fator de forma elástico foi calculado levando-se em consideração a aproximação de impulso padrão. Além disso, foi também estudado o efeito da contribuição de ordem superior no fator de forma.

Palavras Chaves: Equação de Bethe-Salpeter, Representação integral de Nakanishi, dinâmica na frente de luz.

Áreas do conhecimento: Física nuclear e física de hadrons.

Abstract

The work presented in this thesis was dedicated in exploring bound-state solutions of the Bethe-Salpeter equation directly in the Minkowski space. For that, we consider a method that combines the Nakanishi integral representation for the Bethe-Salpeter amplitude, developed by Noboru Nakanishi in the sixties, together with the projection of the Bethe-Salpeter amplitude onto the null-plane, also known as the light-front projection. This approach, besides of allowing to compute the binding energies, which are accessible from the usual Euclidean calculation, enables to obtain the Bethe-Salpeter amplitude in the Minkowski space and the light-front wave function. The feasibility of such an approach is further verified by comparing the Bethe-Salpeter amplitude obtained directly in the Euclidean space with the corresponding amplitude obtained by solving the Bethe-Salpeter equation, using the Nakanishi integral representation, once the Wick rotation is performed to this latter. The success of the approach when applied to study the bound state problem of two-scalar particles exchanging another scalar particle in the ground state, as well as the corresponding study at the zero-energy limit, has encouraged us to extend this method to another interesting problems. In particular, we start by extending the method to study problems in (2+1) dimensions due to the increasing interest in the condensed-matter physics, like the study of Dirac electrons in graphene. In this initial examination we restrict to the scalar model, which enables us to access to the main difficulties that we will face when studying the fermion-fermion bound state problem. Hence, this calculation can be considered as the first step towards the implementation of the method to real fermionic problems. The previous calculations have been performed by considering the ladder approximation for the irreducible interacting kernel for s-wave states. Therefore, one of the extensions that is explored in this thesis is the effect of introducing the next contribution in the interacting kernel, known as the scalar-scalar cross-ladder contribution. The effects in the eigenvalues and the light-front wave functions are analyzed in detail, by considering the computed results. A particular interesting subject, extensively studied in this thesis, is concerned to the spectrum of the Bethe-Salpeter equation for the scalar-scalar bound-state problem. The spectrum of excited states obtained with the Nakanishi integral representation approach is compared with that obtained in the Euclidean

calculation. Besides, the ratio energies excited/ground of the relativistic spectrum is reduced to the non-relativistic one by choosing small binding energies and the mass of the exchanged boson approaching to zero. The valence light-front wave function and the impact-parameter space valence wave function are displayed, revealing the main features of excited states known from the non-relativistic framework. In the analysis of the spectrum, we also studied the transverse-momentum amplitudes for the ground and first-excited state, which can be equivalently obtained in the Minkowski or Euclidean spaces. Finally, we focus on the study of electromagnetic elastic form factors within the Bethe-Salpeter approach. Aware that the correct calculation of form factors should be performed in the Minkowski space, the calculation of the elastic form factor is carried out with the standard impulse approximation and in addition the effect of the next contribution to the form factor is studied.

Key words: Bethe-Salpeter equation, Nakanishi integral representation, Light-front dynamics.

Subject: Nuclear and hadron physics.

Contents

Chapter 1

Introduction

The theoretical investigations on few-body systems within relativistic frameworks are of great relevance in view of the uncountable number of applications that one can imagine in theoretical approaches of high-energy nuclear physics and hadronic structures; in particular, when considering quark degrees of freedom within Quantum Chromodynamics to study hadron structure and particle interactions. The most adequate approach to study the relativistic few-body systems is the quantum field theory, which is the quantum and relativistic description of these systems. In the framework of this theory, the interactions between the constituents is represented by the set of covariant Feynman graphs, which are written in terms of the coupling constant of the theory. The complete amplitude is expanded in terms of orders of the coupling constant: perturbative expansion. Therefore, the success of the perturbative expansion relies on the smallness of the coupling constant. For instance, in atomic systems where the electromagnetic interaction dominates, the smallness of the electromagnetic coupling constant allows for a perturbative treatment. Instead, in nuclear and hadron systems, mostly dominated by the strong interaction where the coupling constant is not small, the same perturbative treatment is not appropriated since in this case the Feynman graphs of higher order give large contribution to the amplitude. In some cases the perturbative treatment is valid, for instance, in strong interaction the asymptotic freedom of the Quantum Chromo Dynamics allows for the perturbative treatment in the high energy regime, where the coupling constant becomes small [1]. Differently from the scattering processes, where one can obtain a reasonable estimation of the scattering amplitude by calculating a few Feynman diagrams of the lowest order, the description of a bound state requires the sum of the infinite set of Feynman diagrams, since that the bound and continuum

states of hadrons and nuclear systems belong to the non-perturbative regime, making in this form the perturbative treatment non-suitable. Therefore the non-perturbative methods to study these systems are necessary to get an adequate and accurate description of the physics. The approaches for dealing with the non-perturbative regime within the field theory framework, are two: the path-integral methods (developed in the Euclidean space) and the relativistic integral equations, like the Bethe-Salpeter (BS) equation (the homogeneous BS equation for bound states, and the inhomogeneous one for the scattering states). In this thesis we focus on the studies of the BS equation for bound states.

The covariant BS equation formulated in the fifties [2], represents the first complete covariant treatment of two-body systems in quantum field theory and in a certain sense has solved the a long-standing problem of the quantum mechanics. The natural and simple way which the relativistic invariance is achieved really represents a progress. Nevertheless, one of the problems of the BS equation when formulating in Minkowski space are the singularities present in propagators and the interaction kernel [3]. The kernel contains the sum of the two-body irreducible Feynman diagrams contributing to a given amplitude. The mentioned singularities turns the integral equation unavailable to be solved using any numerical methods. Historically, this difficulty was overcome by analytical continuation of the "relative energy" to the complex values: Wick rotation [3]. The validity of this procedure has been shown for the ladder kernel, that is, a kernel retaining only the first term in the expansion of the interaction in powers of g^2. However, in the general case for other more complicate kernels, the validity of the Wick rotation is not clear. Additionally, when using dressed propagators of the constituents particles the Wick-rotated Dyson-Schwinger equation contains complex ghost poles [4]. Thus, for simple ladder kernels and free propagators the Wick rotation turns the BS equation available to be solved numerically and obtain the coupling constants, which are invariants under the Wick rotation *. Another consequence of this procedure is the fact that the BS amplitude computed after performing the Wick rotation is obtained as a function of the imaginary relative energy, avoiding to evaluate other physical quantities by means of the BS amplitude, like e.g., the parton distribution function. Therefore a method to solve the BS equation directly in the Minkowski

---

*The Euclidean BS equation is an integral equation, which can be considered as an eigenvalue problem. As a result of solving the equation in the Euclidean space one obtains the eigenvalues (binding energies) and the eigenvectors (Euclidean BS amplitudes)

space is required.

The problem of studying the BS equation in the Minkowski space has been undertaken in the last two decades. For this purpose, the Nakanishi integral representation (NIR) derived by Noboru Nakanishi in the sixties, see Ref. [5], have been implemented to solve the BS equation. The NIR is a natural extension of the spectra representation for a two-point Green's function to n-point function in relativistic field theories. This is technically possible in perturbation theory since the Feynman parametric integral always exists for any Feynman diagram and it is possible to define the integral representation such that the number of independent integration parameters is equal to that of the invariants constructed with the external momenta. Within the NIR approach, BS amplitude can be written as an integral, whose integrand is given by a weight-function, the so-called Nakanishi weight-function, divided by a denominator that contains the analytic structure of the amplitude itself. By writing the BS amplitude in terms of the NIR, the initial BS equation is transformed in a new integral equation for the Nakanishi weight-function. Among the interesting features of NIR, one has: i) the dependence of the Nakanishi weight-function upon real variables, equal in number to the independent invariants of the problem; ii) the explicit analytic structure of the BS amplitude, that allows one to perform analytic integration, when requested (indeed, this will be the case). This procedure was implemented for first time by K. Kusaka and A.G. Williams [6, 7]. They studied the system composed by two scalars particles interacting by means of another scalar, in ladder approximation. The NIR was used to represent the interaction kernel as well as the BS amplitude itself. The singularities were removed by using a suitable analytical treatment. Finally, they were able to solve numerically the integral equation for the Nakanishi weight-function, and obtained the coupling constant and the BS amplitude.

A substantial simplification in the derivation of the equation for the Nakanishi weight-function was achieved in the work developed by J. Carbonell and V. Karmanov in 2006 [8]. In addition to using the NIR for the BS amplitude, the light-front (LF) projection was implemented to remove the singularities present in the integral equation for the Nakanishi weight-function once the NIR for the BS amplitude has been introduced. The LF projection formally is done by integration over k^- ($k^\pm = k^0 \pm k^3$ and $\mathbf{k}_\perp \equiv \{k^1, k^2\}$) to both sides of the BS equation. This integration leads to the integral equation, free of singularities, which is solved numerically by some known method. An important point to emphasize is the fact that the LF projection of the

BS amplitude extracts the probabilistic interpretation of the amplitude, since this projection formally allows us to obtain the valence LF wave function, i.e, the Fock component of the inter-acting state corresponding with the lower number of constituents, for this case two [9, 10, 11]. Thus, it represents another achievement of the direct calculation in Minkowski space within LF dynamics; once the BS amplitude is known one can obtain the LF wave function, which is obviously not available in the Euclidean space. The LF wave function obtained in LF dynamics represents the relativistic counterparts of the non-relativistic wave functions.

Despite of the several attractive advantages provided by the NIR, it is important to point out, that the Nakanishi representation has been devised within a perturbative approach, even if the infinite sum of Feynman diagrams is formally performed through the introduction of the weight-function, one cannot establish a priori the convergence of the series. Hence, the NIR for the BS amplitude is considered as an *ansatz*, that belongs to the perturbative regime. Therefore, one has to check its validity, which is simply done by looking for solutions of the integral equation satisfied by the weight-function, which one exactly deduces from the BS equation in Minkowski space after introducing the chosen ansatz.

Further simplifications to the integral equation derived in Ref. [8] can be achieved by using the uniqueness of the Nakanishi weight-function, as shown in Ref. [9]. In Ref. [12] numerical tests of the uniqueness were done by comparing solutions of the BS equation for two-boson bound states, in ladder approximation, with two integral equations for the Nakanishi weight-function, namely with and without using uniqueness.

Moreover, within the NIR the effect of the self-energy contribution in the binding energy of the ground state has been explored in the scalar theory [13, 14]. In these analyses in addition of using the NIR for the vertex function, the NIR for the two-leg function or the so-called *Lehmann representation* is adopted to introduce the self-energy contribution in the free propagators of the constituents and the exchanged boson.

The next order in the perturbative expansion of the interaction kernel, i.e, g^4, which is called the cross-ladder contribution, has been also explored within the NIR and LF projection frame-work [15] in 3+1 dimensions. Corrections in the coupling constant have been obtained, showing that the cross-ladder contribution relative to the ladder one, results in a stronger attractive effect.

The formal extension of the method to the continuum was carried out in Ref. [9] and tested

numerically in Ref. [16]. Again, the two-boson system in ladder approximation was considered. The computed scattering lengths are in agreement with those computed within a quite different framework, based on the direct calculation of the contributions from the singularities of the inhomogeneous BS equation [17]. It is important to point out that the very interesting problem of two-fermion bound state has been investigated in the framework of the explicit covariant formulation [18]. Also, advances in the same problem within the non-explicit covariant formulation have been reported very recently [19], much analytic and numerical effort was spent in this subject.

The previous successful analysis encourages us to extend the NIR to other problems, some of extensions in current developing are shown in this thesis. In particular, of great interest is the 2+1 dimensions problem in view of the applications in condensed-matter physics, like the study of Dirac electrons in graphene, see Refs. [20, 21]. Quantum fields models describe effective forces among Dirac electrons living on the graphene layer by exchanging bosons [22, 23]. For studying this problem, the validity of the Nakanishi representation in lower dimensions is proved analytically and used to represent the BS amplitude. The BS equation for the two-spatial dimensional problem is solved for the bound state composed of two-scalar bosons exchanging another scalar boson, in the ladder approximation [24]. In addition to the ladder kernel, we also include the cross-ladder contribution in the irreducible interaction kernel still in 2+1 dimensions. We analyze the effect of this kernel in the eigenvalues as well as in the Euclidean BS amplitude and the LF wave function. This scalar model developed here enables us to access to the difficulties, which we face when studying the fermion-fermion bound state problem.

An important subject developed in this thesis, which deserves much attention is the study of the spectrum of the excited states within BS approach in 3+1 dimensions [25]. As a natural extension of the previous analysis done only for the ground state, considering *s*-wave states and the ladder kernel approximation, it is possible to obtain a set of excited states. By slightly changing the integral equation for the Nakanishi weight-function used to study the ground state problem, one can fix the value of the coupling constant obtained from the ground state calculation to obtain the spectrum of excited states. As usual, the reliability of the method is verified by comparing with the Euclidean calculation, which is in fair agreement within the accuracy of our calculations. Furthermore, it is possible to obtain the non-relativistic limit of this calculation by choosing small binding energies and the mass of the exchanged boson approaching to zero.

An important result is obtained when analyzing the LF valence wave function for the excited states, since that differently from the ground state, it presents the expected node structure of excited states, i.e, one and two nodes for the first- and second-excited state, respectively. In this analysis of the spectrum of the scalar theory, we have taken profit of this calculation to explore the transverse-momentum BS amplitudes. These quantities show the dependence of the BS amplitude with the transverse-momentum and can be computed once the BS amplitude is known. The calculation of the transverse-momentum amplitude can be done independently in the Minkowski space by means of the NIR method or in the Euclidean space. Hence, this quantity provides another evidence of the reliability of the NIR method to solve the BS equation. In fact, as we will show the transverse-momentum amplitudes present nice agreement for the ground and the first-excited state when computed by the two methods. In this thesis we also studied the valence LF wave function in the Impact parameter space, obtained as the Fourier transform of the valence LF wave function in the transverse-momentum and keeping the longitudinal momentum. Therefore, this quantity provides the correlation between the longitudinal momentum carried by one of the constituents, and the probability distribution in the so-called Impact parameter space. A node structure is also encountered in the Impact parameter space for the LF wave function. We were encouraged to study the latter quantity because of the increasing interest on this topic in hadron physics, where the valence component plays an important role in determining the structural properties of hadrons, like parton transverse-momentum distributions [26, 27, 28].

Finally, we complete this thesis with the study of the electromagnetic form factors. These quantities have been investigated for a long time on account of its relevance in the understanding of the internal structure of composite systems. The information about the charge and magnetization distributions inside of the composite systems are contented in these quantities. Within the BS framework, the form factors are computed by using the BS amplitude of the bound state, obtained when solving the BS equation. As it will be explained later on, the calculation of form factors by means of the Euclidean BS amplitude leads to an approximate result. Hence, the correct calculation is performed by using the BS amplitude obtained directly from the Minkowski space. Therefore, the approach provided by the NIR to obtain solutions in the Minkowski space is quite convenient to the form factor calculation. It represents another motivation to undertake a study in the Minkowski space, even that its complexity increases. In this scheme, we compute the form factor in the impulse approximation, which was already studied in Ref. [29]. Further-

more, we add the next contribution to the form factor, analyzing its effect relative to the Impulse Approximation, which appears when the kernel of the BS equation contains a cross-ladder term.

This thesis is organized as follows: in Chapter 2 we present the general structure of the BS equation. We display the derivation to obtain the inhomogeneous BS equation and later the homogeneous BS equation to study bound states. The analytic properties of the BS amplitude are also studied in view of the application of the Wick rotation. Finally, we present the normalization of the BS amplitude. Chapter 3 is devoted to study the LF dynamics, we present the general features of this approach, emphasizing in the advantages of LF dynamics with respect to other forms of relativistic dynamics. Then, we explore the meaningful fact of LF dynamics by performing the LF projection of the BS amplitude onto the null-plane, what allows us to extract valence LF wave function for the composite state. In Chapter 4, we derive the NIR for *N*-external legs. In particular, we emphasize in the Nakanishi representation for the three-external legs or vertex function, which plays an important role when studying the bound-state problem. The Nakanishi representation is studied in 3+1 dimensions as well as in 2+1 dimensions. In Chapter 5, the integral equation for the Nakanishi weight-function is obtained. Starting from the usual BS equation for the bound states, we obtain a generalized integral equation for the Nakanishi weight-function, once the NIR for the vertex function is adopted and after integrating the singularities with the LF projection. The explicit calculation is carried out for ladder and cross-ladder in 3+1 and 2+1 dimensions. Chapter 6 is devoted to the standard analysis of the BS equation in the Euclidean space for ladder and cross-ladder kernels. We have decided to spend this chapter to the study of the Euclidean formulation, since this framework allows us to have some results to compare with the corresponding ones obtained with Minkowski space calculations. In Chapter 7, the results obtained by numerical solution of the BS equation are presented. In the initial part we present the numerical method employed to solve the integral equation for the Nakanishi weight-function. The numerical results are shown for the bound state problem in 2+1 dimensions. Chapter 8 is devoted to the study of the spectrum of excited states in the scalar theory. Because, the spectrum analysis is done for first time we restrict it to 3+1 dimensions. The spectrum, valence LF wave functions, transverse-momentum amplitudes and LF wave functions in the impact-parameter space are analyzed for excited states. In Chapter 9 the electromagnetic properties of the composite scalar system are studied. This represents one of the motivations to undertake the calculation in the Minkowski space. As it will be shown

the calculation of form factors forces us to obtain the BS amplitudes in the Minkowski space if one wants to compute form factors without any approximation. The usual impulse approximation and next order in the calculation of form factors are considered and analyzed. Finally, in Chapter 10 the conclusions and perspectives are outlined.

Chapter 2

The Bethe-Salpeter equation

The initial chapter is devoted to the derivation and general features of the BS equation. The BS equation was first proposed by Salpeter and Bethe in 1951 [2] and then derived from field-theoretic foundations by Gell-Mann and Low [30] and Schwinger [31, 32]. The number of derivations of this equation since its initial proposal is huge, we do not discuss all these derivations here but we adopt the pedagogical derivation considering as starting point the four-point Green's function, which is the relevant quantity in quantum field theory to study a two-particle interacting system. From this quantity we derivate an integral equation for the BS amplitude suitable to study problems in the non-perturbative regime. In particular, the occurrence of poles in the four point Green's function leads to a homogeneous integral equation describing the bound state of two interacting particles. This equation will be the starting point for the forthcoming investigation. The derivation present here is quite general, hence it can be used in Minkowski or Euclidean space. We also discuss the analytic properties of the BS amplitude and its normalization at the end of this chapter.

2.1 Derivation of the Bethe-Salpeter equation

In the case of free particles the two-point Green's function plays an important role in determining the properties of the single particle. It determines the mass of the physical particle (after including the radiative corrections), the propagation in the space-time of the physical particle and the scattering of the physical particle on the external potential. In other words, all properties and the complete behavior of single physical particles are fully determined by the exact propagator. Presumably, the n-points Green's function for higher order can give an analogous description for

11

many-particle systems. Indeed, this is the case for a system of two interacting particles, where one should consider the *four-point* Green's function in the coordinate representation. We focus on the system composed by two scalar particles interacting by means of another scalar particle, which will be the model used in this thesis. For this case we have the interaction Lagrangian $\mathcal{L}_{\text{inter}} = g \; \phi^2 \chi$. Then, the four-point Green's functions reads:

$$G(x_1, x_2; y_1, y_2) = \langle \Omega | T\{\phi_1(x_1)\phi_2(x_2)\phi_1^\dagger(y_1)\phi_2^\dagger(y_2)\} | \Omega \rangle, \tag{2.1}$$

where $|\Omega\rangle$ stands for the vacuum of the interacting theory and the operators are written in the Heisenberg representation. As usual, the Heisenberg operators are written in the interaction picture where the evolution of the operators is given by the free Hamiltonian. Within of this picture the evolution operator, which contains the interaction, can be expanded in powers of the coupling constant g. Summing all orders in g we obtain all of graphs that can be constructed with four external legs. In the perturbative regime the expansion can be truncated considering only the graphs of lowest order that provide the large contribution. In the study of bound states the main difficulty comes because of the inadequacy of retaining only a few Feynman diagrams, which is the basis of any perturbative calculation in high-energy physics. The reason is that bound states produce poles in the scattering matrix in the channel in which they appear. However, no such poles exist in any Feynman diagram or any finite sum of them, a pole can only be generated by an infinite sum. The latter issue will be dealt throughout this chapter.

We can rearrange the set of Feynman diagrams which can be reproduced by means of Eq. (2.1) into two sets: *irreducible* and *reducible*. We define a graph as reducible if, in a given diagram, by cutting vertically through two ϕ_i internal lines and no χ line, the graph can be split into two connected graphs. It turns out that the infinity series of reducible Feynman graphs can be obtained by iterations of the irreducible ones. Taking into account the above considerations, the four-point Green's function can be written as the following integral equation

$$G(x_1, x_2; y_1, y_2) = G_0(x_1, x_2; y_1, y_2) + \int dz_1 dz_2 dz_1' dz_2' G_0(x_1, x_2; z_1, z_2) K(z_1, z_2; z_1', z_2') G(z_1', z_2'; y_1, y_2), \tag{2.2}$$

where $G_0(x_1, x_2; y_1, y_2) = \Delta_1(x_1 - y_1)\Delta_2(x_2 - y_2)$ is the product of the free-propagators:

$$\Delta_i(x_i - y_i) = \langle 0|T\{\phi_i(x_i)\phi_i^\dagger(y_i)\}|0\rangle, \tag{2.3}$$

and $K(z_1, z_2; z_1', z_2')$ is the interaction kernel that contains all the irreducible diagrams of two particles.

The four-point Green's functions as written in Eq. (2.2) is in the coordinate space, however it is more useful to write it in the momentum representation. For this aim it is convenient to introduce the relative and global coordinates as in the non-relativistic case:

$$\begin{aligned} x &= x_1 - x_2 & X &= \eta_1 x_1 + \eta_2 x_2 \\ y &= y_1 - y_2 & Y &= \eta_1 y_1 + \eta_2 y_2, \end{aligned} \tag{2.4}$$

where the Jacobian of the transformation is given by:

$$J = \eta_1 + \eta_1. \tag{2.5}$$

In analogy with the non-relativistic case one can choose

$$\eta_1 = \frac{m_1}{m_1 + m_2} \qquad \eta_2 = \frac{m_2}{m_1 + m_2}, \tag{2.6}$$

where m_1 and m_2 are the masses of the particles and $\eta_1 + \eta_2 = 1$, therefore $\eta_i \in [0, 1]$. By using the relative and global coordinates Eq. (2.4), it is possible to have space-time translational invariance if we consider the following function

$$F(x_1, x_2; y_1, y_2) = F(x, y, X - Y). \tag{2.7}$$

We perform the Fourier transformation of this quantity as follows:

$$\begin{aligned} F(p_1, p_2; q_1, q_2) &= \int dx_1\, dx_2\, dy_1\, dy_2\; e^{-ip_1 x_1} e^{-ip_2 x_2} e^{-iq_1 y_1} e^{-iq_2 y_2} F(x_1, x_2; y_1, y_2) \\ &= (2\pi)^4 \delta(P - Q) \int dx\, dy\, dW e^{-iPW} e^{-ikx} e^{iqy} F(x, y; W), \end{aligned} \tag{2.8}$$

where for shorthand notation we use $dx \equiv d^4x$ throughout of this chapter and $W = X - Y$, x, y were defined in Eq. (2.4). $P = p_1 + p_2$, $k = \eta_2 p_1 - \eta_1 p_2$ and $q = \eta_2 q_1 - \eta_1 p_2$ are corresponding

conjugate momenta. Now, we apply the Fourier transformation defined in Eq. (2.8) to the four-point Green's function Eq. (2.2). We proceed as follows:

(i) the first term is computed by using in (2.2) the expression

$$\Delta(x_1 - x_2) = \frac{1}{(2\pi)^4} \int dp\ \Delta(p) e^{ip(x_1 - x_2)}, \tag{2.9}$$

for the free-propagators and performing the Fourier transformation to obtain

$$G^{(1)}(k, q; P) = (2\pi)^4 \delta^{(4)}(k - q) \Delta_1(\eta_1 P + k) \Delta_2(\eta_2 P - k). \tag{2.10}$$

We have obtained this expression with standard procedure: with the exponential functions and with the aid of the dx, dy, dW one generates three delta functions. Then, we use two delta functions for performing the integration in the momenta.

(ii) For the calculation of the second term of the four-point Green's function, one considers the following form for the kernel and the Green's function:

$$K(z_1, z_2; z_1', z_2') = K(z, z'; Z - Z')$$
$$G(z_1', z_2'; y_1, y_2) = G(z', y; Z' - Y), \tag{2.11}$$

where $\{z, z'\}$ stand for the relatives coordinates and $\{Z, Z'\}$ for the global ones. After that we write the kernel and the Green's function in the momentum space through the Fourier transformation Eq. (2.8). A straightforward but rather lengthy derivation leads to

$$G^{(2)}(k, q; P) = \Delta_1(\eta_1 P + k) \Delta_2(\eta_2 P - k) \int \frac{dq'}{(2\pi)^4} K(k, q'; P) G(q', q; P). \tag{2.12}$$

The four-point Green's function in the momentum space is written as:

$$G(k, q; P) = (2\pi)^4 \delta^{(4)}(k - q) G_0(k; P) + G_0(k; P) \int \frac{dq'}{(2\pi)^4} K(k, q'; P) G(q', q; P), \tag{2.13}$$

with $G_0(k; P) = \Delta_1(\eta_1 P + k) \Delta_2(\eta_2 P - k)$. Consequently, the first term in Eq. (2.13) accounts for the propagation of the free particles and the other term for the interaction between them. A diagrammatic representation of the four-point Green's function is given in Fig. 2.1.

As mentioned previously in studying the bound state problem one should consider the pole terms related with the four-point Green's function. This leads to the *homogeneous* integral
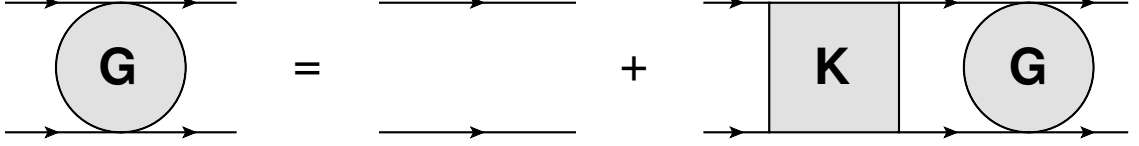
Figure 2.1: Diagrammatic representation of the integral equation for four-point Green function in the momentum space Eq. (2.13).

equation for the so-called BS amplitude. This quantity contains all the needed information about a bound state, therefore it allows us to evaluate several physical observables. To define this quantity let us consider the state $|P_B, \alpha\rangle$, which represents the two-body bound state. The BS amplitude is defined as:

$$\Phi(x_1, x_2; P_B, \alpha) = \langle 0|T\{\phi_1(x_1)\phi_2(x_2)\}|P_B, \alpha\rangle, \tag{2.14}$$

and its conjugate

$$\bar{\Phi}(x_1, x_2; P_B, \alpha) = \langle P_B, \alpha|T\{\phi_1^\dagger(x_1)\phi_2^\dagger(x_2)\}|0\rangle, \tag{2.15}$$

P_B is the four-momentum of the bound state, with $P_B^2 = M^2$ and α the set of quantum numbers. It is important to emphasize that Φ and $\bar{\Phi}$ cannot be considered as the usual wave functions, instead for recovering the probabilistic character, it is necessary to expand the bound state $|P_B, \alpha\rangle$ in a complete Fock basis, to obtain the relativistic counterparts of the non-relativistic wave functions. This fact will be studied in detail in Chapter. 3.

Applying a translational transformation in Eq. (2.14) one obtains

$$\Phi(x_1 + a, x_2 + a; P_B, \alpha) = e^{-iP_B \cdot a}\Phi(x_1, x_2; P_B, \alpha), \tag{2.16}$$

this can be easily seen, by considering that the field operators in Eq. (2.14) are in the Heisenberg representation $\phi_j(x) = e^{-i\hat{P}x_j}\phi_j(0)e^{i\hat{P}x_j}$ and taking into account the translation invariance of the vacuum. In terms of the relative and global coordinates Eq. (2.4), the BS amplitude can be written as:

$$\Phi(x_1, x_2; P_B, \alpha) = \langle 0|T\{\phi_1(x_1)\phi_2(x_2)\}|P_B, \alpha\rangle = \theta(x^0)\langle 0|e^{i\hat{P}\cdot X}\phi_1(\eta_2 x)\phi_2(-\eta_1 x)e^{-i\hat{P}\cdot X}|P_B, \alpha\rangle$$

$$+ \theta(-x^0)\langle 0|e^{i\hat{P}\cdot X}\phi_2(-\eta_1 x)\phi_1(\eta_2 x)e^{-i\hat{P}\cdot X}|P_B, \alpha\rangle$$

$$= \theta(x^0)e^{-iP_B\cdot X}\langle 0|\phi_1(\eta_2 x)\phi_1(-\eta_1 x)|P_B, \alpha\rangle$$

$$+ \theta(-x^0)e^{-iP_B\cdot X}\langle 0|\phi_2(-\eta_1 x)\phi_1(\eta_2 x)|P_B, \alpha\rangle$$

$$= \frac{e^{-iP_B\cdot X}}{(2\pi)^{3/2}}\varphi(x; P_B, \alpha),$$

$$(2.17)$$

where we have introduced the *reduced* BS amplitude defined as

$$\varphi(x; P_B, \alpha) = (2\pi)^{3/2}\langle 0|T\{\phi_1(\eta_2 x)\phi_2(-\eta_1 x)\}|P_B, \alpha\rangle. \tag{2.18}$$

Now, we continue with the objective of obtaining a homogeneous integral equation for the BS amplitude for the two body bound state. We consider again the initial four point Green's function in the coordinate space Eq. (2.1). We restrict ourselves to the case $x_1^0,\ x_2^0 > y_1^0,\ y_2^0$ hence we can write

$$G(x_1, x_2; y_1, y_2) = \theta[min(x_1^0, x_2^0) - max(y_1^0, y_2^0)]\langle 0|T\{\phi_1(x_1)\phi_2(x_2)\}T\{\phi_1(y_1)^\dagger\phi_2(y_2)^\dagger\}|0\rangle,$$

$$(2.19)$$

then we insert a full set of states $\sum_n |n\rangle\langle n|$=1 into the four-point Green's function

$$G(x_1, x_2; y_1, y_2) = \theta[min(x_1^0, x_2^0) - max(y_1^0, y_2^0)]\sum_n \langle 0|T\{\phi_1(x_1)\phi_2(x_2)\}|n\rangle\langle n|T\{\phi_1(y_1)^\dagger\phi_2(y_2)^\dagger\}|0\rangle,$$

$$(2.20)$$

and let us consider the contribution from the two-body bound state: $|n\rangle \to |P_B, \alpha\rangle$

$$\sum_n |n\rangle\langle n| \to \int dP\delta(P^2 - m_B^2)\theta(P_0)|P_B, \alpha\rangle\langle P_B, \alpha| = \int \frac{d^3P}{2E_B}|P_B, \alpha\rangle\langle P_B, \alpha|, \tag{2.21}$$

with $P_B = (E_B, \mathbf{P})$, $E_B = \sqrt{\mathbf{P}^2 + m_B^2}$ and m_B is the mass of bound state. Taking into account this contribution, the four-point Green's function becomes

$$G(x_1, x_2; y_1, y_2) = \theta[min(x_1^0, x_2^0) - max(y_1^0, y_2^0)]$$

$$\times \int \frac{d^3 P}{2E_B} \langle 0|T\{\phi_1(x_1)\phi_2(x_2)\}|P_B, \alpha\rangle \langle P_B, \alpha|T\{\phi_1(y_1)^\dagger \phi_2(y_2)^\dagger\}|0\rangle. \tag{2.22}$$

By introducing the reduced BS amplitude Eq. (2.18) we obtain:

$$G(x_1, x_2; y_1, y_2) = \theta[min(x_1^0, x_2^0) - max(y_1^0, y_2^0)] \int \frac{d^3 P}{(2\pi)^3} \frac{1}{2E_B} e^{-iP_B \cdot (X-Y)} \varphi(x; P_B, \alpha) \bar{\varphi}(y; P_B, \alpha). \tag{2.23}$$

Next, we analyze the argument of the θ function in Eq. (2.23). We can write the functions $min(x_1^0, x_2^0)$ and $max(y_1^0, y_2^0)$ as follows

$$min(x_1^0, x_2^0) = \frac{x_2^0}{2}\left[\frac{(x_1^0 - x_2^0)}{|x_1^0 - x_2^0|} + 1\right] + \frac{x_1^0}{2}\left[\frac{(x_2^0 - x_1^0)}{|x_2^0 - x_1^0|} + 1\right]$$

$$max(y_1^0, y_2^0) = \frac{y_1^0}{2}\left[\frac{(y_1^0 - y_2^0)}{|y_1^0 - y_2^0|} + 1\right] + \frac{y_2^0}{2}\left[\frac{(y_2^0 - y_1^0)}{|y_2^0 - y_1^0|} + 1\right], \tag{2.24}$$

using the relative coordinates Eq. (2.4) we obtain

$$min(x_1^0, x_2^0) = -\frac{x^0}{|x^0|}\frac{x^0}{2} + \frac{2X^0 + (\eta_2 - \eta_1)x^0}{2}$$

$$min(y_1^0, y_2^0) = \frac{y^0}{|y^0|}\frac{y^0}{2} + \frac{2Y^0 + (\eta_2 - \eta_1)y^0}{2}, \tag{2.25}$$

thus, the θ function in Eq. (2.23) is written as:

$$\theta[min(x_1^0, x_2^0) - max(y_1^0, y_2^0)] = \theta[X^0 - Y^0 + f(x^0, y^0)]$$

$$f(x^0, y^0) = -\frac{|x^0|}{2} - \frac{|y^0|}{2} + \frac{(\eta_2 - \eta_1)}{2}(x^0 - y^0). \tag{2.26}$$

We can resort to the integral representation of the θ function:

$$\theta(z) = \frac{i}{2\pi} \int \frac{e^{-itz}}{t + i\epsilon} dt, \tag{2.27}$$

to write four-point Green's function as

$$G(x_1, x_2; y_1, y_2) = \int \frac{d^3P}{2E_B} \frac{dt}{(2\pi)^3} \varphi(x; P_B, \alpha) \bar{\varphi}(y; P_B, \alpha) e^{-iE_B(X_0 - Y_0)} e^{i\mathbf{P} \cdot (\mathbf{X} - \mathbf{Y})}$$
$$\times \frac{i}{2\pi} \frac{e^{-i(X_0 - Y_0 + f(x_0, y_0))t}}{t + i\epsilon}. \qquad (2.28)$$

By performing the substitution $t \to P_0 - E_B$ in Eq. (2.28)

$$G(x_1, x_2; y_1, y_2) = \int \frac{dP}{(2\pi)^4} \frac{i}{2E_B} \varphi(x; P_B, \alpha) \bar{\varphi}(y; P_B, \alpha) e^{-i(P_0 - E_B)f(x_0, y_0)} \frac{e^{-i(X - Y) \cdot P}}{P_0 - E_B + i\epsilon}, \qquad (2.29)$$

one realizes the presence of a pole at $P^0 = E_B$ in Eq. (2.29), just at the mass of the bound state. This allows us to separate the Green's function as follows:

$$G = G_B + \text{regular terms for } P_0 \to E_B, \qquad (2.30)$$

where the regular terms do not contain poles in $P_0 = E_B$. We want to use the Green's function structure of the initial BS equation Eq. (2.13), hence we should perform the Fourier transformation of Eq. (2.29) as before:

$$G(k, q; P) = \int dx \; dy \; dW e^{ik \cdot x} e^{-iq \cdot y} e^{iP \cdot W} G(x, y; W), \qquad (2.31)$$

this leads to the following expression for the Green's function in the momentum space

$$G_B(k, q; P) = \frac{i\varphi(q; P_B, \alpha) \bar{\varphi}(k; P_B, \alpha)}{2E_B(P_0 - E_B + i\epsilon)}. \qquad (2.32)$$

We introduce Eq. (2.32) into the BS equation Eq. (2.13), after multiplying to both sides by $(P_0 - E_B + i\epsilon)$ and taking the limit $P_0 \to E_B$, the integral equation for the two-body bound state reads as

$$\varphi(k; P_B, \alpha) \bar{\varphi}(q; P_B, \alpha) = G_0(k; P_B) \int \frac{dq'}{(2\pi)^4} K(k, q'; P_B) \varphi(q'; P_B, \alpha) \bar{\varphi}(q; P_B, \alpha), \qquad (2.33)$$

which leads to the following equation for the BS amplitude

$$\varphi(k; P_B) = \Delta_1(\eta_1 P_B + k)\Delta_2(\eta_2 P_B - k) \int \frac{dq'}{(2\pi)^4} K(k, q'; P_B) \varphi(q'; P_B), \qquad (2.34)$$

this integral equation written in terms of the BS amplitude is known as the *homogeneous BS equation.* In Fig. 2.2, a schematic representation of the equation is shown. This equation describes the relativistic bound state of two scalars particles. We will deal with this equation throughout of this thesis.
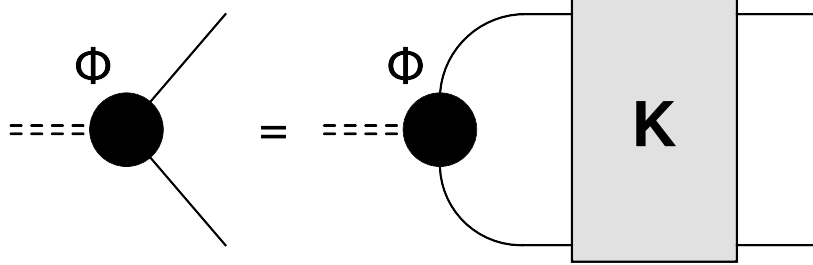

Figure 2.2: Schematic representation of the homogeneous BS equation.

2.2 Analytical properties of the Bethe-Salpeter amplitude

In this section, we study the analytic behavior of the BS amplitude. This issue, which will be explored formally in this Section, is used later on when solving the BS equation in the Euclidean space. As it will be shown, since the analytic behavior of the BS amplitude, it is possible to perform the analytic continuation to the Euclidean space, allowing to obtain an equivalent integral equation. On one hand, this procedure allows us to avoid the well known singular behavior of the BS equation, however it also prevents of obtaining the BS amplitude in the Minkowski space, which can be useful to computed other interesting physical quantities. We deal with this subject later when we study the Euclidean BS equation in Chapter. 6.

We consider again the BS amplitude Eq. (2.14) in the following form:

$$(2\pi)^{-3/2}\Phi(x;P_B,\alpha) = \langle 0|T\{\phi_1(\eta_2 x)\phi_1(-\eta_1 x)\}|P_B,\alpha\rangle = \theta(x_0)f(x;P_B,\alpha) + \theta(-x_0)g(x;P_B,\alpha),$$

(2.35)

with

$$f(x;P_B,\beta) = \langle 0|\phi_1(\eta_2 x)\phi_2(-\eta_1 x)|P_B,\alpha\rangle$$

$$g(x;P_B,\beta) = \langle 0|\phi_2(-\eta_1 x)\phi_1(\eta_2 x)|P_B,\alpha\rangle,$$

(2.36)

introducing a set of complete states: $1 = \sum_n |n\rangle\langle n| \equiv \sum_\beta \int dp|p,\beta\rangle\langle p,\beta|$, the functions f and g reads

$$f(x; P_B, \alpha) = \sum_\beta \int dp\langle 0|\phi_1(\eta_2 x)|p,\beta\rangle\langle p,\beta|\phi_2(-\eta_1 x)|P_B, \alpha\rangle$$

$$g(x; P_B, \alpha) = \sum_\beta \int dp\langle 0|\phi_2(-\eta_1 x)|p,\beta\rangle\langle p,\beta|\phi_1(\eta_2 x)|P_B, \alpha\rangle.$$

(2.37)

Recalling that the ϕ_1 and ϕ_2 operators are written in the Heisenberg representation, we get the expressions for the f and g functions as

$$f(x; P_B, \alpha) = \sum_\beta \int dp \; e^{-i(p-\eta_1 P_B)x}\langle 0|\phi_1(0)|p,\beta\rangle\langle p,\beta|\phi_2(0)|P_B, \alpha\rangle = \int dp \; e^{-i(p-\eta_1 P_B)\cdot x}f(p; P_B, \alpha)$$

$$g(x; P_B, \alpha) = \sum_\beta \int dp \; e^{-i(\eta_2 P_B-p)x}\langle 0|\phi_2(0)|p,\beta\rangle\langle p,\beta|\phi_1(0)|P_B, \alpha\rangle = \int dp \; e^{-i(\eta_2 P_B-p)\cdot x}g(p; P_B, \alpha),$$

(2.38)

where we have designated

$$f(p; P, \alpha) = \sum_\beta \langle 0|\phi_1(0)|p,\beta\rangle\langle p,\beta|\phi_2(0)|P_B, \alpha\rangle$$

$$g(p; P, \alpha) = \sum_\beta \langle 0|\phi_2(0)|p,\beta\rangle\langle p,\beta|\phi_1(0)|P_B, \alpha\rangle,$$

(2.39)

The matrix element $\langle 0|\phi_1(0)|p,\beta\rangle$ is different to zero only if the field $\phi_1(0)$ has the same quantum numbers of the state $|p,\beta\rangle$. Since the stability conditions, the particle 1 cannot decay into any state spontaneously, therefore among the states with the same quantum numbers of the particle 1, this particle should have the smallest invariant mass. This condition can be expressed through the relation: $p_0 \geq \sqrt{m_1^2 + \mathbf{p}^2}$

$$f(x; P_B, \alpha) = \int dp \; e^{-i(p-\eta_1 P_B)\cdot x}f(p; P_B, \alpha)\theta\left(p_0 - \sqrt{m_1^2 + \mathbf{p}^2}\right)$$

$$= \int d^3q \int_0^\infty dq^0 e^{-iq\cdot x}f(q + \eta_1 P_B; P_B, \alpha)\theta(q^0 - E_{min})$$

$$f(x; P_B, \alpha) = \int d^3q \int_{E_{min}}^\infty dq^0 e^{-iq\cdot x}f(q + \eta_1 P_B; P_B, \alpha),$$

(2.40)

where the substitution $q = p - \eta_1 P_B$ has been used and $E_{min} = \sqrt{m_1^2 + (\mathbf{q} + \eta_1 \mathbf{P}_B)^2} - \eta_1 P_B^0$. Analogously for $g(x; P_B, \alpha)$

$$g(x; P_B, \alpha) = \int d^3q \int_{-\infty}^{E_{max}} dq^0 e^{-iq \cdot x} g(\eta_2 P_B - q; P_B, \alpha), \tag{2.41}$$

with $q = \eta_2 P_B - p$ and $E_{max} = \eta_2 P_B^0 - \sqrt{m_2^2 + (\eta_2 \mathbf{P}_B - \mathbf{q})^2}$. The BS amplitude is written as:

$$\begin{aligned}
\Phi(x; P_B, \alpha) = &(2\pi)^{3/2} \theta(x_0) \int d^3q \int_{E_{min}}^{\infty} dq^0 e^{-iq \cdot x} f(q + \eta_1 P_B; P_B, \alpha) \\
&+ (2\pi)^{3/2} \theta(-x_0) \int d^3q \int_{-\infty}^{E_{max}} dq^0 e^{-iq \cdot x} g(\eta_2 P_B - q; P_B, \alpha).
\end{aligned} \tag{2.42}$$

The case when $E_{min} \leq 0$ or $E_{max} \geq 0$ is usually avoided, since in this case there is no gap between the integration interval and the BS amplitude cannot be continued analytically. For avoiding this unpleasant situation, we restrict ourselves to the condition: $|P_B^0| < m_1 + m_2$. Thus $E_{min} > E_{max}$ and a gap in the q^0-axis appears. Additional, choosing the rest frame, $\mathbf{P}_B = 0$, this ensures that $E_{min} > 0$ and $E_{max} < 0$. Therefore, imposing these conditions the BS amplitude can be analytically continued in the complex plane: (i) if $x_0 > 0$ it can be continued to the bottom half-plane and (ii) if $x_0 < 0$ it can be continued to the upper half-plane. This is allowed given the falling exponential behavior in Eq. (2.42).

More instructive is to analyze the BS amplitude in the momentum space. Therefore, we perform the Fourier transformation of Eq. (2.42):

$$\begin{aligned}
\Phi(p'; P, \alpha) = &\int dx e^{ip' \cdot x} \Phi(x; P_B, \alpha) \\
\Phi(p'; P, \alpha) = &(2\pi)^{3/2} \theta(x_0) \int dx \int d^3q \int_{E_{min}}^{\infty} dq^0 e^{i(p'-q) \cdot x} \tilde{f}(q; P_B; \alpha) \\
&+ (2\pi)^{3/2} \theta(-x_0) \int dx \int d^3q \int_{-\infty}^{E_{max}} dq^0 e^{i(p'-q) \cdot x} \tilde{g}(q; P_B; \alpha),
\end{aligned} \tag{2.43}$$

after performing the integration in $\mathbf{q}$ using $\delta(\mathbf{p'} - \mathbf{q})$ one obtains

$$\begin{aligned}
\Phi(p'; P, \alpha) = &(2\pi)^{9/2} \int_0^{\infty} dx^0 \int_{E_{min}}^{\infty} dq^0 \ e^{i(p'_0 - q_0)x_0} \tilde{f}(q_0, \mathbf{p'}; P_B; \alpha) \\
&+ (2\pi)^{9/2} \int_{-\infty}^{0} dx^0 \int_{-\infty}^{E_{max}} dq^0 \ e^{i(p'_0 - q_0)x_0} \tilde{g}(q_0, \mathbf{p'}; P_B; \alpha),
\end{aligned} \tag{2.44}$$

in the integration upon x^0 one has to add the imaginary part in the argument of the exponential, $i(p_0 - q_0 \pm i\epsilon)$ in order that the integral is converged

$$\Phi(p'; P, \alpha) = (2\pi)^{9/2} \int_{E_{min}}^{\infty} dq_0 \frac{i}{(p'_0 - q_0 + i\epsilon)} \tilde{f}(q_0, \mathbf{p'}; P_B; \alpha)$$
$$- (2\pi)^{9/2} \int_{-\infty}^{E_{max}} dq_0 \frac{i}{(p'_0 - q_0 - i\epsilon)} \tilde{g}(q_0, \mathbf{p'}; P_B; \alpha). \tag{2.45}$$

According to Eq. (2.45), the BS amplitude in the momentum space has *cuts* in the complex q_0-plane, which should be considered if one wants to do an analytical continuation to the imaginary axis. We display these cuts in the complex plane in Fig. 2.3. As we can see later when considering the simpler interaction kernel in the BS equation known as the *ladder* kernel, these cuts should be taken into account to perform the analytical continuation. For this kernel it is possible to realize that the analytical continuation is allowed since the analytical properties of the BS amplitude given in Eq. (2.45) and the positions of the singularities of the ladder kernel. For a detailed survey about this issue see Refs. [5, 33].
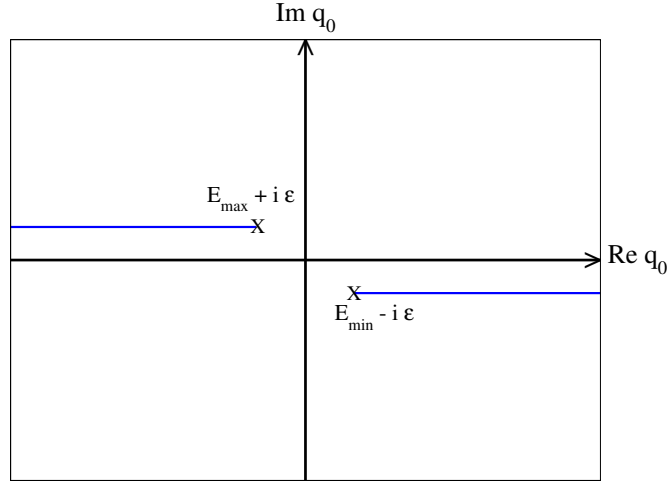

Figure 2.3: Analytical behavior of the BS amplitude.

2.3   Normalization of the Bethe-Salpeter amplitude

Since the initial derivation of the BS equation, the normalization of the BS amplitude has presented difficulties. The earlies derivation required the existence of a conserved quantity such as baryon number or the electric charge [34, 35, 36], therefore inapplicable to neutral systems making those procedures restricted. Afterwards, the normalization was derived without assume the existence of conserved quantities [37, 38, 39], showing that the results are equivalent to the

previous ones. Here, we do not present an exhaustive derivation of the BS amplitude, but we use the result presented in Ref. [39].

By considering the four-point Green function Eq. (2.13), we recall the expression

$$G(k, q; P) = (2\pi)^4 \delta^{(4)}(k - q)G_0(k; P) + G_0(k; P) \int \frac{dq'}{(2\pi)^4} K(k, q'; P)G(q', q; P),$$

now, we introduce the following notation, which has been widely used in the standard analysis of the normalization of the BS amplitude:

$$
\begin{aligned}
A \otimes B &= \int dq' A(p, q'; P)B(q', q : P) \\
\mathcal{K} &= \frac{\delta(k - q')}{\Delta_1(\eta_1 P + k)\Delta_2(\eta_2 P - k)} \\
\mathcal{I} &= (2\pi)^4 \int dq' \delta(k - q')\delta(q' - q),
\end{aligned}
\tag{2.46}
$$

where $\Delta_1(\eta_1 P + k)$ and $\Delta_2(\eta_2 P - k)$ stand for the free-propagators. By using this operator notation the four-point Green's function reads as:

$$\mathcal{K} \otimes G = \mathcal{I} + K \otimes G \Rightarrow (\mathcal{K} - K) \otimes G = \mathcal{I}. \tag{2.47}$$

Deriving to both sides respect of P_0 and using $(\mathcal{K} - K) \otimes G = \mathcal{I}$, we get

$$\frac{\partial G}{\partial P_0} = -G \otimes \left(\frac{\partial \mathcal{K}}{\partial P_0} + \frac{\partial K}{\partial P_0} \right) \otimes G. \tag{2.48}$$

Recalling the expression for the Green's function in the neighborhood of the pole

$$G_B(p, q; P) = \frac{i\varphi(p; P_B, \alpha)\bar{\varphi}(q; P_B, \alpha)}{2E_B(P_0 - E_B + i\epsilon)}, \tag{2.49}$$

we obtain

$$
\begin{aligned}
\frac{\partial G}{\partial P_0} &= -i \frac{\varphi(p; P_B)\bar{\varphi}(q; P_B)}{2E_P(P_0 - E_P + i\epsilon)^2} \\
G \otimes \frac{\partial}{\partial P_0}(\mathcal{K} + K) &= \int \frac{dq''}{(2\pi)^4} G(p, q''; P) \frac{\partial}{\partial P_0}(\mathcal{K} + K)(q'', q'; P) \\
G \otimes \frac{\partial}{\partial P_0}(\mathcal{K} + K) \otimes G &= \int \frac{dq'}{(2\pi)^4} \frac{dq''}{(2\pi)^4} G(p, q''; P) \left[\frac{\partial}{\partial P_0}(\mathcal{K} - K) \right](q'', q'; P)G(q', q; P)
\end{aligned}
\tag{2.50}
$$

introducing these pieces into Eq. (2.48), the result is:

$$-2iE_P = \int \frac{dq'}{(2\pi)^4} \frac{dq''}{(2\pi)^4} \bar{\varphi}(q''; P_B) \left[\frac{\partial}{\partial P_0}(\mathcal{K} + K) \right]_{P_0 = E_P} (q'', q'; P)\varphi(q'; P_B). \qquad (2.51)$$

It should be pointed out that this unfamiliar way of normalizing the BS amplitude is the closer analog of the usual normalization conditions for free elementary particle wave functions. As illustrated in Ref. [39], this normalization condition leads to the usual orthogonality relations. That example has been done for spin-$\frac{1}{2}$ particles, but the procedure is quite general.

Chapter 3

Light-front dynamics

In the Dirac's seminal work [40], presented in the 40's, it was clear the existence of several forms of relativistic dynamics, differently from the non-relativistic quantum mechanics where only one is allowed. After the introduction of the special relativity, since the upper bound for the speed, the dynamics is restricted to the space-time light-cone: inside of the light-cone two points in the space-time are connected causally, outside the points are not connected and over the hyper-surface the points are connected by a signal of light. Thus, for describing the dynamics of a physical system is necessary to specify the values of the dynamical variables on a given initial 3-dimensional hyper-surface. The choice of this hyper-surface determines the type of variables that one can use to describe the physical evolution. The evolution of a system with non-relativistic dynamics is governed fully by the Hamiltonian: given the state of the system at some time $t=0$, one may calculate its state at any another time using the evolution operator $U(t) = e^{-iHt}$. The state specification at the surface $t=0$, an instant in time, represents the initial conditions.

3.1 A short review of the Poincarè group

In this section we present the general structure of the Poincarè group (PG) to better understand the situation in the relativistic framework. The general transformation of the PG is given for the ten-parameter transformation written as

$$x^\mu \longrightarrow x'^\mu = \Lambda^\mu_\nu x^\nu + a^\mu, \tag{3.1}$$

where a^μ is a constant four-vector, which accounts for a translation in the space-time and it depends on four parameters. Λ^μ_ν stands for a Lorentz transformation, that contains boosts transformations and spatial rotations. For Lorentz transformations six parameters are necessary; three of them are related with the velocities and the remaining related with the Euler angles to perform the spatial rotations. From the requirement of the special relativity of maintaining the square of the four-vectors one obtains

$$g_{\rho\sigma} = g_{\mu\nu}\,\Lambda^\mu_\rho\,\Lambda^\nu_\sigma, \tag{3.2}$$

$g_{\mu\nu}$ is the symmetric metric tensor. This relation implies that

$$\det(\Lambda) = \pm 1. \tag{3.3}$$

The two values of the determinant allow to classify the Lorentz transformations in two kinds of transformations: *proper (improper)* Lorentz transformation if the determinant is positive (negative). There is an additional classification of the Lorentz transformations: if $\Lambda^0_0 \geq 1$ it is called *orthochronous* and if $\Lambda^0_0 \leq 1$ it is called *non-orthochronous*.

The structure of group of the Lorentz transformation is explored by considering the infinitesimal transformation

$$x'^\mu = x^\mu + \alpha^\mu + \beta^\mu_\nu x^\mu, \tag{3.4}$$

where α^μ is an infinitesimal four-vector and β^μ_ν is an antisymmetric tensor depend on the six parameters of the transformation. Once introduced the generators, it is possible to obtain their Lie algebra

$$\begin{aligned}
&[P_\mu, P_\nu] = 0, \\
&[M_{\mu\nu}, P_\rho] = -ig_{\mu\rho}P_\nu + ig_{\nu\rho}P_\mu, \\
&[M_{\mu\nu}, M_{\rho\sigma}] = ig_{\nu\rho}M_{\mu\sigma} - ig_{\mu\rho}M_{\nu\sigma} - ig_{\nu\sigma}M_{\mu\rho} + ig_{\mu\sigma}M_{\mu\rho}.
\end{aligned} \tag{3.5}$$

A more familiar expressions can be obtained by introducing the new operators $J_i \equiv \frac{1}{2}\epsilon_{ijk}M_{jk}$, which lead to the well known expressions of the Lie algebra for the rotation group $SU(2)$

$$[J_i, J_j] = i\epsilon_{ijk}J_k, \tag{3.6}$$

also for boosts generators defined as $K_i \equiv M_{0i}$, one has the following expression for the Lie algebra

$$
\begin{aligned}
[K_i, K_j] &= -i\epsilon_{ijk}J_k \\
[J_i, K_j] &= i\epsilon_{ijk}K_k.
\end{aligned}
\tag{3.7}
$$

For a very clear and instructive discussion of the PG see Ref. [41].

According to Dirac, see Ref. [40], one can point out that the Hamiltonian dynamics is described by a certain number of pairs of dynamical variables, e.g. (ξ, η), usually the coordinates and momentums. These variables change when applying a transformation of the PG, but given the principle of relativity, their Poisson brackets must remain unchanged. There exists only a unique way to satisfy such a constraint. For the dynamical variable ξ, it has to change according to the following relation

$$
\xi' = \xi + \{\xi, F\},
\tag{3.8}
$$

where F is an infinitesimal dynamical variable, independent of ξ. The F associated with the transformation of Eq. (3.4) should depend linearly on the infinitesimal numbers α^μ, β^μ_ν. The most general form of F is given by:

$$
F = -\alpha^\mu P_\mu + \frac{1}{2}M_{\mu\nu}\beta^{\mu\nu}.
\tag{3.9}
$$

The aim of relativistic dynamics is to find representations of these generators in physical form, e.g, as differential, integral or matrix operators on the states. For the case of non-interacting particles the task is almost trivial. Much more difficult is the construction of such representations in the case of interacting particles. This is the topic of the relativistic dynamics proper.

As mentioned above, one should choose a hyper-surface, which we call Σ, in the Minkowski space such that it does not contain time-like directions, because the points in these hyper-surfaces are connected by means of Lorentz transformations. These are included anyway in a covariant formalism. In principle, the choice is infinity, but one should choose the surface with further advantages from the physical point of view. In terms of the group theory, from the set of all generators of the PG, the subset of these generators that leave the initial hyper-surface invariant are called kinematical generators and their set composes the *stability* group of Σ. The other generators those that transform the initial Σ in a Σ' are called hamiltonian generators. Therefore, the dynamics of the system is determined by the hamiltonian generators of the PG.

3.2   Dirac's forms of relativistic dynamics

Dirac in his work explained three forms of relativistic dynamic. The first of them is the *Instant form*, equivalent to the hyperplane $x^0=0$. In this case the dynamical variables are referred to physical conditions to a certain instant in time, e.g. the coordinates and their conjugate momenta at $x^0=0$ as in the non-relativistic case. The kinematical operators are the P^i, since that they generate translations along the three spatial directions and leave x^0 unchanged and the J^i that generates rotations. The hamiltonian generators are P^0 and the boosts K^i, which clearly modify x^0.

The second form of relativistic dynamic is given by the hyper-plane tangent to the light-cone: $x^0 + x^3 = 0$ know as the *light-front* (LF). For classifying the generators in the LF dynamics, we first introduce the LF coordinates of a four-vector. Given a four-vector $x^\mu = (x^0, x^1, x^2, x^3)$, it is possible to write it in LF components as follows

$$x^\mu = (x^+, x^-, \mathbf{x}_\perp), \tag{3.10}$$

where

$$x^+ = x^0 + x^3 \qquad x^- = x^0 - x^3 \qquad \mathbf{x}_\perp = (x^1, x^2), \tag{3.11}$$

with these coordinates the scalar product reads as

$$x_\mu y^\mu = \frac{1}{2}x^+ y^- + \frac{1}{2}x^- y^+ - \mathbf{x}_\perp \mathbf{y}_\perp. \tag{3.12}$$

Thus, we may classify the generators as follows:

- **Kinematical generators**

   P^1, P^2 which generate spatial translations in x^1 and x^2. J^3 that generates rotations in x^3. P^+ that produces translations in x^-. The boost K^3 is also a kinematical generator. In order to see clearly that the plane $x^+ = 0$ is unchanged under this transformation, consider the Lorentz transformation along the x^3-axis:

$$\begin{aligned} x'^0 &= \gamma(x^0 + \beta x^3) \\ x'^3 &= \gamma(x^3 + \beta x^0), \end{aligned} \tag{3.13}$$

by using the LF coordinates of Eq. (3.10), we get

$$
\begin{aligned}
x'^+ &= \gamma(1 + \beta)x^+ \\
x'^- &= \gamma(1 - \beta)x^-,
\end{aligned}
\tag{3.14}
$$

therefore the plane $x^+ = 0$ remains unchanged. In the same way it is possible to obtain that the "boost" defined as $E_1 = K_1 + J_2$ and $E_2 = K_2 + J_2$ behaves like kinematical generators in the LF dynamics.

- **Hamiltonian generators**

  P^- that produces translations in x^+ and the LF "rotations" defined as: $F_1 = K_1 - J_2$ and $F_2 = K_2 + J_1$.

The third relativistic form discussed by Dirac is called *Point form*, which is given by the hyper-surface $x^\mu x_\mu - a^2 > 0$ with $x^0 > 0$. In this case the kinematical generators are the boots K^i since that $x_\mu x^\mu$ remains unchanged and the rotation generators J^i because $x_i x^i$ is invariant. The Hamiltonian generators are the generators of space-time translation P^μ, since the change in the coordinates will change the scalar product.

In principle there is no reason to use a particular form of relativistic dynamics. In fact, it has been demonstrated that the Dirac's forms are unitarily equivalent, i.e, one can change of form by means of the unitary transformation [42]. However, one can choose a particular form to take advantage from the physical point of view. LF dynamics is singled out for corresponding to the smallest number of dynamical generators: three*. This property by itself is not important enough to prefer the LF, however since the three boost generators are kinematical this enables to separate the center of mass motion of the intrinsic one in a similar way of the non-relativistic framework [44].

Another advantage, already stressed by Dirac, is the *spectrum property*. Consider a particle with four-momenta $p^\mu = (p^-, p^+, \mathbf{p}_\perp)$, where p^- is interpreted as the energy and p^+ the longitudinal momentum. If $p^\mu p_\mu \geq 0$ and $p_0 \geq 0$, then $p_0 \geq |p_3|$. Now, by considering the dispersion relation in LF dynamics

---

*It is important to emphasize that a hypersurface $x^+ = c$, with $c \neq 0$ loss the invariance respect to the longitudinal boost and so the number of kinematical generators is reduced to six. Hence, the importance of the hypersurface $x^+ = 0$.

$$p^\mu p_\mu = p^+ p^- - \mathbf{p}_\perp^2 \geq 0, \tag{3.15}$$

one obtains that $p^+ \geq 0$ and $p^- \geq 0$. The sign $=$ holds only for massless paricles. In the instant form dynamics this condition should be implement separately, instead in LF dynamics the positivity of p^+ entails the positivity of p^-. This feature of the LF dynamics is quite relevant in the definition of the vacuum of the theory, since the vacuum is defined as the state with zero momentum thus only particles with zero longitudinal momentum can compose it. Differently, in the instant form the state is specified by its ordinary three-momentum $\mathbf{p} = (p^1, p^2, p^3)$. Since each component of $\mathbf{p}$ can be either positive or negative, there exist zero total momentum Fock states of arbitrary particle number, and these will mix with the zero-particle state to build up the physical vacuum. In the LF dynamics the vacuum is nothing but emptiness and here is the main advantage of this approach.

Before closing this section it is worthy to present the relative LF coordinates of a system composed by two particles and its relation with the total mass of the system, which will be used in mostly of this thesis, for details in this issue see Ref. [43]. Consider the four-momenta of the composite system

$$P = p_1 + p_2 \qquad P^2 = M^2, \tag{3.16}$$

according to the relation dispersion Eq. (3.15)

$$M^2 = P^+ P^- - \mathbf{P}_\perp^2, \tag{3.17}$$

for the case that we are considering, i.e, composed by two particles, one has

$$P^\pm = p_1^\pm + p_2^\pm \qquad \mathbf{P}_\perp = \mathbf{p}_{1\perp} + \mathbf{p}_{2\perp}. \tag{3.18}$$

Now, we introduce the relative coordinates

$$\xi = \frac{p_1^+}{P^+} \qquad \mathbf{k}_\perp = (1 - \xi)\,\mathbf{p}_{1\perp} - \xi\,\mathbf{p}_{2\perp}, \tag{3.19}$$

and their inverse relations

$$\mathbf{p}_{1\perp} = \xi\,\mathbf{P}_\perp + \mathbf{k}_\perp \qquad \mathbf{p}_{2\perp} = (1 - \xi)\,\mathbf{P}_\perp - \mathbf{k}_\perp. \tag{3.20}$$

We write Eq. (3.17) in the following form

$$M^2 = P^+(p_1^- + p_2^-) - \mathbf{P}_\perp^2 = P^+ \left[\frac{m_1^2 + (\mathbf{p}_{1\perp})^2}{p_1^+} + \frac{m_2^2 + (\mathbf{p}_{2\perp})^2}{p_2^+} \right] - \mathbf{P}_\perp^2, \qquad (3.21)$$

by introducing Eq. (3.20) into Eq. (3.21) and using the definition of ξ, we get the following expression for the total invariant mass M:

$$M^2 = \left[\frac{\mathbf{k}_\perp^2 + m_1^2}{\xi} + \frac{\mathbf{k}_\perp^2 + m_2^2}{(1-\xi)} \right]. \qquad (3.22)$$

The third component of k is given by

$$k_3 = \xi(1-\xi)\frac{\partial M}{\partial \xi} = \left(\xi - \frac{1}{2} \right) M - \frac{(m_1^2 - m_2^2)}{2M}, \qquad (3.23)$$

in order to justify the denomination of vector for $\mathbf{k}$, we can compute its square

$$\mathbf{k}^2 = \mathbf{k}_\perp^2 + k_3^2 = \frac{(M^2 - m_1^2 - m_2^2)^2 - 4m_1^2 m_2^2}{4M^2}, \qquad (3.24)$$

it depends only of invariants, therefore $\mathbf{k}^2$ is an invariant independently of the frame. Indeed, $\mathbf{k}$ is the momentum of particle 1 in the rest frame ($\mathbf{P}{=}0$). Thus, we can equate the invariant mass with the energy in this frame

$$E = \sqrt{m_1^2 + \mathbf{k}^2} + \sqrt{m_2^2 + \mathbf{k}^2}. \qquad (3.25)$$

The above relations are useful in view of the analysis of the bound state composed by two particles carried out in the next sections.

3.3 Light-front projection of the Bethe-Salpeter amplitude

In this section, we outline the meaningful feature of the LF dynamics when applied to the BS approach; we show that the BS amplitude when projected onto LF hyperplane allows to extract the valence wave function. In other words, this projection enables to recover the probabilistic interpretation of the BS amplitude.

As starting point, let us consider the BS amplitude of Eq. (2.14)

$$\Phi(x_1, x_2; P_B) = \langle 0|T\{\phi_1(x_1)\phi_2(x_2)\}|p, \Psi_{\text{int}}\rangle,$$

for shorthand notation we skip the index corresponding to the set of all quantum numbers, and we have set $|P_B\rangle = |p, \Psi_{\text{int}}\rangle$, which stands for the bound state of two interacting particles. Note the separation of the internal and total motion, fact that will be justified in shortly. The vector state $|p, \Psi_{\text{int}}\rangle$ can be taken in different representations, but in LF dynamics by considering only massive quanta, it can be written in terms of an infinity sum over Fock components because of the simplicity of the LF vacuum as mentioned in the previous Section. The eigenstate $|p, \Psi_{\text{int}}\rangle$ is expanded in multiparticle Fock eigenstates $\{|n\rangle\}$ of the free Hamiltonian, i.e. a basis constructed by using the LF plane waves, $|\tilde{q}\rangle$.

The one-particle free state is defined by $|\tilde{q}\rangle = (2\pi)^{3/2}\sqrt{2q^+}a^\dagger(\tilde{q})|0\rangle$, describing the motion of a particle with mass m and it is an eigenstate of the LF momentum operators $\hat{p}^+$ and $\hat{\mathbf{p}}_\perp$, i.e. $\tilde{q} \equiv \{q^+, \mathbf{q}_\perp\}$. The dependence in q^- is given by $q^- = (m^2 + |\mathbf{q}_\perp|^2)/q^+$. The normalization of the free-state is

$$\langle \tilde{k}|\tilde{q}\rangle = 2(2\pi)^3 k^+ \delta(k^+ - q^+)\delta^{(2)}(\mathbf{k}_\perp - \mathbf{q}_\perp) = 2(2\pi)^3 k^+ \delta^{(3)}(\tilde{k} - \tilde{q}), \tag{3.26}$$

and therefore the completeness relation is given by

$$\int \frac{d^3\tilde{q}}{2q^+(2\pi)^3}|\tilde{q}\rangle\langle\tilde{q}|. \tag{3.27}$$

We recall that for a particle with mass m one has

$$\int dq\, \delta(q^2 - m^2)\theta(q^0) = \frac{1}{2}\int d^3\tilde{q}\int dq^- \delta(q^+ q^- - |q_\perp|^2 - m^2)\theta(q^+) = \int \frac{d^3\tilde{q}}{2q^+}\theta(q^+), \tag{3.28}$$

the positivity of q^+ entails the positivity of q^0, since $q^0 = [q^+ + (m^2 + |q_\perp|^2)/q^+]/2$. The expansion of $|p, \Psi_{\text{int}}\rangle$ in the Fock basis reads

$$|p, \Psi_{\text{int}}\rangle = 2(2\pi)^3 \sum_{n\geq 2}^\infty \int [d\xi_i][d^2\mathbf{k}_{i\perp}]\psi(\xi_i, \mathbf{k}_{i\perp})|n; \xi_i p^+, \mathbf{k}_{i\perp} + \xi_i\mathbf{p}_\perp\rangle, \tag{3.29}$$

where $n \geq 2$, since we are dealing with a two-body composite system. We recall that $\xi_i = q_i^+/p^+$ and $\mathbf{q}_{i\perp} = \mathbf{k}_{i\perp} + \xi_i\mathbf{p}_\perp$ with $\mathbf{k}_{i\perp}$ being the intrinsic transverse momentum of the i-th constituent. The coefficients $\psi(\xi_i, \mathbf{k}_{i\perp})$ of the Fock expansion are called the light-front wave functions (LFWF). The set of intrinsic variables fulfill the following relations

$$\sum_{j=1}^{n} \xi_j = 1 \qquad \sum_{j=1}^{n} \mathbf{k}_{j\perp} = 0, \tag{3.30}$$

thus the phase-space factors are given by

$$\int [d\xi_j] \equiv \prod_{j=1}^{n} \int \frac{d\xi_j}{2(2\pi)\xi_j} \delta \left(1 - \sum_{i=1}^{n} \xi_i \right)$$

$$\int [d^2\mathbf{k}_{j\perp}] \equiv \prod_{j=1}^{n} \int \frac{d^2\mathbf{k}_{j\perp}}{(2\pi)^2} \delta^2 \left(\sum_{i=1}^{n} \mathbf{k}_{i\perp} \right), \tag{3.31}$$

the delta functions have been added to fulfill the constraints Eq. (3.30). It is important to emphasize that given the kinematical separation of the global motion and intrinsic one in LF dynamics, it leads to the normalization of the intrinsic motion in terms of the LFWFs, this is the reason of the notation that we have adopted, namely $|p, \Psi_{\text{int}}\rangle$. For obtaining explicitly this fact, consider the overlap $\langle n; \xi_i p^+, \mathbf{k}_{i\perp} + \xi_i \mathbf{p}_\perp | p, \Psi_{\text{int}}\rangle$, which can be written in terms of the global motion and the LFWF

$$\langle n; \xi_i p^+, \mathbf{k}_{i\perp} + \xi_i \mathbf{p}_\perp | p, \Psi_{\text{int}}\rangle = 2p^+ (2\pi)^3 \delta^3 \left(\sum_{i}^{n} \tilde{q}_i - \tilde{p} \right) \psi(\xi_i, \mathbf{k}_{i\perp})$$

$$= 2(2\pi)^3 \delta \left(1 - \sum_{i}^{n} \xi_i \right) \delta^{(2)} \left(\sum_{1}^{n} \mathbf{k}_{i\perp} \right) \psi(\xi_i, \mathbf{k}_{i\perp}), \tag{3.32}$$

the plane waves corresponding to the global motion have the standard normalization, which can be factorized out

$$\langle \tilde{p}'; \Psi_{\text{int}} | \tilde{p}; \Psi_{\text{int}}\rangle = 2p^+ (2\pi)^3 \delta^{(3)} \left(\tilde{p}' - \tilde{p} \right) \langle \Psi_{\text{int}} | \Psi_{\text{int}}\rangle$$

$$= [2p^+ (2\pi)^3]^2 \sum_{n \geq 2} \int [d^3\tilde{q}_i] \delta^3 \left(\sum_{i=1}^{n} \tilde{q}_i - \tilde{p} \right) \psi(\xi_i, \mathbf{k}_{i\perp}) \delta^3 \left(\sum_{i=1}^{n} \tilde{q}_i - \tilde{p}' \right) \psi(\xi_i, \mathbf{k}_{i\perp})$$

$$= 2p^+ (2\pi)^3 \delta^3 (\tilde{p}' - \tilde{p}) 2(2\pi)^3 \sum_{n \geq 2} \int [d\xi_i][d^2\mathbf{k}_{i\perp}] |\psi(\xi_i, \mathbf{k}_{i\perp})|^2, \tag{3.33}$$

therefore, the LFWF $\psi(\xi_i, \mathbf{k}_{i\perp})$ are normalized according to

$$\langle \Psi_{\text{int}} | \Psi_{\text{int}}\rangle = 2(2\pi)^3 \sum_{n \geq 2} \int [d\xi_i][d^2\mathbf{k}_{i\perp}] |\psi(\xi_i, \mathbf{k}_{i\perp})|^2 = 1. \tag{3.34}$$

The normalization clearly shows the physical content associated to the LFWF, these yield the probability distributions to find n constituents with intrinsic coordinates $\{\xi_i, \mathbf{k}_{i\perp}\}$ inside the interacting state. The corresponding $\psi(\xi_i, \mathbf{k}_{i\perp})$ for the bound state with the minimal number of constituents, i.e. $n = 2$ is known as the *light-front valence wave function*. The probability of finding the valence component for the bound state is given by

$$N_2 = 2(2\pi)^3 \int \frac{d\xi_1}{2(2\pi)\xi_1} \frac{d\xi_2}{2(2\pi)\xi_2} \delta(1 - \xi_1 - \xi_2) \int \frac{d^2\mathbf{k}_{1\perp}}{(2\pi)^2} \frac{d^2\mathbf{k}_{2\perp}}{(2\pi)^2} \delta^2(\mathbf{k}_{1\perp} + \mathbf{k}_{2\perp}) |\psi(\xi_1, \mathbf{k}_{1\perp}; \xi_2, \mathbf{k}_{2\perp})|^2$$
$$= \frac{1}{(2\pi)^3} \int \frac{d\xi}{2\xi(1-\xi)} \int d^2\mathbf{k}_\perp |\psi(\xi, \mathbf{k}_\perp)|^2.$$

$$(3.35)$$

We have formally presented the structure of the Fock state in LF dynamics. Now, we explain how to extract the LFWF from the BS amplitude given its relevance in the forthcoming analysis. As we show below the constraint $x^+ = 0$ lead us to the relation between the valence component and the BS amplitude.

Before continuing, we explain the simplicity of the field operators in LF quantization. The constituents of the composite system appear as excitations of the dynamical fields $\phi(x)$ expanded in terms of creation and annihilation operators with coordinates $x = (x^+, x^-, \mathbf{x}_\perp)$. However, in LF dynamics, $x^+ = 0$, the Heisenberg operators turn into the Schrödinger ones, since $\phi(x) = \exp(-iP^-x^+/2)\phi(\tilde{x})\exp(iP^-x^+/2)$ and the field operator is written as

$$\phi(\tilde{x}) = \int \frac{dk^+}{\sqrt{2k^+}} \frac{d^2\mathbf{k}_\perp}{(2\pi)^{3/2}} \theta(k^+) \left(a^\dagger(\tilde{k})e^{-i\tilde{k}\cdot\tilde{x}} + a(\tilde{k})e^{i\tilde{k}\cdot\tilde{x}} \right), \qquad (3.36)$$

with $\tilde{x} = (x^-, \mathbf{x}_\perp)$ and $\tilde{k}\cdot\tilde{x} = k^+x^-/2 - \mathbf{x}_\perp\cdot\mathbf{k}_\perp$. The creation and annihilation operators satisfy the commutation relations

$$[a(\tilde{k}), a^\dagger(\tilde{k}')] = \delta(k^+ - k'^+)\delta^{(2)}(\mathbf{k}_\perp - \mathbf{k'}_\perp). \qquad (3.37)$$

After this clarification, we can consider the reduced BS amplitude Eq. (2.18) in the limit $x^+ \to 0_+$

$$\lim_{x^+\to 0_+} \varphi(x, p) = \langle 0|\phi(\tilde{x}/2)\phi(-\tilde{x}/2)|p\rangle, \qquad (3.38)$$

note that in the expression Eq. (2.18) we have chosen $\eta_1 = \eta_2 = 1/2$ because we will deal with the bound state composed by two particles with the same mass $m_1 = m_2 = m$. The quantity

written in Eq. (3.38) is equivalent to consider $\varphi(x,p)\delta(x^+)$, we take the Fourier transform of this quantity

$$
\begin{aligned}
\int dx\ e^{-ix\cdot q}\varphi(x,p)\delta(x^+) &= \int d^3\tilde{x}\ e^{-i\tilde{x}\cdot\tilde{q}}\varphi(\tilde{x},x^+=0,p) \\
&= \int d^3\tilde{x}\ e^{-i\tilde{x}\cdot\tilde{q}}\int\frac{dk^-}{(2\pi)}\int\frac{d^3\tilde{k}}{(2\pi)^3}e^{i\tilde{x}\cdot\tilde{k}}\varphi(k,p) = \int\frac{dk^-}{(2\pi)}\int\frac{d^3\tilde{k}}{(2\pi)^3}\int d^3\tilde{x}\ e^{i(\tilde{k}-\tilde{q})\cdot\tilde{x}}\varphi(k,p) \quad (3.39) \\
&= \int\frac{dk^-}{(2\pi)}\int d^3\tilde{k}\ \varphi(k,p)\delta^3(\tilde{k}-\tilde{q}) = \int\frac{dq^-}{(2\pi)}\varphi(q,p).
\end{aligned}
$$

On the other hand one has

$$
\int d^3\tilde{x}\ e^{-i\tilde{x}\cdot\tilde{q}}\varphi(\tilde{x},x^+=0,p) = \int d^3\tilde{x}\ e^{-i\tilde{k}\cdot\tilde{x}}\langle 0|\phi(\tilde{x}/2)\phi(-\tilde{x}/2)|p\rangle, \quad (3.40)
$$

we can introduce in the above expression the Fock expansion for the state $|p\rangle$ for $n=2$ given in Eq. (3.29), the expression for Schrödinger fields given in Eq. (3.36) and taking into account the commutation relations Eq. (3.37) one obtains

$$
\int d^3x e^{-i\tilde{x}\cdot\tilde{q}}\varphi(\tilde{x},x^+=0,p) = \frac{\sqrt{2}\ p^+}{(p/2+k)^+(p/2-k)^+}\psi(\xi,\mathbf{k}_\perp) = \frac{\sqrt{2}}{p^+}\frac{1}{\xi(1-\xi)}\psi(\xi,\mathbf{k}_\perp). \quad (3.41)
$$

We have obtained the pivotal result in this calculation: *the LF projection allows to extract the LFWF from the Fock interacting state.* Formally, this projection is obtained by integrating the BS amplitude in the LF variable k^-. We summarize the results as:

$$
\psi(\xi,\mathbf{k}_\perp) = \frac{p^+}{\sqrt{2}}\xi(1-\xi)\int\frac{dk^-}{(2\pi)}\varphi(k,p). \quad (3.42)
$$

Thus, once the BS amplitude is obtained for some available method the LFWF can be obtained. Despite that all the physical information is provided by the BS amplitude and several physical observables are computed by means of the BS amplitude, the knowledge of the LFWF allows us to access to the main features of the bound state in a closer relation with their non-relativistic counterparts.

Chapter 4

Nakanishi integral representation for the Bethe-Salpeter amplitude

This chapter is devoted to show the formalism of the Nakanishi integral representation (NIR), to the transition amplitude for a generic scattering process involving N-external particles. This representation was introduced in 60's by Noboru Nakanishi in the basis of a perturbative treatment [5]. Despite, that the NIR has been devised in the perturbative regime, its applicability has been extended to the non-perturbative one. Recently, this representation has been adopted to the study of bound state problems in the non-perturbative regime [6, 7, 8, 9], obtaining satisfactory results. Satisfactory results mean that the results obtained using the NIR are in agreement with those obtained with other unrelated method. There exist many studies where the NIR has given good results, only remains a formal proof of the validity of this representation also in the non-perturbative regime. For this reason, in this thesis we decided to slightly change the name initially used for this representation, namely perturbation theory integral representation to the Nakanishi integral representation.

After deriving the NIR for the N-external legs, we emphasize in the case $N=3$, which represent the vertex function used to study the bound state problem by means of the BS equation. Finally, we formally show that the NIR can be extended to lower dimensions, in particular, for 2+1 dimensions. Since, in this thesis we also perform a study of the three-dimensional bound state problem, it is needed to establish the validity of the NIR in this case.

4.1 Introducing the Nakanishi integral representation

Nowadays, the best known theory for describing reactions in the relativistic framework is quantum field theory. In the framework of this theory the probability amplitudes of a given process are given in terms of the S-matrix, which may be formally written in terms of a power series of the coupling constant associated with the theory. Each term of this sum is by itself a sum of the Feynman integrals corresponding to the Feynman graphs. A Feynman graph is a representation of the interaction process, which contains the propagation of a free particles and the interaction is represented by a vertex. Each propagation and the vertex depend on the nature of the constituents and the type of interaction of the theory.

A Feynman integral is a multiple, singular integral over infinite ranges of four-momenta, and it is not necessarily well defined *a priori*. It is important, therefore, from both theoretical and practical point of view, to convert the Feynman integral into a *Feynman-parametric integral*. We explore this parametrization since it leads to the NIR providing a compact representation of all Feynman graphs for a given set of external particles.

We start by considering a connected Feynman diagram, G, with N external legs, n internal propagations, V vertex and k loops. We adopt the following notation,

- p_i (with $i = 1, ..., N$) are the external four-momenta, with chosen signs such that the four-momentum conservation reads as follows (the covariant indexes are dropped out for simplifying the notation)

$$\sum_{i=1}^{N} p_i = 0. \tag{4.1}$$

- ℓ_j and m_j (with $j = 1, ..., n$) are four-momenta and masses associated to the particles propagating inside the loops, respectively.

- q_r, with $(r = 1, ..., k)$ are the four-momenta on which one has to integrate inside the r-th loop.

After considering the four-momentum conservation at each vertex one can write the general equations

$$\ell_j = \sum_{r=1}^{k} b_{jr} \; q_r + \sum_{i=1}^{N} c_{ji} \; p_i, \tag{4.2}$$

where b_{jr} and c_{ji} can assume the values -1, 0 and 1. The *Feynman integral* associated with G is a formal multiple integral

$$f_G(p_1, p_2, ..., p_N) = \int \left(\prod_{j=1}^{n} d^4 l_j \right) \frac{\prod_{b \in V} \delta^{(4)}(p_b)}{\prod_{j=1}^{n} (l_j^2 - m_j^2 + i\epsilon)}, \tag{4.3}$$

the expression is a product of Feynman propagators corresponding to all internal lines and the four dimensional δ-function in the numerator accounts for the momentum conservation in each vertex b (p_b is the ingoing momentum in each vertex). The number of independent δ-functions involving integration variables is $V - 1$. After carrying out those $V - 1$ trivial integrations, the number of the remaining four-dimensional integrations is $n - (V - 1) = k$. Thus, Eq. (4.3) turns into

$$f_G(p_1, p_2, ..., p_N) = \delta^{(4)} \left(\sum_{i=1}^{N} p_i \right) \int \left(\prod_{r=1}^{k} d^4 q_r \right) \frac{1}{\prod_{j=1}^{n} (l_j^2 - m_j^2 + i\epsilon)}, \tag{4.4}$$

the conservation of the external four-momentum appears explicitly. Note, that the dependence of l_j in q_r is given by Eq. (4.2). The n denominators in Eq. (4.4) can be combined in only one denominator with the aid of the Feynman parametric formula

$$\frac{1}{A_1 A_2 ... A_n} = (n-1)! \int_0^1 d\alpha_1 \int_0^1 d\alpha_2 ... \int_0^1 d\alpha_n \frac{\delta \left(1 - \sum_{i=1}^{n} \alpha_i \right)}{(A_1 \alpha_1 + ... + A_n \alpha_n)^n}, \tag{4.5}$$

one gets

$$f_G(p_1, p_2, ..., p_N) \propto \delta^{(4)} \left(\sum_{i=1}^{N} p_i \right) \int \left(\prod_{r=1}^{k} d^4 q_r \right) \int_0^1 \left(\prod_{j=1}^{n} d\alpha_j \right) \frac{\delta \left(1 - \sum_{j=1}^{n} \alpha_j \right)}{\left[\sum_{j=1}^{n} (l_j^2 - m_j^2 + i\epsilon) \alpha_j \right]^n}. \tag{4.6}$$

We analyze the first term in the denominator, l_j^2. By using Eq. (4.2) it can written as

$$l_j^2 = \sum_{r=1}^{k} \sum_{r'=1}^{k} b_{jr} b_{j'r} (q_r \cdot q_{r'}) + \sum_{i=1}^{N} \sum_{i'=1}^{N} c_{ij} c_{i'j} (p_i \cdot p_{i'}) + 2 \sum_{r=1}^{k} \sum_{i=1}^{N} b_{jr} c_{ij} (q_r \cdot p_i) \tag{4.7}$$

therefore the denominator becomes

$$\left[\sum_{j=1}^{n}(l_j^2 - m_j^2 + i\epsilon)\alpha_j\right]^n = \left[\sum_{j=1}^{n}l_j^2\alpha_j - \sum_{j=1}^{n}m_j^2\alpha_j + i\epsilon\right]^n =$$

$$\left[\sum_{j=1}^{n}\left\{\sum_{r=1}^{k}\sum_{r'=1}^{k}b_{jr}b_{jr'}(q_r\cdot q_{r'})\alpha_j + \sum_{i=1}^{N}\sum_{i'=1}^{N}c_{ij}c_{i'j}(p_i\cdot p_{i'})\alpha_j + 2\sum_{r=1}^{k}\sum_{i=1}^{N}b_{jr}c_{ij}(q_r\cdot p_i)\alpha_j - m_j^2\alpha_j\right\} + i\epsilon\right]^n.$$
(4.8)

Let us analyze the first term

$$\sum_{j=1}^{n}\sum_{r=1}^{k}\sum_{r'=1}^{k}b_{jr}b_{jr'}(q_r\cdot q_{r'})\alpha_j = \sum_{r=1}^{k}\sum_{r'=1}^{k}(q_r\cdot q_{r'})\left(\sum_{j=1}^{n}b_{jr}b_{jr'}\alpha_j\right) = \sum_{r=1}^{k}\sum_{r'=1}^{k}(q_r\cdot q_{r'})D_{rr}, \quad (4.9)$$

with $D_{rr'} = \sum_j \alpha_j b_{jr}b_{jr'}$ being a diagonalizable symmetric $k \times k$ matrix. Once the diagonalization is performed, one can rewrite

$$\sum_{r,r'}q_r\cdot q_{r'}D_{rr'} = \sum_r d_r q_r^2, \tag{4.10}$$

where d_r is the set of eigenvalues corresponding to $D_{rr'}$. The denominator turns into

$$\left[\sum_{j=1}^{n}(l_j^2 - m_j^2 + i\epsilon)\alpha_j\right]^n = \left[\sum_{r=1}^{k}d_r q_r^2 + 2\sum_{r=1}^{k}\sum_{i=1}^{N}B_{ri}(q_r\cdot p_i) + \sum_{i=1}^{N}\sum_{i'=1}^{N}C_{ii'}(p_i\cdot p_{i'}) - \sum_{j=1}^{n}m_j^2\alpha_j + i\epsilon\right]^n,$$
(4.11)

where $B_{ri} = \sum_j \alpha_j \, b_{jr}c_{ji}$ and $C_{ii'} = \sum_j \alpha_j \, c_{ji}c_{ji'}$. We clearly see the dependence on quadratic and linear terms in q_r. In order to eliminate the linear dependence we use the following shift

$$\tilde{q}_r = q_r + \frac{1}{d_r}\sum_{i=1}^{N}B_{ri}p_i, \tag{4.12}$$

we get

$$\left[\sum_{j=1}^{n}(l_j^2 - m_j^2 + i\epsilon)\alpha_j\right]^n = \left[\sum_{r=1}^{k}d_r\tilde{q}_r^2 + F(n, N, \alpha_j, p_i) + i\epsilon\right]^n, \tag{4.13}$$

with $F(n, N, \alpha_j, p_i)$ defined as

$$F(n, N, \alpha_j, p_i) = -\sum_{j=1}^{n}m_j^2\alpha_j + \sum_{i=1}^{N}\sum_{i'=1}^{N}E_{ii'}(p_i\cdot p_i'), \tag{4.14}$$

and $E_{ii'} = C_{ii'} - \sum_{r=1}^{k} \frac{1}{d_r} B_{ri} B_{ri'}$. Once eliminated the linear dependence in $\tilde{q}_r$, one can carry out the set of integrations in $\tilde{q}_r$ using the well known formula

$$\int d\tilde{q}_r \frac{1}{(d_r \tilde{q}_r^2 + A_r + i\epsilon)^n} = \frac{i\pi^2}{(n-1)(n-2)d_r^2 (A_r + i\epsilon)^{n-2}}, \tag{4.15}$$

the result is

$$\int \prod_{r=1}^{k} d\tilde{q}_r \frac{1}{\left[\sum_{r=1}^{k} d_r \tilde{q}_r^2 + F(n, N, \alpha_j, p_i) + i\epsilon\right]^n} = \frac{(n-2k-1)!(i\pi^2)^k}{(n-1)! \, U^2(\alpha_j)[F(n, N, \alpha_j, p_i) + i\epsilon]^{n-2k}} \tag{4.16}$$

with $U(\alpha_j) = det[D(\alpha_j)] = d_1 d_2 .... d_k$. Therefore, after the cumbersome algebraic steps, the initial Feynman integral Eq. (4.3) takes the following form

$$f_G(p_1, p_2, ..p_N) \propto \delta^{(4)}\left(\sum_{i=1}^{N} p_i\right)(i\pi^2)^k \frac{(n-2k-1)!}{(n-1)! \, U^2(\alpha)} \int_0^1 \prod_{j=1}^{n} d\alpha_j \frac{\delta(1 - \sum_j^n \alpha_j)}{[F(n, N, \alpha_j, p_i) + i\epsilon]^{n-2k}}. \tag{4.17}$$

Let us consider again the function $F(n, N, \alpha_j, p_i)$ in the following form

$$F(n, N, \alpha_j, p_i) = -\sum_{j=1}^{n} m_j^2 \alpha_j + \sum_{i=1}^{N} \sum_{i'=1}^{N} E_{ii'}(p_i \cdot p_{i'})$$

$$= -\sum_{j=1}^{n} m_j^2 \alpha_j + \sum_{h} \eta_h s_h \tag{4.18}$$

$$F(n, N, \alpha_j, s_h) = -\beta \left\{ \frac{1}{\beta} \sum_{j=1}^{n} \alpha_j \, m_j^2 - \sum_{h} \frac{\eta_h}{\beta} \, s_h \right\},$$

with $\{s_h\}$ the set of all independent invariants that can be constructed with N external momentum. $\eta_h \geq 0$ (see Ref. [5]) and $\beta \doteq \sum_h \eta_h$. It is clear that the relevance dependence of the Feynman integral appears in the denominator, i.e. the number of loops and the internal masses m_j. The Nakanishi's idea is to move this dependence to the numerator. For this purpose we rewrite Eq. (4.17) as follows

$$f_G(s) \propto \prod_{j=1}^{n} \int d\alpha_j \frac{\delta(1 - \sum_{j=1}^{n} \alpha_j)}{U^2(\alpha_j)(-\beta)^{n-2k}} \prod_h \int_0^1 dz_h \delta\left(z_h - \frac{\eta_h}{\beta}\right)$$

$$\times \int_0^\infty d\chi \, \delta\left(\chi - \sum_l \frac{\alpha_l m_l^2}{\beta}\right) \frac{1}{[\chi - \sum_h z_h s_h + i\epsilon]^{n-2k}}. \tag{4.19}$$

The Feynman integral can be written as

$$f_G(s) \propto \prod_h \int_0^1 dz_h \delta\left(1 - \sum_h z_h\right) \int_0^\infty d\chi \frac{\phi_G(z, \chi)}{[\chi - \sum_h z_h s_h + i\epsilon]^{n-2k}}, \tag{4.20}$$

with

$$\phi_G(z, \chi)\delta\left(1 - \sum_h z_h\right) \equiv \text{const} \prod_{j=1}^{n} \int d\alpha_j \frac{\delta(1 - \sum_{j=1}^{n} \alpha_j)}{U^2(\alpha_j)(-\beta)^{n-2k}} \tag{4.21}$$

$$\times \delta\left(z_h - \frac{\eta_h}{\beta}\right) \delta\left(\chi - \sum_l \frac{\alpha_l m_l^2}{\beta}\right) \delta\left(1 - \sum_h z_h\right), \tag{4.22}$$

where the constraint $\sum_h z_h = 1$ has been added and $\phi_G(z, \chi, \alpha_j)$ is called the *weight-function*. The information about the n internal propagators and k loops is contained in this function. The final step to be performed for implementing the Nakanishi's idea, is to remove the dependence on n and k from the denominator. This can be achieved by integrating by parts the expression Eq. (4.20), thus one has

$$\int_0^\infty d\chi \frac{\phi_G(z, \chi)}{[\chi - \sum_h z_h s_h + i\epsilon]^{n-2k}} =$$

$$-\frac{1}{(n - 2k + 1)} \frac{\phi_G(z, \chi)}{[\chi - \sum_h z_h s_h + i\epsilon]^{n-2k-1}}\bigg|_0^\infty + \frac{1}{(n - 2k + 1)} \int_0^\infty d\chi \frac{\partial \phi_G}{\partial \chi} \frac{1}{[\chi - \sum_h z_h s_h + i\epsilon]^{n-2k-1}}, \tag{4.23}$$

the boundary terms vanish given the dependence of the weight-function in χ as $\delta\left(\chi - \sum_l \frac{\alpha_l m_l^2}{\beta}\right)$. Applying this integration $n - 2k - 1$ times, the result is:

$$\int_0^\infty d\chi \frac{\phi_G(z, \chi)}{[\chi - \sum_h z_h s_h - i\epsilon]^{n-2k}} = \frac{1}{(n - 2k - 1)!} \int_0^\infty d\chi \frac{1}{[\chi - \sum_h z_h s_h - i\epsilon]} \frac{\partial^{n-2k-1} \phi_G(z, \chi)}{\partial \chi^{n-2k-1}},$$

the equation Eq. (4.20) turns into

$$f_G(s) \propto \prod_h \int_0^1 dz_h \; \delta \left(1 - \sum_h z_h\right) \int_0^\infty d\chi \; \frac{\tilde{\phi}_G(z,\chi)}{[\chi - \sum_h z_h s_h - i\epsilon]}, \tag{4.24}$$

where the weight-function has been redefined according to

$$\tilde{\phi}_G(z,\chi) = \frac{1}{(n-2k-1)!} \frac{\partial^{n-2k-1}\phi_G(z,\chi)}{\partial\chi^{n-2k-1}}. \tag{4.25}$$

Once the same steps described above are repeated for each pair (n,k), i.e. for all the diagrams G contributing to the transition amplitude with N external legs, one can obtain the integral representation for the transition amplitude

$$\boxed{f_N(s) = \prod_h \int_0^1 dz_h \delta(1 - \sum_h z_h) \int_0^\infty d\chi \frac{\phi_N(z,\chi)}{(\chi - \sum_h z_h s_h - i\epsilon)},} \tag{4.26}$$

where

$$\phi_N(z,\chi) = \sum_G \mathcal{N}_G \; \tilde{\phi}_G(z,\chi)$$

with $\mathcal{N}_G$ a proper factor. In view of the further applications, we emphasize the following points:

- The expression of the N-leg transition amplitude Eq. (4.26), has been certainly obtained within a perturbative framework, but summing up all the infinite, possible contributions, due to the introduction of an unknown weight-function, $\phi_N(z,\chi)$.

- The weight-function, $\phi_N(z,\chi)$ depends upon real variables: i) the set of compact variables z_h and ii) the non-compact one χ.

- The amplitude depends only on the independent invariants that can be built by the external four-momenta.

- The overall structure in the analytic plane is explicitly given, and contained in the denominator. This is a fundamental feature that will be fully exploited in the application to the BS equation.

4.2   Nakanishi representation for the vertex function

We perform explicitly the calculation for the case of three external legs, which is the main point in our analysis since it represents the vertex function related with the BS amplitude as explained below. For $N = 3$ one has

$$f_3(s) = \int_0^1 dz_1 \int_0^1 dz_2 \int_0^1 dz_3 \, \delta(1 - z_1 - z_2 - z_3) \int_0^\infty d\chi \frac{\phi_3(z_1, z_2, z_3, \chi)}{\chi - z_1 s_1 - z_2 s_2 - z_3 s_3 - i\epsilon},$$

we carry out the integration in z_3, which is trivially done by using the delta function. We obtain

$$\begin{aligned}
f_3(s) &= \int_0^1 dz_1 \int_0^1 dz_2 \int_0^\infty d\chi \frac{\phi_3(z_1, z_2, \chi)\theta\left(1 - z_1 - z_2\right)\theta\left(z_1 + z_2\right)}{\chi - z_1 s_1 - z_2 s_2 - (1 - z_1 - z_2)s_3 - i\epsilon} \\
&= \int_0^1 dz_1 \int_0^1 dz_2 \int_0^\infty \frac{d\chi}{(z_1 + z_2)} \frac{\phi_3(z_1, z_2, \chi)\theta\left(1 - z_1 - z_2\right)\theta\left(z_1 + z_2\right)}{\left[\frac{\chi}{z_1+z_2} - \frac{(1-z_1-z_2)}{z_1+z_2}s_3 - \frac{z_1}{z_1+z_2}s_1 - \frac{z_2}{z_1+z_2}s_2 - i\epsilon\right]},
\end{aligned} \tag{4.27}$$

the theta functions accounts for the constrains $1 - z_1 - z_2 > 0$ and $1 - z_1 - z_2 < 1$ introduced by integrating in z_3. Now, by considering the next change of variable

$$\gamma = \frac{\chi}{z_1 + z_2} - \frac{(1 - z_1 - z_2)}{z_1 + z_2}s_3, \tag{4.28}$$

we get

$$f_3(s) = \int_0^1 dz_1 \int_0^1 dz_2 \int_{\gamma_0}^\infty d\gamma \, \frac{\phi_3(z_1, z_2, \gamma)\theta\left(1 - z_1 - z_2\right)\theta\left(z_1 + z_2\right)}{\left[\gamma - \frac{z_1}{z_1+z_2}s_1 - \frac{z_2}{z_1+z_2}s_2 - i\epsilon\right]},$$

with the negative lower limit

$$\gamma_0 = -(1 - z_1 - z_2)\frac{s_3}{(z_1 + z_2)}. \tag{4.29}$$

In order to eliminate the dependence in one of the variables, we perform the following change of variables

$$\begin{cases} \zeta = \frac{z_1}{z_1+z_2}, \\ \\ y = z_1 + z_2, \end{cases} \tag{4.30}$$

once computed the Jacobian of this transformation one has: $dz_1 dz_2 = y \, d\zeta dy$. The f_3 transforms into

$$f_3(s) = \int_0^1 d\zeta \int_0^1 dy \int_{\gamma_0}^\infty d\gamma \frac{y \, \phi_3(z, y, \gamma)\theta(y)\theta(1-y)}{[\gamma - \zeta s_1 - (1-\zeta)s_2 - i\epsilon]}, \tag{4.31}$$

with

$$\gamma_0 = -\frac{1-y}{y} s_3, \tag{4.32}$$

we can redefined the weight-function as follows once the dependence in y has been removed from the denominator

$$g_3(\zeta, \gamma) = \int_0^1 dy \, y \phi_3(\zeta, y, \gamma)\theta(y)\theta(1-y)\theta\left[\gamma + \frac{(1-y)}{y} s_3\right], \tag{4.33}$$

the additional theta function is introduced to extend the interval of γ to $[-\infty, \infty]$. Finally, we obtain

$$f_3(s) = \int_0^1 d\zeta \int_{-\infty}^\infty d\gamma \frac{g_3(\zeta, \gamma)}{[\gamma - \zeta s_1 - (1-\zeta)s_2 - i\epsilon]}. \tag{4.34}$$

For the vertex function we have $p = p_1 + p_2$, therefore we can choose as independent invariants p_1^2 and p_2^2, which written in terms the global and relative coordinates reads as

$$\begin{aligned}
p_1 &= \frac{p}{2} - k & p_1^2 &= \frac{M^2}{4} + k^2 - p \cdot k, \\
p_2 &= \frac{p}{2} + k & p_2^2 &= \frac{M^2}{4} + k^2 + p \cdot k,
\end{aligned} \tag{4.35}$$

introducing the above invariants into Eq. (4.34) we obtain

$$f_3(s) = \int_0^1 d\zeta \int_{-\infty}^\infty d\gamma \frac{g_3(\zeta, \gamma)}{[\gamma - \frac{M^2}{4} - k^2 - (1-2\zeta)(p \cdot k) - i\epsilon]}, \tag{4.36}$$

additional we can define the variable $z = 1 - 2\zeta$, thus one obtains the expression for the vertex function widely used [5, 13, 14]:

$$\Gamma(k, p) = \int_{-1}^1 dz \int_{-\infty}^\infty d\gamma \frac{g_3^{(n)}(z, \gamma)}{[\gamma - \frac{M^2}{4} - k^2 - z(p \cdot k) - i\epsilon]^n}, \tag{4.37}$$

we have used the common notation for the vertex function: $\Gamma = f_3(s)$ and we have also introduced the non-negative integer dummy parameter n in the NIR. To justify the denominator of dummy parameter, one can perform a integration by parts upon γ' of Eq. (4.37)

$$-i \int_{-\infty}^{\infty} d\gamma' \int_{-1}^{1} dz \frac{g_3^{(n)}(z,\gamma')}{[\gamma' - \frac{M^2}{4} - k^2 - z(p \cdot k) - i\epsilon]^n} =$$
$$(n)(-i) \int_{-\infty}^{\infty} d\gamma' \int_{-1}^{1} dz \frac{\left[\int_{-\infty}^{\gamma'} d\gamma'' g_3^{(n)}(z,\gamma'')\right]}{\left[\gamma' - \frac{M^2}{4} - k^2 - z(p \cdot k) - i\epsilon\right]^{n+1}},$$

(4.38)

and comparing with

$$\Gamma(k,p) = \int_{-1}^{1} dz \int_{-\infty}^{\infty} d\gamma' \frac{g_3^{(n+1)}(z,\gamma')}{[\gamma' - \frac{M^2}{4} - k^2 - z(p \cdot k) - i\epsilon]^{n+1}},$$

(4.39)

one realizes that the Nakanishi weight-function for different n are related as

$$g_3^{(n+1)}(\gamma',z) = n \int_{-\infty}^{\gamma'} g_3^{(n)}(\gamma'',z) \, d\gamma''$$

(4.40)

Despite that the choice of n is arbitrary, this parameter can be chosen adequately to take advantage in the numerical calculation.

As explained before, throughout of this analysis we deal with the integral equation of the BS amplitude for describing the bound state of two particles. For this reason, we write the BS amplitude in terms of the NIR, which can be obtained from the vertex function Eq. (4.37). We recall the relation between the BS amplitude and the vertex function $\varphi = (G_1)(i\Gamma)(G_2)$, where G_i stands for the free propagators, since that in this analysis we are disregarding the self-energy contributions. The expression for the BS amplitude reads

$$\varphi(k,p) = \frac{i}{(\frac{p}{2} - k)^2 - m^2 - i\epsilon} \left[i \int_{-1}^{1} dz \int_{-\infty}^{\infty} d\gamma \frac{g_3(z,\gamma)}{[\gamma - \frac{M^2}{4} - k^2 - z(p \cdot k) - i\epsilon]^n}\right] \frac{i}{(\frac{p}{2} + k)^2 - m^2 - i\epsilon}.$$

(4.41)

Now, we can put together the three denominators using the Feynman parametrization. The procedure is shown below: i) we put together the two free-propagators using the symmetric Feynman parametrization

$$G_1(k,p)G_2(k,p) = \frac{1}{2}\int_{-1}^{1}\frac{d\eta}{[m^2 - f(k,p,\eta) - i\epsilon]^2}, \tag{4.42}$$

with $f(p,k,\eta) = \frac{M^2}{4} + k^2 + (p\cdot k)\eta$. ii) we add the Nakanishi denominator with the usual Feynman parametrization

$$\varphi(k,p) = -i\int_{-1}^{1}dz\int_{-\infty}^{\infty}d\gamma\frac{\Gamma(n+2)}{2\Gamma(n)}\int_{-1}^{1}d\eta\int_{0}^{1}dt\frac{(1-t)t^{n-1}g_3(\gamma,z)}{[\gamma t - tm^2 + m^2 - f(p,k,z') - i\epsilon]^{n+2}} \tag{4.43}$$

with $z' = tz + (1-t)\eta$. Considering the domain of t, η and z it is possible to see that $z' \in (-1,1)$. Also, we consider $\gamma' = \gamma t - tm^2$, clearly $\gamma' \in (0,\infty)$. By using these substitutions the BS amplitude becomes

$$\varphi(k,p) = -i\int_{-1}^{1}dz\int_{-\infty}^{\infty}d\gamma'\frac{g(\gamma',z')}{\left[\gamma' + m^2 - \frac{p^2}{4} - k^2 - p\cdot kz' - i\epsilon\right]^{n+2}}. \tag{4.44}$$

The Nakanishi function is also redefined to incorporate the integration in the Feynman parameters η and t

$$g(\gamma',z') = \frac{\Gamma(n+2)}{2\Gamma(n)}\int_{-1}^{1}d\eta\int_{0}^{1}dt(1-t)t^{n-2}g_3(\gamma',z',t,\eta). \tag{4.45}$$

The expression Eq. (4.44) will be the workable *ansatz* for the BS amplitude. The main point will be to investigate if such ansatz will lead to actual solutions of the BS equation.

4.3   Nakanishi representation in 2+1 dimensions

In view of the applications in condensed-matter physics, graphene [22, 23], it is worthy to extend the Nakanishi representation presented in the previous section to other spatial dimensions, in particular 2+1 dimensions. For 2+1 dimension problem we intend to reduce one of the spatial dimensions, in the LF dynamics where we have $x = (x^+, x^-, \mathbf{x}_\perp)$ with $\mathbf{x}_\perp = (x^1, x^2)$, we neglect one of the perpendicular coordinates. Thus, mostly of the formalism used in $3 + 1$ dimensions remains unchanged.

In general, for d-dimension the analogous Feynman integral Eq. (4.3) reads as

$$f_G^{(d)}(p_1, p_2, ..p_n) \propto \int\prod_{r=1}^{k}d^{(d)}q_r\frac{1}{\prod_{j=1}^{n}(l_j^2 - m_j^2 + i\epsilon)}, \tag{4.46}$$

recalling $l_j = \sum_{r=1}^{k} b_{jr} q_r + \sum_{i=1}^{N} c_{ij} p_i$. We can do the same steps as in the case $d = 4$, the Feynman integral becomes

$$f_G^{(d)}(p_1, p_2, ..p_n) = \prod_h \int_0^1 dz_h \delta(1 - \sum_h z_h) \int_0^\infty d\chi \frac{\phi_G^{(d)}(z, \chi)}{[\chi - \sum_h z_h s_h + i\epsilon]^{n - \frac{d}{2}k}}. \tag{4.47}$$

According to Nakanishi's idea of removing the dependence in the number of loops and the internal propagators from the denominator, one should perform partial integration. However, differently from the case with $d = 4$, where the partial integration removes that dependence, when dealing with other dimensions the exponent of the denominator is no longer integer and the partial integration will not eliminate the dependence in n and k. However, we can treat the difficulty of the non-integer exponent. We restrict to the case $N = 3$ (vertex function) in $2 + 1$ dimensions with the restriction $n - \frac{d}{2}k > 0$. Consider the integral

$$\frac{2}{\sqrt{\pi}} \frac{\Gamma\left(n - \frac{d.k}{2} + \frac{1}{2}\right)}{\Gamma\left(n - \frac{d.k}{2}\right)} \int_0^\infty \frac{d\Lambda}{(\Lambda^2 + C)^{\frac{2n - d.k + 1}{2}}} = \frac{1}{(C)^{n - \frac{d.k}{2}}}, \tag{4.48}$$

in the case when the product $d.k$ is an odd number, the exponent in the right-hand side of Eq. (4.48) is fractionary. The corresponding exponent in the right-hand side before perform the integration is integer number. In this form the problem of the fracionary exponent can be avoided if we take $C = \chi - \sum_h z_h s_h + i\epsilon$ in Eq. (4.47). The NIR in 2+1 dimensions reads as

$$f_G^{(d)}(p_1, p_2, ..p_n) = \prod_h \int_0^1 dz_h \delta(1 - \sum_h z_h)$$
$$\times \frac{2}{\sqrt{\pi}} \frac{\Gamma\left(n - \frac{d.k}{2} + \frac{1}{2}\right)}{\Gamma\left(n - \frac{d.k}{2}\right)} \int_0^\infty d\chi \int_0^\infty d\Lambda \frac{\phi_G^{(d)}(z, \chi)}{[\Lambda^2 + \chi - \sum_h z_h s_h + i\epsilon]^{n - \frac{d}{2}k}}. \tag{4.49}$$

We can perform the shift $\chi \to \chi + \Lambda^2$ and we obtain

$$f_G^{(d)}(p_1, p_2, ..p_n) = \prod_h \int_0^1 dz_h \delta(1 - \sum_h z_h) \int_0^\infty d\chi \frac{\varphi_G^{(d)}(z, \chi)}{[\chi - \sum_h z_h s_h + i\epsilon]^{\frac{2n - d.k + 1}{2}}}, \tag{4.50}$$

the integration in Λ is absorbed by the Nakanishi weigh-function

$$\varphi_G^{d}(z, \chi) = \frac{2}{\sqrt{\pi}} \frac{\Gamma\left(n - \frac{d.k}{2} + \frac{1}{2}\right)}{\Gamma\left(n - \frac{d.k}{2}\right)} \int_0^\infty d\Lambda \, \phi_G^{(d)}(z, \chi - \Lambda^2). \tag{4.51}$$

Having removed the fractionary exponent in Eq. (4.50) the steps to obtain the expression final of the NIR are the same as we have done for 3+1 dimensions.

4.3.1 An alternative derivation

We provide an alternative way of obtaining the NIR in 2+1 dimensions, this relies on the projection of the NIR in 3+1 dimension to 2+1 dimensions. Therefore, it is more restricted than the derivation presented in the preceding section.

As starting point consider the Nakanishi representation for three external legs in 3+1 dimensions Eq. (4.44)

$$\varphi(k,p) = -i \int_{-1}^{1} dz' \int_{-\infty}^{\infty} d\gamma \frac{g(\gamma',z')}{\left[\gamma' + m^2 - \frac{p^2}{4} - k^2 - p \cdot k z' - i\epsilon\right]^{n+2}}.$$

To prove that the NIR is valid also in 2+1 dimensions, one performs the following integration to both sides

$$\tilde{\varphi}(k,p) = \int_{-\infty}^{\infty} dk_2 \int_{-\infty}^{\infty} dp_2 \, \varphi(k,p), \tag{4.52}$$

this integration leads to amplitude with one of the spatial coordinates equal to zero. In LF dynamics with $x = (x^+, x^-, \mathbf{x}_\perp)$ and $\mathbf{x}_\perp = (x^1, x^2)$, we can set one of the perpendicular coordinates equal to zero: $x^2 = 0$.

In the first integration over p_2, we write the integral in the following form

$$\int_{-\infty}^{\infty} dp_2 \, \varphi(k,p) = (-i) \int d\gamma' dz' \int_{-\infty}^{\infty} \frac{dp_2}{(k_2 z')^{n+2}} \frac{g(\gamma',z')}{\left[p_2 - \left\{\frac{(-\gamma'-\kappa^2+k^2)}{k_2 z'} + \frac{(p_0 k_0 - p_1 k_1 - p_3 k_3)z'}{k_2 z'} + \frac{i\epsilon}{k_2 z'}\right\}\right]^{n+2}}$$

$$= (-i) \int d\gamma' dz' \int_{-\infty}^{\infty} \frac{dp_2}{z'^{n+2} k_2 (k_2)^{n+1}}$$

$$\times \frac{g(\gamma',z')}{\left[p_2 - \left\{\frac{(-\gamma'-\kappa^2+k^2)}{k_2 z'} + \frac{(p_0 k_0 - p_1 k_1 - p_3 k_3)z'}{k_2 z'} + \frac{i\epsilon}{k_2 z'}\right\}\right]\left[p_2 - \left\{\frac{(-\gamma'-\kappa^2+k^2)}{k_2 z'} + \frac{(p_0 k_0 - p_1 k_1 - p_3 k_3)z'}{k_2 z'} + \frac{i\epsilon}{k_2 z'}\right\}\right]^{n+1}}, \tag{4.53}$$

in order to evaluate this integral by the Cauchy's residue theorem, we add a quantity $\Delta^+ > 0$ to k_2, in such a way that the poles in Eq. (4.53) are moved toward the upper and lower complex plane. Hence, the evaluation of the integral does not vanish. At the end of the calculation we take the limit $\Delta^+ \to 0$

$$
\int_{-\infty}^{\infty} dp_2 \varphi(k,p) = lim_{\Delta^+ \to 0}(-i) \int d\gamma' dz' \int_{-\infty}^{\infty} \frac{dp_2}{z'^{n+2}(k_2 + \Delta^+)(k_2)^{n+1}} \times
$$

$$
\frac{g(\gamma', z')}{\left[p_2 - \left\{\frac{(-\gamma' - \kappa^2 + k^2)}{(k_2 + \Delta^+)z'} + \frac{(p_0 k_0 - p_1 k_1 - p_3 k_3)z'}{(k_2 + \Delta^+)z'} + \frac{i\epsilon}{(k_2 + \Delta^+)z'}\right\}\right]\left[p_2 - \left\{\frac{(-\gamma' - \kappa^2 + k^2)}{k_2 z'} + \frac{(p_0 k_0 - p_1 k_1 - p_3 k_3)z'}{k_2 z'} + \frac{i\epsilon}{k_2 z'}\right\}\right]^{n+1}}.
$$

$$(4.54)$$

Now, we impose the conditions: $k_2 z' < 0$ and $(\Delta^+ + k_2)z' > 0$, and we choose to close the path in the upper half complex plane. In this way, one gets rid of the evaluation of the $(n+1)$ order pole. We have

$$
\int_{-\infty}^{\infty} dp_2 \varphi(k,p) = lim_{\Delta^+ \to 0}(-i) \int d\gamma' dz'
$$

$$
2\pi i \frac{(z'\Delta^+ + z'k_2)^n}{z'^{n+1}} \frac{\theta(-z'k_2)\theta[z'(\Delta^+ + k_2)]}{(-\Delta^+)^{n+1}} \frac{g(\gamma', z')}{[-\gamma' - \kappa^2 + k^2 + (p_0 k_0 - p_1 k_1 - p_2 k_3)z' + i\epsilon]^{n+1}}.
$$

$$(4.55)$$

Finally, to take the limit $\Delta^+ \to 0$, one has to concern with the integral

$$
\int_{-\infty}^{\infty} dx \, \theta(x)\theta(z'\Delta^+ - x)\frac{1}{z'^{n+1}}\frac{(-x + z'\Delta^+)^n}{(-\Delta^+)^{n+1}} = \int_0^{z'\Delta^+} dx \frac{1}{z'^{n+1}}\frac{(-x + z'\Delta^+)^n}{(-\Delta^+)^{n+1}},
$$

$$(4.56)$$

where we have defined $x = -z'k_2$ and in the last step the theta functions have been used to restrict the interval of integration. It is convenient to make the substitution $y = x/\Delta^+$ to perform the integration

$$
\int_0^{z'\Delta^+} dx \frac{1}{z'^{n+1}}\frac{(-x + z'\Delta^+)^n}{(-\Delta^+)^{n+1}} = \frac{(-1)^{n+1}}{z'^{n+1}}\int_0^{z'} dy(z' - y)^n = \frac{-(-1)^{n+1}}{(n+1)}.
$$

$$(4.57)$$

Because of the theta functions in the integral, $z'k_2$ is restricted as: $-z'\Delta^+ < z'k_2 < 0$, therefore in the limit $\Delta^+ \to 0$ one has $\delta(k_2)$. The result of the integration reads as

$$
\int_{-\infty}^{\infty} dp_2 \varphi(k,p) = 2\pi i \frac{-(-1)^{n+1}(-i)}{(n+1)} \int d\gamma' dz' \frac{g(\gamma', z')\delta(k_2)}{[-\gamma' - \kappa^2 + k^2 + (p_0 k_0 - p_1 k_1 - p_3 k_3)z' + i\epsilon]^{n+1}}.
$$

$$(4.58)$$

The integration over k_2 is trivially done by using the delta function. One gets

$$\tilde{\varphi}(k,p) = \int_{-\infty}^{\infty} dk_2 \int_{-\infty}^{\infty} dp_2 \varphi(k,p)$$

$$= \frac{-2\pi}{(n+1)} \int d\gamma' dz' \frac{g(\gamma', z')}{[\gamma' + \kappa^2 - (k_0^2 - k_1^2 - k_3^2) - (p_0 k_0 - p_1 k_1 - p_3 k_3)z' - i\epsilon]^{n+1}}. \tag{4.59}$$

Therefore, the NIR is valid in 2+1 dimensions as we can appreciate from Eq. (4.59). We rewrite the NIR as follows

$$\tilde{\varphi}(k,p) = \int d\gamma' dz' \frac{\tilde{g}(\gamma', z')}{[\gamma' + \kappa^2 - k^2 - (p \cdot k)z' - i\epsilon]^{n+1}}, \tag{4.60}$$

where we have redefined the Nakanishi weight-function as $\tilde{g}(\gamma', z') = \frac{-2\pi}{(n+1)} g(\gamma', z')$. Note that the exponent of the denominator has changed from $n+2$ to $n+1$. However, as it was mentioned before n is a dummy parameter which can be chosen freely with the only restriction being positive.

Chapter 5

Integral equation for the Nakanishi weight-function

In this chapter, a general integral equation for Nakanishi weight-function will be derived, which should be valid for any irreducible Feynman diagram. This equation is obtained within a *non-explicitly-covariant LF framework* (see Ref. [11]) and using the NIR for the BS amplitude. In particular, the contribution of the ladder and crossed-ladder diagrams to the irreducible kernel of the BS equation and consequently to the Nakanishi kernel is analyzed. It should be pointed out that ladder and cross-ladder contribution to the Nakanishi kernel within an explicitly-covariant LF framework was already derived in Ref. [8, 15]. For a detailed explanation in this approach see Ref. [10].

As we have seen in Sec. 3.42, the LF projection of the BS amplitude allows to extract the valence wave function, this fact in turn leads to well defined integral equation for the LFWF Eq. (3.42)

$$\psi(\xi, \mathbf{k}_\perp) = \frac{p^+}{\sqrt{2}} \xi(1-\xi) \int_{-\infty}^{\infty} \frac{dk^-}{(2\pi)} \varphi(k, p).$$

The LFWF ψ, as any wave function, has no singularities in its physical domain. Hence, the LF projection can be viewed as an integral transformation of the BS amplitude leading to a non-singular function. This suggests to apply this transformation to the BS equation itself:

$$\int \frac{dk^-}{(2\pi)} \varphi(k, p) = \int_{-\infty}^{\infty} \frac{dk^-}{(2\pi)} G_1(k, p) G_2(k, p) \int \frac{d^4 k'}{(2\pi)^4} i K(k, k', p) \varphi(k', p), \qquad (5.1)$$

this transformation should provide an equivalent integral equation to the initial BS equation

but free of singularities. For obtaining an integral equation for ψ, it requires to invert the LF projection Eq. (3.42) in order to have explicitly ψ in the right-hand side of Eq. (5.1), as it has been done in Ref. [8]. Instead in this analysis, we use the *ansatz* for the BS amplitude in terms of the NIR introduced in the previous section Eq. (4.44), to obtain an integral equation for the Nakanishi weight-function. The steps are sketched below, we start recalling the NIR for the BS amplitude:

$$\varphi(k,p) = -i \int_{-1}^{1} dz' \int_{0}^{\infty} d\gamma' \frac{g(\gamma',z')}{\left[\gamma' + m^2 - \frac{p^2}{4} - k^2 - p \cdot kz' - i\epsilon\right]^3}, \tag{5.2}$$

where we have chosen the minimal value of the dummy parameter, i.e, $n = 1$. A larger value of n results into smoother solution. Note that the range of γ' has been shrunk respect to that used in Eq. (4.44). It is allowed since the support properties of $g(\gamma',z')$ when studying the bound state. The support of the Nakanishi weight-function has been widely discussed in Refs. [5, 6, 16]. In particular in Ref. [16], they have studied the scattering process of two-scalar bosons of the same mass exchanging another scalar boson in ladder approximation. For that study, it is considered the inhomogeneous BS equation and the NIR is adopted for the inhomogeneous BS amplitude. Starting with the open interval $\gamma' \in (-\infty, \infty)$, by analyzing the transition between scattering and bound state, which is accomplished by considering $\left(m^2 - \frac{M^2}{4}\right) \to 0_-$, where m is the mass of the constituent particles and M is the mass of the composite system, the range of γ' is reduced to (0,∞) in this limit. Therefore, to study the bound state problem where $\left(m^2 - \frac{M^2}{4}\right) > 0$ one has to concern with the NIR as written in Eq. (5.2).

Now, we perform explicitly the integral transformation in the BS equation Eq. (5.1) by using the NIR for the BS amplitude Eq. (5.2). In the left-hand side one has:

$$\int_{-\infty}^{\infty} \frac{dk^-}{(2\pi)} \varphi(k,p) = -i \int_{-\infty}^{\infty} \frac{dk^-}{(2\pi)} \int_{-1}^{1} dz' \int_{0}^{\infty} d\gamma' \frac{g(\gamma',z')}{\left[\gamma' + m^2 - \frac{p^2}{4} - k^2 - p \cdot kz' - i\epsilon\right]^3}. \tag{5.3}$$

To perform the integration in k^-, we have to express the Nakanishi denominator in terms of the LF variables introduced in Chapter. 3, viz

$$p^2 = p^+p^- - \mathbf{p}_\perp^2 \qquad k^2 = k^+k^- - \mathbf{k}_\perp^2 \qquad p \cdot k = \frac{p^+k^-}{2} + \frac{p^-k^+}{2} - \mathbf{p}_\perp \cdot \mathbf{k}_\perp. \tag{5.4}$$

We can boost the system to the frame $\mathbf{p}_\perp = 0$, what is allowed since the kinematical nature of the boost in the LF dynamics, we obtain

$$\int_{-\infty}^{\infty} \frac{dk^-}{(2\pi)} \varphi(k,p) =$$
$$- i \int_{-\infty}^{\infty} \frac{dk^-}{(2\pi)} \int_{-1}^{1} dz' \int_{0}^{\infty} d\gamma' \frac{g(\gamma',z')}{\left[\gamma' + m^2 + k^- \left(-k^+ - \frac{p^+ z'}{2}\right) - \frac{p^+ p^-}{4} + \mathbf{k}_\perp^2 - \frac{(p^- k^+)}{2} z' - i\epsilon\right]^3},$$
(5.5)

the integration in k^- can be done by using the formula

$$\int_{-\infty}^{\infty} \frac{d\beta}{(\beta x - y - i\epsilon)^3} = \frac{i\pi}{y^2} \delta(x),$$
(5.6)

one obtains

$$\int_{-\infty}^{\infty} \frac{dk^-}{(2\pi)} \varphi(k,p) = \frac{1}{p^+} \int_{-1}^{1} dz' \int_{0}^{\infty} d\gamma' g(z',\gamma') \frac{\delta(z'-z)}{\left[\frac{p^+ p^-}{4} + \frac{(p^- k^+)}{2} z' - \mathbf{k}_\perp^2 - \gamma' - m^2 - i\epsilon\right]^2},$$
(5.7)

with $z = -\frac{2k^+}{p^+} = 1 - 2\xi$. The last relation can be obtained by writing the momentum of each particles in terms of relative momentums and ξ, namely

$$\xi = \frac{p_1^+}{p^+} = \frac{1}{2} + \frac{k^+}{p^+} \qquad (1 - \xi) = \frac{p_2^+}{p^+} = \frac{1}{2} - \frac{k^+}{p^+}.$$
(5.8)

The integration in z' can be trivially done using the delta function

$$\int_{-\infty}^{\infty} \frac{dk^-}{(2\pi)} \varphi(k,p) = \frac{1}{p^+} \int_{0}^{\infty} d\gamma' \frac{g(\gamma',z)}{\left[\gamma' + \gamma + m^2 - (1 - z^2)\frac{M^2}{4}\right]^2},$$
(5.9)

we have defined $\gamma = \mathbf{k}_\perp^2$. Note that the term $i\epsilon$ has been dropped out since that the denominator is always positive for bound states. It is convenient to introduce the quantity κ defined as

$$\kappa^2 = m^2 - \frac{M^2}{4},$$
(5.10)

which is positive for bound states, hence the dependence of the bound state mass is introduced by means of this parameter. In terms of κ^2, we write Eq. (5.9) as

$$\int_{-\infty}^{\infty} \frac{dk^-}{(2\pi)} \varphi(k,p) = \frac{1}{p^+} \int_0^{\infty} d\gamma' \frac{g(\gamma',z)}{[\gamma' + \gamma + z^2 m^2 + (1-z^2)\kappa^2]^2}. \tag{5.11}$$

Resorting to the LFWF definition obtained from the projection onto the null-plane, we get

$$\psi(z,\gamma) = \frac{(1-z^2)}{4\sqrt{2}} \int_0^{\infty} d\gamma' \frac{g(\gamma',z)}{[\gamma' + \gamma + z^2 m^2 + (1-z^2)\kappa^2]^2}. \tag{5.12}$$

This expression shows the relation between the Nakanishi weight-function and the valence LFWF. As it will be showed in the forthcoming sections, the aim is to find numerical solutions for the Nakanishi weight-function, corresponding to the well defined integral equation for a given interaction kernel iK. Once obtained numerically the weight-function, one can easily compute the LFWF by means of Eq. (5.12), since the LF projection has removed the singular behavior in the Nakanishi denominator. Differently, the expression Eq. (4.44) to compute the BS amplitude contains singularities, showing the expected behavior of the BS amplitude in Minkowski space.

Continuing with the aim of formulating an integral equation for the Nakanishi weight-function, we have arranged the left-hand side of Eq. (5.1) in a convenient form. The next step is to analyze the right-hand side, which is clearly is more complicated due to the interaction kernel. We rewrite it as follows

$$\int_{-\infty}^{\infty} \frac{dk^-}{(2\pi)} G_1(k,p) G_2(k,p) \int \frac{d^4 k'}{(2\pi)^4} iK(k,k',p) \varphi(k',p) =$$
$$\int_{-\infty}^{\infty} \frac{dk^-}{(2\pi)} G_1(k,p) G_2(k,p) \int \frac{d^4 k'}{(2\pi)^4} iK(k,k',p)(-i) \int_{-1}^{1} dz' \int_0^{\infty} d\gamma' \frac{g(\gamma',z')}{[\gamma' + \kappa^2 - k'^2 - (p \cdot k')z' - i\epsilon]^3} =$$
$$\int_{-1}^{1} dz' \int_0^{\infty} d\gamma' \left[i \int_{-\infty}^{\infty} \frac{dk^-}{(2\pi)} G_1(k,p) G_2(k,p) \int \frac{d^4 k'}{(2\pi)^4} \frac{iK(k,k',p)}{[k'^2 + (p \cdot k')z' - \gamma' - \kappa^2 + i\epsilon]^3} \right] g(\gamma',z'). \tag{5.13}$$

Equaling the both sides of the BS equation Eq. (5.11) and Eq. (5.13) we have

$$\int_0^{\infty} d\gamma' \frac{g(\gamma',z)}{[\gamma' + \gamma + z^2 m^2 - (1-z^2)\kappa^2]^2} =$$
$$\int_{-1}^{1} dz' \int_0^{\infty} d\gamma' \left[ip^+ \int_{-\infty}^{\infty} \frac{dk^-}{(2\pi)} G_1(k,p) G_2(k,p) \int \frac{d^4 k'}{(2\pi)^4} \frac{iK(k,k',p)}{[k'^2 + (p \cdot k')z' - \gamma' - \kappa^2 + i\epsilon]^3} \right] g(\gamma',z'), \tag{5.14}$$

or in a more compact form

$$\int_0^\infty d\gamma' \frac{g(\gamma', z)}{[\gamma' + \gamma + z^2 m^2 + (1 - z^2)\kappa^2]^2} = \int_{-1}^1 dz' \int_0^\infty d\gamma' \, V(\gamma, z, \gamma', z') g(\gamma', z'), \qquad (5.15)$$

with

$$V(\gamma, z, \gamma', z') = i p^+ \int_{-\infty}^\infty \frac{dk^-}{(2\pi)} G_1(k, p) G_2(k, p) \int \frac{d^4 k'}{(2\pi)^4} \frac{iK(k, k', p)}{[k'^2 + (p \cdot k')z' - \gamma' - \kappa^2 + i\epsilon]^3}. \quad (5.16)$$

We have not worked out the right-hand side, since that its explicit form depends on the chosen interaction kernel. This will be explicitly done in the next sections.

At this point we can trace out the steps to obtain the integral equation Eq. (5.15). The integral equation for the Nakanishi weight-function has been obtained by using the NIR for the vertex function and then multiplying by the free propagators to obtain the corresponding representation for the BS amplitude. After that we perform the exact projection onto the hyperplane $x^+ = 0$, which has lead to a generalized integral equation free of singularities and it is valid for any irreducible kernel. This equation is physically equivalent to the initial BS equation but with the improvement of having removed the singular behavior, what represents a remarkable advantage for the numerical calculation.

The integral equation once arranged in the form Eq. (5.15) can be written in a symbolic form

$$\mathcal{B}(M)g = \mathcal{A}(M, \alpha)g, \qquad (5.17)$$

being $\mathcal{B}(M)$ and $\mathcal{A}(M, \alpha)$ the integral operators acting in the Nakanishi weight-function. α is the coupling constant of the theory, which is contained in the irreducible interaction kernel and M is the mass of the bound state. As one can see this is a generalized eigenvalue problem since the operators appear to both sides of the equation. Therefore, in solving the integral equation one should invert one of the operators in order to get the usual eigenvalue problem. We deal with this issue in the Section. 7.1.

As we mentioned earlier, the NIR has been devised in a perturbative scheme. However, the anzast for the BS amplitude is being used for solving the BS equation, which is an approach of non-perturbative character. Apparently it should be inconsistence however if the equation for

the Nakanishi weight-function admits solutions one can claim that the Nakanishi representation of the BS amplitude is also valid in the non-perturbative regime.

5.1 Ladder kernel in 3+1 dimensions

In this section we will obtain explicitly the Nakanishi kernel corresponding to the ladder kernel. Once obtained analytically the expressions for the kernel, it will be introduced into Eq. (5.15) and then the equation should be solved numerically.

The simplest interaction kernel for the theory with the interaction Lagrangian $\mathcal{L}_{inter} = g\phi^2\chi$ is known as the ladder approximation. This kernel accounts for the exchange of a spinless scalar particle of mass μ between of two spinless scalar particles with the same mass m. In Fig. 5.1, we draw the Feynman graph associated to this contribution

Figure 5.1: Irreducible BS kernel in the ladder approximation.

the expression of the ladder kernel reads as:

$$iK(k, k') = \frac{i(-ig)^2}{(k - k')^2 - \mu^2 + i\epsilon}. \tag{5.18}$$

By introducing the above kernel into Eq. (5.15), the Nakanishi kernel becomes

$$
\begin{aligned}
V_{3+1}^{(L)}(\gamma, z; \gamma', z') = &- g^2 p^+ \int_{-\infty}^{\infty} \frac{dk^-}{2\pi} \frac{1}{[(\frac{p}{2} + k)^2 - m^2 + i\epsilon]} \frac{1}{[(\frac{p}{2} - k)^2 - m^2 + i\epsilon]} \\
&\times \int \frac{dk'}{(2\pi)^4} \frac{1}{[k'^2 + (p \cdot k')z' - \gamma' - \kappa^2 + i\epsilon]^3} \frac{1}{(k - k')^2 - \mu^2 + i\epsilon},
\end{aligned}
\tag{5.19}
$$

To compute the integrations in the above kernel we start by performing the integration in k'. We proceed as usual, putting together the two denominators containing k' by means of the Feynman parametrization

$$\frac{1}{A^3}\frac{1}{B} = \frac{\Gamma(4)}{\Gamma(3)\Gamma(1)}\int_0^1 dv\frac{v^2}{[Av + B(1-v)]^4},$$

being

$$A = k'^2 + (p\cdot k')z' - \gamma' - \kappa^2 + i\epsilon \qquad B = (k-k')^2 - \mu^2 + i\epsilon.$$

The integration in k' is done by means of the formula

$$\int\frac{d^dk}{(2\pi)^d}\frac{1}{(k^2 - m^2 + i\epsilon)^n} = (-1)^{d/2}\frac{i}{(4\pi)^{d/2}}\frac{\Gamma(n-d/2)}{\Gamma(n)}\frac{(-1)^{n-d/2}}{(m^2-i\epsilon)^{n-d/2}}, \qquad (5.20)$$

which for $d = 4$ reads as

$$\int\frac{d^4k}{(2\pi)^4}\frac{1}{(k^2 - (C-i\epsilon))^\alpha} = \frac{i}{(4\pi)^2}\frac{\Gamma(\alpha-2)}{\Gamma(\alpha)}\frac{(-1)^\alpha}{(C-i\epsilon)^{\alpha-2}}. \qquad (5.21)$$

The result of the integration yields

$$\int\frac{dk'}{(2\pi)^4}\frac{1}{[k'^2 + (p\cdot k')z' - \gamma' - \kappa^2 + i\epsilon]^3}\frac{1}{(k-k')^2 - \mu^2 + i\epsilon} = \frac{i}{2(4\pi)^2}\int_0^1 dv\frac{v^2}{[C-i\epsilon]^2}, \qquad (5.22)$$

with

$$C = -\mu^2(v-1) + (\gamma' + \kappa^2 + k^2(v-1))v + (k\cdot p)(v-1)vz' + \frac{p^2}{4}v^2z'^2, \qquad (5.23)$$

and the kernel $V_{3+1}^{(L)}(\gamma, z; \gamma', z')$ reduces to

$$V_{3+1}^{(L)}(\gamma, z; \gamma', z') = -g^2p^+\int_{-\infty}^\infty\frac{dk^-}{(2\pi)}\frac{1}{[(\frac{p}{2}+k)^2 - m^2 + i\epsilon]}\frac{1}{[(\frac{p}{2}-k)^2 - m^2 + i\epsilon]}\frac{i}{2(4\pi)^2}\int_0^1 dv\frac{v^2}{[C-i\epsilon]^2}. \qquad (5.24)$$

Now, we perform the integration in k^- by means of the Cauchy's residuum theorem, since the presence of three poles in the expression. Two of the poles are related with the propagation of the constituents particles and the other with the propagation of the exchange particle. To perform the integration we write the free-propagators and the C function in terms of the LF coordinates

$$\left(\frac{p}{2} \pm k\right)^2 = \left(\frac{p}{2} \pm k\right)^- \left(\frac{p}{2} \pm k\right)^+ - \mathbf{k}_\perp^2$$

$$C = l_D - v(1-v)k^- \frac{M}{2}\left(z' + \frac{2}{M}k^+\right) \tag{5.25}$$

$$l_D = (1-v)v\left(\gamma + \frac{M^2}{4}zz' + \kappa^2\right) + \mu^2(1-v) + \gamma'v + v^2\left(\frac{M^2}{4}z'^2 + \kappa^2\right),$$

we recall that $\mathbf{p}_\perp = 0$ and $p^\pm = M$. The kernel becomes

$$V_{3+1}^{(L)}(\gamma, z; \gamma', z') = -g^2 M \frac{i}{2(4\pi)^2} \frac{1}{(\frac{p}{2}-k)^+} \frac{1}{(\frac{p}{2}+k)^+}$$

$$\times \int_0^1 dv v^2 \int_{-\infty}^\infty \frac{dk^-}{(2\pi)} \frac{1}{\left[(\frac{p}{2}-k)^- - \frac{(\gamma+m^2)}{(\frac{p}{2}-k)^+} + \frac{i\epsilon}{(\frac{p}{2}-k)^+}\right]\left[(\frac{p}{2}+k)^- - \frac{(\gamma+m^2)}{(\frac{p}{2}+k)^+} + \frac{i\epsilon}{(\frac{p}{2}+k)^+}\right]}$$

$$\times \frac{1}{[v(1-v)k^- \frac{M}{2}(z' + \frac{2}{M}k^+) - l_D + i\epsilon]^2}. \tag{5.26}$$

In order to localize the position of the poles of in this integrand, we rearrange the kernel in the following form

$$V_{3+1}^{(L)}(\gamma, z; \gamma', z') = -g^2 M \frac{i}{2(4\pi)^2} \frac{1}{(\frac{p}{2}-k)^+} \frac{1}{(\frac{p}{2}+k)^+}$$

$$\times \int_0^1 dv v^2 \int_{-\infty}^\infty \frac{dk^-}{(2\pi)} \frac{-1}{\left[k^- - \frac{M}{2} + \frac{2}{M}\frac{(\gamma+m^2)}{(1+z)} - \frac{i\epsilon}{(1+z)}\right]\left[k^- + \frac{M}{2} - \frac{2}{M}\frac{(\gamma+m^2)}{(1-z)} + \frac{i\epsilon}{(1-z)}\right]}$$

$$\times \frac{1}{v^2(1-v)^2(z'-z)^2\left(\frac{M}{2}\right)^2} \frac{1}{\left[k^- - k_D + \frac{2i\epsilon}{v(1-v)M(z'-z)}\right]^2}, \tag{5.27}$$

with $k_D = \frac{2l_D}{v(1-v)M(z'-z)}$ and we have used $z = -2\frac{k^+}{M}$. Thus, there are two poles of first order:

- $k^- - \left(\frac{M}{2} - \frac{2}{M}\frac{(\gamma+m^2)}{(1+z)} + \frac{i\epsilon}{(1+z)}\right)$

- $k^- - \left(-\frac{M}{2} + \frac{2}{M}\frac{(\gamma+m^2)}{(1-z)} - \frac{i\epsilon}{(1-z)}\right),$

and one pole of second order due to the factor

$$k^- - \left(k_D - \frac{2i\epsilon}{v(1-v)M(z'-z)}\right). \tag{5.28}$$

The poles of first order have a fixed position in the complex plane, since the factor $(1 \pm z)$ is always positive one pole in the lower complex plane and the other one is in the upper complex plane. Instead, the position of the third order pole is not fixed but it depends on the sign of $(z' - z)$. For evaluating the integral in k^- through the residue theorem, the path of integration can be closed in the upper half-plane as well as in the lower one. Therefore, to avoid the complications of evaluating a second-order pole, one can choose to close the path in the upper complex plane if $z' > z$ and in the lower one if $z' < z$. After that evaluation, one obtains

$$
\begin{aligned}
V_{3+1}^{(L)}(\gamma, z; \gamma', z') = & -g^2 M \frac{i}{2(4\pi)^2} \frac{4(-1)}{M^2(1-z^2)} \frac{(2\pi)i}{(2\pi)} \\
& \times \int_0^1 dv \, v^2 \frac{M}{\left[M^2 - \frac{4(\gamma+m^2)}{(1-z^2)} + i\epsilon\right] \left[\frac{M}{2} - \frac{2}{M}\frac{(\gamma+m^2)}{(1+z)} - k_D + i\epsilon\right]^2} \frac{\theta(z'-z)}{v^2(1-v)^2(z'-z)^2 \left(\frac{M}{2}\right)^2},
\end{aligned}
\tag{5.29}
$$

and

$$
\begin{aligned}
V_{3+1}^{(L)}(\gamma, z; \gamma', z') = & -g^2 M \frac{i}{2(4\pi)^2} \frac{4(-1)}{M^2(1-z^2)} \frac{(2\pi)-i}{(2\pi)} \\
& \times \int_0^1 dv \, v^2 \frac{-M}{\left[M^2 - \frac{4(\gamma+m^2)}{(1-z^2)} + i\epsilon\right] \left[-\frac{M}{2} + \frac{2}{M}\frac{(\gamma+m^2)}{(1-z)} - k_D - i\epsilon\right]^2} \frac{\theta(z-z')}{v^2(1-v)^2(z'-z)^2 \left(\frac{M}{2}\right)^2}.
\end{aligned}
\tag{5.30}
$$

We have kept all the prefactors in order to avoid any confusion. Note the minus sign which appears from the evaluation of the clockwise path. However, this minus sign is canceled with the sign coming from the evaluation of the first-order pole in the lower complex plane. We can put together the both parts of the kernel in the following form:

$$
\begin{aligned}
V_{3+1}^{(L)}(\gamma, z; \gamma', z') = & \frac{g^2}{2(4\pi)^2} \frac{1}{[\gamma + \kappa^2(1-z^2) + m^2 z^2]} \\
& \times \int_0^1 dv \frac{v^2}{v^2(1-v)^2(z'-z)^2 \left(\frac{M}{2}\right)^2} \left\{ \frac{\theta(z'-z)}{\left[\frac{M}{2} - \frac{2}{M}\frac{(\gamma+m^2)}{(1+z)} - k_D + i\epsilon\right]^2} + \frac{\theta(z-z')}{\left[\frac{M}{2} - \frac{2}{M}\frac{(\gamma+m^2)}{(1-z)} + k_D + i\epsilon\right]^2} \right\}.
\end{aligned}
\tag{5.31}
$$

We now write the kernel in a more symmetric form. The last line in the above expression can be written as

$$
\begin{aligned}
V_{3+1}^{(L)}(\gamma, z; \gamma', z') \propto & \int_0^1 dv \, v^2 \\
& \left\{ \frac{\theta(z'-z)}{\left[v(1-v)(z'-z)\left(\frac{M^2}{4} - \frac{(\gamma+m^2)}{(1+z)}\right) - l_D + i\epsilon'\right]^2} + \frac{\theta(z-z')}{\left[v(1-v)(z'-z)\left(\frac{M^2}{4} - \frac{(\gamma+m^2)}{(1-z)}\right) + l_D + i\epsilon'\right]^2} \right\},
\end{aligned}
\tag{5.32}
$$

with $\epsilon' = v(1-v)(z'-z)(\frac{M}{2})\epsilon$

$$V_{3+1}^{(L)}(\gamma, z; \gamma', z') \propto \int_0^1 dv\ v^2 \left\{ \frac{\theta(z'-z)(1+z)^2}{\left[v(1-v)(z'-z)\left(\frac{M^2}{4}(1+z)-(\gamma+m^2)\right)-(1+z)l_D+i(1+z)\epsilon'\right]^2} \right.$$
$$\left. + \frac{\theta(z-z')(1-z)^2}{\left[v(1-v)(z'-z)\left(\frac{M^2}{4}(1-z)-(\gamma+m^2)\right)+(1-z)l_D+i(1-z)\epsilon'\right]^2} \right\}.$$
$$(5.33)$$

By writing the kernel in the above form Eq. (5.33), one can define the following quantity

$$D(v, z, z', \gamma, \gamma') = v(1-v)(z'-z)\left[\frac{M^2}{4}(1+z)-(\gamma+m^2)\right]-(1+z)l_D+i(1+z)\epsilon', \quad (5.34)$$

if we consider the transformation $z \to -z$ and $z' \to -z'$ and taking into account that l_D is invariant under this transformation we can write

$$V_{3+1}^{(L)}(\gamma, z; \gamma', z') = \frac{g^2}{2(4\pi)^2} \frac{1}{[\gamma + \kappa^2(1-z^2)+m^2z^2]}$$
$$\times \int_0^1 dv\ v^2 \left\{ \frac{\theta(z'-z)(1+z)^2}{[D(v,z,z',\gamma,\gamma')]^2} + \frac{\theta(z-z')(1-z)^2}{[D(v,-z,-z',\gamma,\gamma')]^2} \right\},$$
$$(5.35)$$

after some algebraic manipulations, the D function takes the form

$$D(v, z, z', \gamma, \gamma') = -v(1-v)(1+z')\left[\gamma + m^2z^2 + \kappa^2(1-z^2) + \Gamma(v,z,z',\gamma')\right]$$
$$\Gamma(v, z, z', \gamma') = \frac{(1+z)}{(1+z')}\left\{ \frac{\mu^2}{v} + \gamma' + \frac{v}{(1-v)}\left(\frac{M^2}{4}z'^2 + \kappa^2 + \gamma'\right)\right\}.$$
$$(5.36)$$

From the above expression, it is possible to see the regular behavior of the D function and in consequence of the kernel $V_{3+1}^{(L)}(\gamma, z; \gamma', z')$, i.e, the singularities in the initial BS equation have been removed, allowing to drop out the term $i\epsilon$. For the numerical treatment we deal with the kernel in Eq. (5.35), which is introduced in the integral equation for the Nakanishi function Eq. (5.15).

It is important to emphasize the advantage of using the NIR together with the LF projection method. The first attempts for the implementation of the NIR for studying the bound state were carried out by K.Kusaka and A.G. Williams, see Ref. [6, 7]. In those analyses without

using the LF projection, they have obtained the same results as those in Ref. [8, 12] where the LF projection is adopted. However, that technique to handle the singularities was clearly more complicated that the LF projection shown above. In addition, those analyses described in Ref. [6, 7] were restricted to the ladder kernel.

5.2 Uniqueness of the Nakanishi weight-function for the ladder kernel

In this section we describe in shortly the application of the *uniqueness conjecture* of the Nakanishi weight-function, which was presented in the Nakanishi's seminal work [5]. For the ladder kernel in 3+1 dimensions, taking as starting point the integral equation for the Nakanishi weight-function derived in the previous section Eq. (5.15), one can arrange the integral equation in a convenient way to apply the uniqueness theorem. Once applied the uniqueness one obtains another integral equation for the Nakanishi weight-function, which has the form of an usual eigenvalue problem. This equation must provide the same solution that the initial integral equation if the uniqueness holds in the non-perturbative regime. In this thesis we do not perform a numerical analysis of this new integral equation, we only mention it for sake of completeness since that it can be useful for future applications.

Consider the Nakanishi kernel for the ladder case Eq. (5.35)

$$
V_{3+1}^{(L)}(\gamma, z; \gamma', z') = \frac{g^2}{2(4\pi)^2} \frac{1}{[\gamma + \kappa^2(1 - z^2) + m^2 z^2]}
$$
$$
\times \int_0^1 dv \; v^2 \left\{ \frac{\theta(z' - z)(1 + z)^2}{[D(v, z, z', \gamma, \gamma')]^2} + \frac{\theta(z - z')(1 - z)^2}{[D(v, -z, -z', \gamma, \gamma')]^2} \right\},
$$

for the next steps it is convenient to define the denominators

$$
A = \gamma + z^2 m^2 + \kappa^2(1 - z^2) + \Gamma(v, \pm z, \pm z', \gamma')
$$
$$
B = \gamma + z^2 m^2 + \kappa^2(1 - z^2).
$$

$$(5.37)$$

To combine the denominators of the ladder kernel we use the Feynman trick

$$
\frac{1}{BA^2} = \lim_{\lambda \to 0^+} \frac{1}{\lambda} \left[\frac{1}{BA} - \frac{1}{B(A + \lambda)} \right] = \lim_{\lambda \to 0^+} \frac{1}{\lambda} \left\{ \int_0^1 \frac{d\xi}{[B - \xi(B - A)]^2} - \int_0^1 \frac{d\xi}{[B - \xi(B - A) + \xi\lambda]^2} \right\},
$$

$$(5.38)$$

and using the denominators Eq. (5.37) in Eq. (5.38) we obtain

$$\frac{1}{BA^2} = \lim_{\lambda \to 0^+} \frac{1}{\lambda} \left\{ \int_0^1 \frac{d\xi}{[\gamma + z^2 m^2 + \kappa^2 (1 - z^2) + \xi \, \Gamma]^2} - \int_0^1 \frac{d\xi}{[\gamma + z^2 m^2 + \kappa^2 (1 - z^2) + \xi \, \Gamma + \xi \lambda]^2} \right\}.$$
(5.39)

Now if we define

$$\mathcal{H}(\gamma, z; \gamma', z', \mu^2, \lambda) = \frac{(1+z)}{(1+z')} \int_0^1 \frac{dv}{(1-v)^2} \int_0^1 d\xi \int_{-\infty}^\infty d\gamma'' \frac{\delta[\gamma'' - \xi\Gamma(v, \pm z, \pm z', \gamma') - \xi\lambda]}{[\gamma + \gamma'' + z^2 m^2 + \kappa^2 (1 - z^2)]^2},$$
(5.40)

and also

$$\mathcal{H}'(\gamma, z; \gamma', z', \mu^2) = \lim_{\lambda \to 0^+} \frac{1}{\lambda} \left[\mathcal{H}(\gamma, z; \gamma', z', \mu^2, \lambda) - \mathcal{H}(\gamma, z; \gamma', z', \mu^2, 0) \right], \tag{5.41}$$

the kernel is written as

$$V_{3+1}^{(L)}(\gamma, z; \gamma', z') = -\frac{g^2}{2(4\pi)^2} \left[\frac{(1+z)}{(1+z')} \theta(z'-z) \mathcal{H}'(\gamma, z; \gamma', z', \mu^2) + \frac{(1-z)}{(1-z')} \theta(z-z') \mathcal{H}'(\gamma, -z; \gamma', -z', \mu^2) \right].$$
(5.42)

From the definition of Γ in Eq. (5.36), one see that $\Gamma > 0$ because $\gamma' > 0$ and hence $(\Gamma + \lambda) > 0$, we use this fact in the next steps. We perform trivially the integration in ξ using the delta function in Eq. (5.40) in the following form

$$\begin{aligned}
\mathcal{H}(\gamma, z; \gamma', z', \mu^2, \lambda) =& \frac{(1+z)}{(1+z')} \int_0^1 \frac{dv}{(1-v)^2} \int_0^1 d\xi \int_{-\infty}^\infty d\gamma'' \frac{1}{(\Gamma + \lambda)} \frac{\delta\left[\frac{\gamma''}{\Gamma+\lambda} - \xi\right]}{[\gamma + \gamma' + z^2 m^2 + \kappa^2 (1 - z^2)]^2} \\
=& \frac{(1+z)}{(1+z')} \int_0^1 \frac{dv}{(1-v)^2} \int_{-\infty}^\infty d\gamma'' \frac{1}{(\Gamma + \lambda)} \frac{\theta[\Gamma + \lambda - \gamma''] \, \theta[\gamma'']}{[\gamma + \gamma'' + z^2 m^2 + \kappa^2 (1 - z^2)]^2} \\
\mathcal{H}(\gamma, z; \gamma', z', \mu^2, \lambda) =& \int_{-\infty}^\infty d\gamma'' \frac{\theta[\gamma'']}{[\gamma + \gamma'' + z^2 m^2 + \kappa^2 (1 - z^2)]^2} \, h(\gamma'', z; \gamma', z', \mu^2, \lambda),
\end{aligned}$$
(5.43)

the θ functions come from the fact that ξ belongs to the interval [0,1] and $h(\gamma'', z; \gamma', z', \mu^2, \lambda)$ is defined as

$$h(\gamma'', z; \gamma', z', \mu^2, \lambda) = \frac{(1+z)}{(1+z')} \int_0^1 \frac{dv}{(1-v)^2} \frac{\theta[\Gamma + \lambda - \gamma'']}{(\Gamma + \lambda)}. \tag{5.44}$$

The derivative in Eq. (5.42) is done as follows

$$h'(\gamma'', z; \gamma', z', \mu^2) = \frac{\partial h(\gamma'', z; \gamma', z', \mu^2)}{\partial \Gamma} = \frac{(1+z)}{(1+z')} \int_0^1 \frac{dv}{(1-v)} \left\{ \frac{\delta(\Gamma - \gamma'')}{\gamma''} - \frac{\theta[\Gamma - \gamma'']}{\Gamma^2} \right\}. \tag{5.45}$$

After this manipulation in the kernel, the integral equation for the Nakanishi weight-function with the kernel Eq. (5.42) can be written in the following form

$$\int_0^\infty d\gamma' \frac{g(\gamma', z)}{[\gamma' + \gamma + z^2 m^2 + \kappa^2(1 - z^2)]^2} = \int_0^\infty d\gamma' \int_{-1}^1 dz' \frac{-g^2}{2(4\pi)^2}$$
$$\times \left[\frac{(1+z)}{(1+z')} \theta(z' - z) \int_0^\infty d\gamma'' \frac{h'(\gamma'', z; \gamma', z', \mu)}{[\gamma + \gamma'' + z^2 m^2 + \kappa^2(1 - z^2)]^2} \right.$$
$$\left. + \frac{(1-z)}{(1-z')} \theta(z - z') \int_0^\infty d\gamma'' \frac{h'(\gamma'', -z; \gamma', -z', \mu)}{[\gamma + \gamma'' + z^2 m^2 + \kappa^2(1 - z^2)]^2} \right] g(\gamma', z'), \tag{5.46}$$

putting outside the denominator and changing $\gamma' \to \gamma''$, we get

$$\int_0^\infty \frac{d\gamma''}{[\gamma'' + \gamma + z^2 m^2 + (1 - z^2)\kappa^2]^2} \left[g(\gamma'', z) - \frac{g^2}{2(4\pi)^2} \int_0^\infty d\gamma' \int_{-1}^1 dz' g(\gamma', z') \right.$$
$$\left. \times \left\{ \frac{(1+z)}{(1+z')} \theta(z' - z) h'(\gamma'', z; \gamma', z', \mu) + \frac{(1-z)}{(1-z')} \theta(z - z') h'(\gamma'', -z; \gamma', -z', \mu) \right\} \right] = 0, \tag{5.47}$$

if the uniqueness holds we get the following integral equation for the Nakanishi weight-function with the ladder kernel

$$g(\gamma'', z) = \frac{-g^2}{2(4\pi)^2} \int_0^\infty d\gamma' \int_{-1}^1 dz'$$
$$\times \left[\frac{(1+z)}{(1+z')} \theta(z' - z) h'(\gamma'', z; \gamma', z', \mu) + \frac{(1-z)}{(1-z')} \theta(z - z') h'(\gamma'', -z; \gamma', -z', \mu) \right] g(\gamma', z'). \tag{5.48}$$

It is important to note that the kernel in the right-hand is symmetric respect to the transformation $\{z, z'\} \to \{-z, -z'\}$ and it vanishes for values $z = \pm 1$ due to the theta functions. As mentioned before, the equation for the Nakanishi weight-function Eq. (5.48) should provide

the same solutions than the initial one Eq. (5.15) if the uniqueness theorem holds in the non-perturbative regime. In fact as shown numerically in Ref. [12], the eigenvalues provided by these two integral equations are in complete agreement.

5.3 Ladder kernel in 2+1 dimensions

As presented in the Sec. 4.3, the Nakanishi representation can be extended for 2+1 dimensions. Therefore, it allows to carry out a complete analysis of the two-dimensional problem in the relativistic scheme. Also, the BS equation can be formulated in two-spatial dimension without difficulty. The BS equation reads as:

$$\varphi(k,p) = G_1(k,p)G_2(k,p) \int \frac{d^3k'}{(2\pi)^3} iK(k,k',p)\varphi(k,p). \tag{5.49}$$

In complete analogy with the calculation in 3+1 dimensions, the calculation for 2+1 dimensions is obtained taking as starting point the Nakanishi kernel

$$
\begin{aligned}
V_{2+1}^{(L)}(\gamma,z;\gamma',z') &= -g^2 p^+ \int \frac{d^3k'}{(2\pi)^3} \frac{1}{[k'^2 + (p \cdot k')z' - \gamma' - \kappa^2 + i\epsilon]^3} \\
&\times \int_{-\infty}^{\infty} \frac{dk^-}{2\pi} \frac{1}{[(\frac{p}{2}+k)^2 - m^2 + i\epsilon]} \frac{1}{[(\frac{p}{2}-k)^2 - m^2 + i\epsilon]} \frac{1}{(k-k')^2 - \mu^2 + i\epsilon}.
\end{aligned}
\tag{5.50}
$$

The Nakanishi kernel can be obtained straightforward only by changing the dimension of the internal momentum $\frac{dk'}{(2\pi)^4} \to \frac{d^3k'}{(2\pi)^3}$, because as explained previously the Nakanishi representation can be implemented to lower dimensions without difficulty. The steps follow as before, performing the integration in k' after putting together the denominators with the aid of the Feynman parametrization using the formula Eq. (5.20). After that, the integration in k^- is done by using the Cauchy's formula, we get the following expression for the kernel

$$
\begin{aligned}
V_{2+1}^{(L)}(\gamma,z;\gamma',z') &= \frac{g^2}{16\pi^{\frac{3}{2}}} \Gamma\left(\frac{5}{2}\right) \frac{1}{[\gamma + (1-z^2)\kappa^2 + z^2 m^2]} \\
&\times \int_0^1 dv \ v^2 \left[\frac{(1+z)^{\frac{5}{2}}\theta(z'-z)}{[v(1-v)(1+z')]^{\frac{5}{2}}[\gamma + m^2 z^2 + \kappa^2(1-z^2) + \Gamma(v,z,z',\gamma)]^{\frac{5}{2}}} \right. \\
&\left. + \frac{(1-z)^{\frac{5}{2}}\theta(z-z')}{[v(1-v)(1-z')]^{\frac{5}{2}}[\gamma + m^2 z^2 + \kappa^2(1-z^2) + \Gamma(v,-z,-z',\gamma)]^{\frac{5}{2}}} \right].
\end{aligned}
\tag{5.51}
$$

The difference of the 2+1 dimensions kernel with the 3+1 dimensions one is the prefactor in front of the kernel, which, together with coupling constant, plays the role of eigenvalue of the eigenvalue equation for the Nakanishi weight-function. The exponent of the D function is also changed. This change will affect the stability of the numerical solution since that in the 2+1 dimension calculation is slightly more difficult to get the convergence in the eigenvalues and eigenvectors than in the 3+1 dimension calculation. However, this difference does not provide a real difficulty. A complete discussion about the 2+1 dimension problem for the scalar theory can be found in Refs. [24, 69].

5.4   Cross-ladder kernel in 3+1 dimensions

The next order contribution in the BS kernel in the theory that we are considering, $\mathcal{L}_{inter} = g\,\phi^2\chi$, is the irreducible kernel with two exchanged bosons, which is known as the *cross-ladder* kernel. As stressed in Ref. [49], it is necessary to introduce the cross-ladder kernel in order to reproduce the results obtained with the Klein-Gordon and Dirac equations. At the same time it removes an undesirable contribution of the order $\alpha^3 log\ \alpha$ obtained from the ladder approximation [50, 51]. The correction in the eigenvalues due to the cross-ladder kernel has already studied in Refs. [15, 52], showing an important contribution respect to the ladder kernel. However, by comparing with the analysis performed by Nieuwenhuis and Tjon [58], where the Feynman-Schwinger representation was adopted to include all ladder and cross-ladder contributions, the two-boson exchanged is not enough and large differences were found. However, although the two-boson exchange kernel ignores large contributions of the complete kernel, this should serve as a mean to infer the behavior of the eigenvalues and the LFWF when higher contributions are considered. In particular, we focus on analyzing the LFWF, which has not been studied in detail so far.

The corresponding Feynman graph for this contribution is depicted below
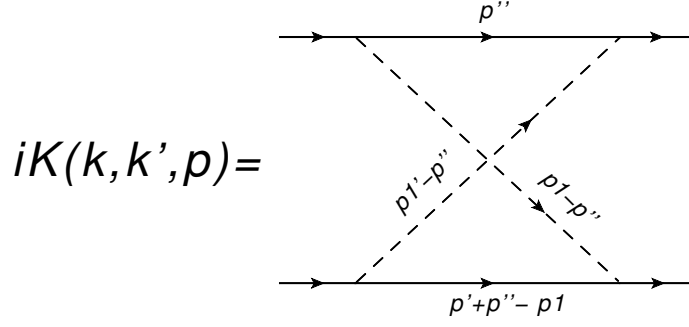
Figure 5.2: Irreducible BS kernel for the cross-ladder contribution.

In this section, we arrange the kernel in a convenient form to introduce it in the BS equation to be solved numerically. The calculation of this diagram demands more algebraic steps with respect to the ladder kernel, since this diagram contains an additional integration in the internal momentum, however the calculation can be done without any difficulty. The expression for the cross-ladder kernel of Fig. 5.2 reads as

$$
iK_{3+1}^{(CL)} = \frac{g^4}{(2\pi)^4} \int \frac{dp''}{p''^2 - m^2 + i\epsilon} \frac{1}{(p' - p_1 + p'')^2 - m^2 + i\epsilon} \tag{5.52}
$$
$$
\times \frac{1}{(p_1 - p'')^2 - \mu^2 + i\epsilon} \frac{1}{(p_1' - p'')^2 - \mu^2 + i\epsilon},
$$

after performing the integration in the internal momenta p'' one has

$$
iK_{3+1}^{(CL)}(k, k', p) = \frac{ig^4}{(4\pi)^2} \frac{\Gamma(2)}{\Gamma(4)} \int_0^1 dy_3 \int_0^{1-y_3} dy_2 \int_0^{1-y_2-y_3} dy_1 \frac{1}{A'^2}, \tag{5.53}
$$

where A' is given by

$$
\begin{aligned}
A' =& k'^2(y_1 + y_3)(1 - y_1 - y_3) + k^2(y_2 + y_3)(1 - y_2 - y_3) + k' \cdot p(y_1(1 - y_1 - y_2) - y_3(y_1 + y_2)) \\
& - k \cdot p(y_2(1 - y_1 - y_2) - y_3(y_1 + y_2)) + 2k \cdot k'((y_1 + y_3)(y_2 + y_3) - y_3) \\
& + \frac{1}{4}M^2(y_1 + y_2)(1 - y_1 - y_2) - \mu^2(1 - y_1 - y_2) - m^2(y_1 + y_2) + i\epsilon.
\end{aligned}
$$
$$\tag{5.54}$$

Now we have to put together the kernel in the form Eq. (5.52) with the Nakanishi denominator to perform the integration in k', with aid of the Feynman parametrization

$$\int \frac{dk'}{(2\pi)^4} \frac{1}{[k'^2 + (p \cdot k')z' - \gamma' - \kappa^2 + i\epsilon]^3 A'^2} = \frac{i}{(4\pi)^2} \int_0^1 dy_4 (1 - y_4)^2 y_4 \frac{\eta}{[H + i\epsilon]^3}, \qquad (5.55)$$

$$I(k,p) = \int \frac{d^3 k'}{(2\pi)^3} \frac{iK(k,k',p)}{[k'^2 + (p \cdot k')z' - \gamma' - \kappa^2 + i\epsilon]^3} = \frac{-g^4}{(4\pi)^4} \int [dy_i](1 - y_4)^2 y_4 \frac{\eta}{[H + i\epsilon]^3}, \quad (5.56)$$

where $\eta = 1 - y_4[1 - (1 - y_1 - y_3)(y_1 + y_3)]$ and

$$\int [dy_i] = \int_0^1 dy_3 \int_0^{1-y_3} dy_2 \int_0^{1-y_2-y_3} dy_1 \int_0^1 dy_4. \qquad (5.57)$$

Finally, we carry out the integration in dk^-

$$\int_{-\infty}^{\infty} \frac{dk^-}{(2\pi)} G_1(k,p) G_2(k,p) I(k,p) =$$

$$\frac{-g^4}{(4\pi)^4} \int [dy_i](1 - y_4)^2 y_4 \eta \int_{-\infty}^{\infty} \frac{dk^-}{(2\pi)} \frac{i}{(k + p/2) - m^2 + i\epsilon} \frac{i}{(k - p/2) - m^2 + i\epsilon} \frac{1}{[H + i\epsilon]^3}. \qquad (5.58)$$

In order to perform the integration by means of the Cauchy's formula, we analyze the position of the poles in the free propagators and the H function in Eq. (5.58). Introducing the LF variables $k^+, k^-, \mathbf{k}_\perp$, one has the following relations for the invariants

$$k^2 = k^+ k^- - \mathbf{k}_\perp{}^2$$

$$k \cdot p = \frac{k^+ p^-}{2} + \frac{k^+ p^-}{2} \qquad (5.59)$$

$$p^2 = p^+ p^-,$$

recalling that $\mathbf{p}_\perp = \mathbf{0}$. By using the above relations, the free propagators can be written as

$$G_1^{-1} = -i\left(k^+ + \frac{p^+}{2}\right)\left[k^- + \frac{(M^2/4 - m^2 - \mathbf{k}_\perp{}^2 + k^+ p^-/2)}{(k^+ + \frac{p^+}{2})} + \frac{i\epsilon}{(k^+ + \frac{p^+}{2})}\right]$$

$$G_2^{-1} = -i\left(k^+ - \frac{p^+}{2}\right)\left[k^- + \frac{(M^2/4 - m^2 - \mathbf{k}_\perp{}^2 - k^+ p^-/2)}{(k^+ - \frac{p^+}{2})} + \frac{i\epsilon}{(k^+ - \frac{p^+}{2})}\right], \qquad (5.60)$$

in this frame one has: $p^+ = p^- = M$. Therefore, the above expressions can be written as

$$G_1^{-1} = -i\left(\frac{M}{2} + k^+\right)\left[k^- - k_L^-\right]$$

$$G_2^{-1} = -i\left(\frac{M}{2} - k^+\right)\left[k_U^- - k^-\right],$$

(5.61)

where

$$k_L^- = -\frac{M}{2} + \frac{(m^2 + \mathbf{k}_\perp{}^2)}{(\frac{M}{2} + k^+)} - \frac{i\epsilon}{(\frac{M}{2} + k^+)}$$

$$k_U^- = \frac{M}{2} - \frac{(m^2 + \mathbf{k}_\perp{}^2)}{(\frac{M}{2} - k^+)} + \frac{i\epsilon}{(\frac{M}{2} - k^+)}.$$

(5.62)

Since $(M/2 \pm k^+) \geq 0$, one has the pole k_L^- in the lower complex plane and k_U^- in the upper complex plane. Let us to analyze the pole in the term H. After some algebraic manipulations, the term H is written in the following form:

$$H = \frac{M}{2}k^-(S_2 - zS_1) - \gamma S_1 - z\frac{M^2}{4}S_2 + S_3 + i\epsilon,$$

(5.63)

where $z = -\frac{2k^+}{M}$ and $\gamma = \mathbf{k}_\perp{}^2$. The functions S_i have the following dependence: $S_1(y_i)$, $S_2(y_i, z')$ and $S_3(m^2, \mu^2, \kappa^2, \gamma', y_i)$. Thus, the position of the third pole is given by:

$$k_3^- = \frac{\gamma S_1 + z\frac{M^2}{4}S_2 - S_3}{\frac{M}{2}(S_2 - zS_1)} - \frac{i\epsilon}{\frac{M}{2}(S_2 - zS_1)},$$

(5.64)

therefore, the position of this pole in the complex plane depends on the sign of $(S_2 - zS_1)$ as we can see from the imaginary part in Eq. (5.64). H reads as:

$$H = \frac{M}{2}(S_2 - zS_1)(k^- - k_3^-).$$

(5.65)

The integral Eq. (5.58) can be done by closing the path in the upper or lower complex plane. In the same way as in the ladder case, for avoiding the evaluation of the third-order pole, we proceed as follows: if $(S_2 - zS_1) > 0$ we close in the upper complex plane and if $(S_2 - zS_1) < 0$ we close in the lower one. Below, we analyze these two cases:

- $(S_2 - zS_1) > 0$

$$\int_{-\infty}^{\infty} \frac{dk^-}{(2\pi)} G_1(k,p) G_2(k,p) I(k,p) \propto$$
$$\int_{-\infty}^{\infty} dk^- \frac{1}{(\frac{M}{2}+k^+)} \frac{1}{(\frac{M}{2}-k^+)} \frac{i}{(k^- - k_L^-)} \frac{i}{(k_U^- - k^-)} \frac{1}{\left[\frac{M}{2}(S_2 - zS_1)(k^- - k_3^-)\right]^3},$$

(5.66)

after closing the path in the upper plane one has

$$\int_{-\infty}^{\infty} \frac{dk^-}{(2\pi)} G_1(k,p) G_2(k,p) I(k,p) \propto$$
$$\times \frac{1}{(\frac{M}{2}+k^+)} \frac{1}{(\frac{M}{2}-k^+)} \frac{1}{(k_U^- - k_L^-)} \frac{1}{\left[\frac{M}{2}(S_2 - zS_1)(k_U^- - k_3^-)\right]^3},$$

(5.67)

using the explicit expressions of the poles, one obtains

$$(k_U^- - k_L^-) = \frac{-4}{M(1-z^2)} \left[\gamma + \kappa^2(1-z^2) + m^2 z^2\right]$$
$$(k_U^- - k_3^-) = \frac{2}{M(1-z^2)(S_2 - zS_1)} \left[-4(S_2 - zS_1)\{m^2 z^2 + \kappa^2(1-z^2) + \gamma\} + 4R\right] \quad (5.68)$$
$$\left(\frac{M}{2}+k^+\right)\left(\frac{M}{2}-k^+\right) = \frac{M^2}{4}(1-z^2),$$

the R function is decomposed in the following form:

$$R = \gamma b_\gamma + \gamma' b_{\gamma'} + m^2 b_m + \kappa^2 k_\kappa + \mu^2 b_\mu. \tag{5.69}$$

The long expressions for these coefficients are shown at the end of this section. Replacing the above relations in Eq. (5.56) and adding carefully the previous factors, we get the expression for the Nakanishi cross-ladder kernel

$$V_{3+1}^{(CL)}(z, z', \gamma, \gamma') =$$
$$\frac{-g^4}{(4\pi)^4} \frac{(1-z^2)^3}{[\gamma + \kappa^2(1-z^2) + m^2 z^2]} \int d[y_i](1-y_4)^2 y_4 \frac{\eta}{[-(S_2 - zS_1)\{m^2 z^2 + \kappa^2(1-z^2) + \gamma\} + R]^3}.$$

(5.70)

- $(S_2 - zS_1) < 0$

  For this case we close the contour in the lower complex plane

$$\int_{-\infty}^{\infty} \frac{dk^-}{(2\pi)} G_0^{12}(k,p) I(k,p) \propto \frac{1}{(\frac{M}{2}+k^+)} \frac{1}{(\frac{M}{2}-k^+)} \frac{-1}{(k_U^- - k_L^-)} \frac{1}{\left[\frac{M}{2}(S_2 - zS_1)(k_L^- - k_3^-)\right]^3}.$$

  (5.71)

  The expression for the factor $(k_L^- - k_3^-)$ is:

$$(k_L^- - k_3^-) = \frac{2}{M(1-z^2)(S_2 - zS_1)} \left[4(S_2 - zS_1)\{m^2 z^2 + \kappa^2(1-z^2) + \gamma\} + 4R\right]. \quad (5.72)$$

  In this case we obtain

$$V_{3+1}^{(CL)}(z, z', \gamma, \gamma') =$$
$$\frac{-g^4}{(4\pi)^4} \frac{(1-z^2)^3}{[\gamma + \kappa^2(1-z^2) + m^2 z^2]} \int d[y_i](1-y_4)^2 y_4 \frac{\eta}{[(S_2 - zS_1)\{m^2 z^2 + \kappa^2(1-z^2) + \gamma\} + R]^3}.$$

  (5.73)

Note the four integrals in the Feynman parameters in the Nakanishi kernel, which demands more numerical capability for computing the kernel.

Finally, we show the coefficients of the R function

$$b_\gamma = y_4(y_2^2(1 + (-1 + y_1 + y_3)y_4)(1 + z) + y_3(-1 + y_3 + (1 + (-1 + y_1)y_1)$$
$$y_4 - y_3 y_4 + y_1 y_3 y_4 + y_1 z - y_1^2 y_4 z - y_1 y_3 y_4 z +$$
$$(-1 + y_1 + y_3)(-1 + y_4)zz') + y_2(-1 + (1 + (-1 + y_1)y_1)y_4 - z + \qquad (5.74)$$
$$y_3^2 y_4(1 + z) + y_3(2 + z + y_4(-3 - 2z + 2y_1(1 + z)) + (-1 + y_4)zz') +$$
$$z(y_4 + y_1(1 - z' + y_4(-2 + y_1 + z')))))$$

$$b_{\gamma'} = (-1 + y_4)(-1 + (1 + y_1^2 + (-1 + y_3)y_3 + y_1(-1 + 2y_3))y_4)(-1 + z^2)$$

$$
\begin{aligned}
b_\kappa = &-((-1 + z^2)(-1 + z'^2 + y_4(2 + (-1 + y_3)y_3 + y_2 \\
&(-1 + y_2 + (-1 + y_2 + y_3)z) - 2y_1^2(-1 + z') - y_1(-2 + y_2(2 + z) + \\
&y_3(2 + z))(-1 + z') - y_3(2y_2 + (-1 + y_2 + y_3)z)z' - 2z'^2) + \\
&y_4^2(-1 + y_2 + y_3 - y_3^2 + y_2^2(-1 + y_3)(1 + z) + \\
&y_2(-1 + y_3)(y_3 + (-1 + y_3)z) + (-1 + y_3)y_3zz' + y_2y_3(2 + z)z' + \\
&z'^2 + y_1^2(-2 + y_2 + y_3 + y_2z - y_3z + 2z') + \\
&y_1(2 + y_2^2(1 + z) - 2z' + y_3(-3 + y_3 - y_3z + (2 + z)z') + y_2 \\
&(-3 - 2z + 2y_3(1 + z) + (2 + z)z')))))
\end{aligned}
$$

(5.75)

$$
\begin{aligned}
b_m = &-(y_1^3 y_4^2(-1 + z^2)) + y_2^2 y_4(1 + (-1 + y_3)y_4)(1 + z)(-1 + z + z^2) + \\
&y_1^2 y_4((1 + z)(-1 + z + y_2y_4z^2) + y_3(y_4 - y_4z^3) + 2(-1 + y_4)(-1 + z^2)z') \\
&+ y_2y_4(z^2(-1 + y_4 + y_3(2 + (-3 + y_3)y_4) - z + (y_3 + (-1 + y_3)^2y_4)z) + \\
&y_3(-1 + y_4)(-2 + z^2(2 + z))z' + (-1 + y_4)(-((-1 + y_3)y_3y_4z^2) + \\
&(-1 + y_3)y_3y_4z^3z' + (-1 + y_4)(-1 + z^2)z'^2) + y_1y_4(-(y_3(y_4(1 + y_3(-1 + z)) - z)z^2) + \\
&y_2^2 y_4(1 + z)(-1 + z + z^2) + (-1 + y_4)(2 - 2z^2 + y_3(-2 + z^2(2 + z)))z' + \\
&y_2(-((-2 + z^2(2 + z))(-1 + z')) + y_4(2 - 2z' + z^2(-3 - 2z + 2y_3(1 + z) + (2 + z)z'))))
\end{aligned}
$$

$$b_\mu = (-1 + y_1 + y_2)y_4(-1 + (1 + y_1^2 + (-1 + y_3)y_3 + y_1(-1 + 2y_3))y_4)(-1 + z^2)$$

$$
\begin{aligned}
(S_2 - zS_1)/y_4 = &y_2^2(1 + (-1 + y_1 + y_3)y_4)(1 + z) + y_3(y_1^2 y_4(-1 + z) \\
&- (-1 + y_3)(-1 + y_4)(z - z') + y_1(1 + y_3y_4(-1 + z) - y_4z + \\
&(-1 + y_4)z')) + y_2((-1 + y_4)(1 + z) + y_1^2 y_4(1 + z) + \\
&y_3^2 y_4(1 + z) + y_3(1 + 2z - z' + y_4(-2 - 3z + z')) + \\
&y_1(1 - z' + y_4(-2 - z + 2y_3(1 + z) + z'))).
\end{aligned}
$$

(5.76)

5.5 Cross-ladder kernel in 2+1 dimensions

In the same form as in the ladder case, we can perform successfully the calculation of the cross-ladder contribution in 2+1 dimensions. For this case the kernel reads as

$$iK_{2+1}^{(CL)} = \frac{g^4}{(2\pi)^3} \int \frac{d^3p''}{p''^2 - m^2 + i\epsilon} \frac{1}{(p' - p_1 + p'')^2 - m^2 + i\epsilon} \tag{5.77}$$
$$\times \frac{1}{(p_1 - p'')^2 - \mu^2 + i\epsilon} \frac{1}{(p_1' - p'')^2 - \mu^2 + i\epsilon}.$$

Performing the same steps as before, taking into account the changing in the dimension we obtain the Nakanishi kernel

- $(S_2 - zS_1) > 0$

$$V_{2+1}^{(CL)}(z, z', \gamma, \gamma') =$$
$$\frac{-3g^4}{(4\pi)^3} \frac{(1 - z^2)^4}{[\gamma + \kappa^2(1 - z^2) + m^2 z^2]} \int d[y_i](1 - y_4)^2 y_4^{3/2} \frac{\eta^{5/2}}{[-(S_2 - zS_1)\{m^2 z^2 + \kappa^2(1 - z^2) + \gamma\} + R]^4}, \tag{5.78}$$

and

- $(S_2 - zS_1) < 0$

$$V_{2+1}^{(CL)}(z, z', \gamma, \gamma') =$$
$$\frac{-3g^4}{(4\pi)^3} \frac{(1 - z^2)^4}{[\gamma + \kappa^2(1 - z^2) + m^2 z^2]} \int d[y_i](1 - y_4)^2 y_4^{3/2} \frac{\eta^{5/2}}{[(S_2 - zS_1)\{m^2 z^2 + \kappa^2(1 - z^2) + \gamma\} + R]^4}. \tag{5.79}$$

The coefficients of the R function are the same as the 3+1 kernel.

The results obtained for ladder and cross-ladder kernel in 3+1 dimensions can be directly compared with the results in Ref. [8, 15], where the explicit covariant LF framework was implemented. The analytic expressions obtained in these references are in quite agreement with the expression that we have derived. Thus, this shows the reliability of the approach that we have implemented.

Chapter 6

Euclidean Bethe-Salpeter equation

As it has been explained in Sec.2.2, in view of the analytic properties of the BS amplitude it is possible to perform the analytic continuation to complex energy values, transformation know as the *Wick rotation*. This procedure allows to transform the initial singular BS equation in the Minkowski space to the Euclidean space where the singularities vanish, at least for the simple kernels, see Ref. [3]. Hence, many numerical methods becomes available for solving the Euclidean BS equation. We deal with this subject in this chapter. Despite of the aim of this thesis be to explore the solutions of the BS equation obtained directly in the Minkowski space, the Euclidean calculation serves as mean to verify the obtained results. We recall that the eigenvalues of the BS equation are invariants under the Wick rotation.

6.1   Euclidean BS equation for the ladder kernel

6.1.1   3+1 dimensions

As starting point we recall the BS equation in the Minkowski space for the ladder kernel

$$\varphi(k,p) = \frac{i}{(k+p/2)^2 - m^2 + i\epsilon} \frac{i}{(k-p/2)^2 - m^2 + i\epsilon} (ig)^2 \int \frac{dk'}{(2\pi)^4} \frac{i}{(k-k')^2 - \mu^2 + i\epsilon} \varphi(k',p).$$

The singularities in the free-propagators and in the kernel are evident. As we studied in Sec.2.2, the BS amplitude has some cuts in the complex plane, which due to their positions allow to carry out an analytic continuation. For applying this transformation we also have to find the position of the poles provided by the kernel. By looking at the kernel of the BS equation we realize the position of the poles in the following points

$$k'^0 = k^0 \pm \sqrt{(\mathbf{k} - \mathbf{k'})^2 + \mu^2 - i\epsilon}, \tag{6.1}$$

taking into account the cuts of the BS amplitude Eq. (2.45) and the positions of the poles, the integration path in k'^0 from $-\infty$ to ∞ can be rotated along to the imaginary axis ik'^0 from $-i\infty$ to $i\infty$ if the variable k^0 is also rotate 90^0 in counter-clockwise, for details see Ref. [3, 33]. In the BS equation, it is only necessary to carry out the replacement $k'^0 \to ik'^0_E$ and $k^0 \to ik^0_E$. Recalling that we restrict to rest frame $\mathbf{p} = 0$, the Euclidean BS equation reads as

$$
\begin{aligned}
\varphi(k^0_E, \mathbf{k}) = & \frac{i^2}{\left[(-(k^0_E)^2 - \mathbf{k}^2 + M^2/4 - m^2)^2 + (k^0_E)^2 M^2\right]} \\
& \times (ig)^2 \int \frac{dk'^0_E d\mathbf{k'}}{(2\pi)^4} \frac{1}{(k^0_E - k'^0_E)^2 + (\mathbf{k} - \mathbf{k'})^2 + \mu^2} \varphi(k'^0_E, \mathbf{k'}),
\end{aligned}
\tag{6.2}
$$

the equation is reduced to an integral equation in the Euclidean vector space with the metric

$$k^2 = -(k^0_E)^2 - k_1^2 - k_2^2 - k_3^2. \tag{6.3}$$

It is clear from Eq. (6.2) that the Euclidean BS equation with the ladder kernel is now free of singularities. In this form, the equation is ready to be solved numerically. We can still simplify the Euclidean BS equation, taking into account that for *s*-wave (ground state) one has $\varphi(k^0_E, \mathbf{k}) = \varphi(k^0_E, |\mathbf{k}|)$. Using this fact the BS equation can be written the following form:

$$
\begin{aligned}
\varphi(k^0_E, |\mathbf{k}|) = & \frac{i^2}{[(-(k^0_E)^2 - |\mathbf{k}|^2 + M^2/4 - m^2)^2 + (k^0_E)^2 M^2]} \\
& \times (ig)^2 \int \frac{dk'^0_E}{2\pi} \int \frac{|\mathbf{k'}|^2 d|\mathbf{k'}| d\Omega_{k'}}{(2\pi)^3} \frac{1}{(k^0_E - k'^0_E)^2 + |\mathbf{k}|^2 + |\mathbf{k'}|^2 - 2|\mathbf{k}||\mathbf{k'}|cos\theta + \mu^2} \varphi(k'^0_E, |\mathbf{k'}|),
\end{aligned}
\tag{6.4}
$$

with $d\Omega_{k'} = sin\theta \, d\theta \, d\phi$. Thus, one can perform the angular integration

$$
\begin{aligned}
\varphi(k^0_E, |\mathbf{k}|) = & \frac{i^2}{[(-(k^0_E)^2 - |\mathbf{k}|^2 + M^2/4 - m^2)^2 + (k^0_E)^2 M^2]} \\
& \times \frac{g^2}{2|\mathbf{k}||\mathbf{k'}|} \int \frac{dk'^0_E \, d|\mathbf{k'}| \, |\mathbf{k'}|^2}{(2\pi)^3} ln\left(\frac{a+b}{a-b}\right) \varphi(k'^0_E, |\mathbf{k'}|),
\end{aligned}
\tag{6.5}
$$

with

$$(a+b) = (k'^0_E - k^0_E)^2 + (|\mathbf{k'}| + |\mathbf{k}|)^2 + \mu^2$$
$$(a-b) = (k'^0_E - k^0_E)^2 + (|\mathbf{k'}| - |\mathbf{k}|)^2 + \mu^2. \tag{6.6}$$

This equation can also be written in symbolic form as

$$\frac{1}{g^2}\varphi = \mathcal{A}(M)\varphi, \tag{6.7}$$

we have the usual eigenvalue problem with $\frac{1}{g^2}$ being the eigenvalue. Thus, for given masses of the constituents and the mass of the bound state M we can obtain the corresponding coupling constant.

6.1.2   2+1 dimensions

We recall the BS equation in 2+1 dimensions

$$\varphi(k,p) = \frac{i}{(k+p/2)^2 - m^2 + i\epsilon}\frac{i}{(k-p/2)^2 - m^2 + i\epsilon}(ig)^2 \int \frac{d^3k'}{(2\pi)^3}\frac{i}{(k-k')^2 - \mu^2 + i\epsilon}\varphi(k',p),$$

following the same steps as before, i.e. after performing the Wick rotation and taking into account the reduction of the dimension, the BS can be written as

$$\varphi(k^0_E, |\mathbf{k}|) = \frac{i^2}{[(-(k^0_E)^2 - |\mathbf{k}|^2 + M^2/4 - m^2)^2 + (k^0_E)^2 M^2]}$$
$$\times (ig)^2 \int \frac{dk'^0_E}{(2\pi)^3}\int |\mathbf{k'}|\, d|\mathbf{k'}|\, d\phi \frac{1}{(k^0_E - k'^0_E)^2 + |\mathbf{k}|^2 + |\mathbf{k'}|^2 - 2|\mathbf{k}||\mathbf{k'}|cos\phi + \mu^2}\varphi(k'^0_E, |\mathbf{k'}|), \tag{6.8}$$

also the angular integration can be done, we obtain

$$\varphi(k^0_E, |\mathbf{k}|) = \frac{1}{[(-(k^0_E)^2 - |\mathbf{k}|^2 + M^2/4 - m^2)^2 + (k^0_E)^2 M^2]}$$
$$\times g^2 \int \frac{dk'^0_E}{(2\pi)^2}\int |\mathbf{k'}|\, d|\mathbf{k'}| \frac{1}{\left\{[(k^0_E - k'^0_E)^2 + |\mathbf{k}|^2 + |\mathbf{k'}|^2 + \mu^2]^2 - 4|\mathbf{k}|^2|\mathbf{k'}|^2\right\}^{\frac{1}{2}}}\varphi(k'^0_E, |\mathbf{k'}|). \tag{6.9}$$

As solution of the equations (6.5) and (6.9), we will obtain the coupling constant and the Euclidean BS amplitude to be compared with those obtained from the calculation in the Minkowski space *.

6.2 The Euclidean Cross-Ladder kernel

6.2.1 3+1 dimensions

Now, we concern with the Euclidean cross-ladder kernel. The calculation involving this kernel is more tedious, however after some analytical manipulations we can obtain a suitable expression for the kernel. This treatment is showed below in detail. We show explicitly the treatment for 3+1 dimension, which is easily extended to 2+1 dimensions.

Considering the cross-ladder kernel of Eq. (5.52), we use the Feynman parametrization to put together the denominators. Then, the integration in the internal momentum is carried out, which leads to the expression Eq. (5.53) for the kernel. Once the Wick rotation is performed, the A' function in Eq. (5.53) is written in the following form

$$
\begin{aligned}
A'_E &= (-1)\Bigg[[(k'^{0\,2}_E + \mathbf{k'}^2)(y_1 + y_3)(1 - y_1 - y_3) + (k^{0\,2}_E + \mathbf{k}^2)(y_2 + y_3)(1 - y_1 - y_3)] \\
&\quad - ik'^0_E M\left(y_1(1 - y_1 - y_2) - y_3(y_1 + y_2)\right) + ik^0_E M\left(y_2(1 - y_1 - y_2) - y_3(y_1 + y_2)\right) \\
&\quad + 2(k^0_E k'^0_E + |\mathbf{k}||\mathbf{k'}|\cos\theta)\left((y_1 + y_3)(y_2 + y_3) - y_3\right) - \frac{1}{4}M^2\left(y_1 + y_2\right)(1 - y_1 - y_2) \\
&\quad + \mu^2\left(1 - y_1 - y_2\right) + m^2\left(y_1 + y_2\right) - i\epsilon \Bigg],
\end{aligned}
\tag{6.10}
$$

recalling that $\mathbf{p} = 0$, the Euclidean kernel becomes

$$
K^{(CL)}_{3+1}(k^0_E, k^{0\,\prime}_E, |\mathbf{k}|, |\mathbf{k'}|, \cos\theta) = \frac{g^4}{(4\pi)^2}\frac{\Gamma(2)}{\Gamma(4)}\int_0^1 dy_3 \int_0^{1-y_3} dy_2 \int_0^{1-y_2-y_3} dy_1 \frac{1}{A'^2_E}.
\tag{6.11}
$$

The next step is the angular integration, however this is not immediate as in the ladder case and further analytical treatment is necessary, as we show below. In order to improve the numerical

---

computation, we use the property that the BS amplitude is symmetric in k_0 to construct a real equation. First we write the BS equation as

$$\varphi(k_E^0, |\mathbf{k}|) = \mathcal{O}^{(3+1)} \int_{-\infty}^{\infty} dk_E'^0 \int_0^{\infty} d|\mathbf{k'}| \ |\mathbf{k'}|^2 \tag{6.12}$$

$$\times \ \frac{1}{\left[\mathcal{A}_1(k_E'^{0\,2}, k_E^{0\,2}, \mathbf{k'}^2, \mathbf{k}^2) + \mathcal{A}_2(k_E'^0 k_E^0) + ik_E'^0 \mathcal{C'} - ik_E^0 \mathcal{C} + \mathcal{D}\right]^2} \varphi(k_E'^0, |\mathbf{k'}|),$$

where the operator $\mathcal{O}^{(3+1)}$ is defined as:

$$\mathcal{O}^{(3+1)} = G_E^{(10)} G_E^{(20)} \frac{g^4}{(4\pi)^2} \frac{\Gamma(2)}{\Gamma(4)} \int_0^1 dy_3 \int_0^{1-y_3} dy_2 \int_0^{1-y_2-y_3} dy_1 \int d\Omega_{k'}, \tag{6.13}$$

$G_E^{(i0)}$ are the free propagators in the Euclidean space. The explicit expressions of the coefficients in Eq. (6.12) are

$$\mathcal{A}_1(k_E'^{0\,2}, k_E^{0\,2}, |\mathbf{k'}|^2, |\mathbf{k}|^2) = (k_E'^{0\,2} + |\mathbf{k'}|^2)(y_1 + y_3)(1 - y_1 - y_3) + (k_E^{0\,2} + |\mathbf{k}|^2)(y_2 + y_3)(1 - y_1 - y_3),$$

$$\mathcal{A}_2(k_E'^0 k_E^0) = 2k_E^0 k_E'^0 \left((y_1 + y_3)(y_2 + y_3) - y_3\right),$$

$$\mathcal{C'} = -M\left(y_1(1 - y_1 - y_2) - y_3(y_1 + y_2)\right), \quad \mathcal{C} = -M\left(y_2(1 - y_1 - y_2) - y_3(y_1 + y_2)\right),$$

$$\mathcal{D} = 2|\mathbf{k}||\mathbf{k'}|\cos\theta\left((y_1 + y_3)(y_2 + y_3) - y_3\right) - \frac{1}{4}M^2\left(y_1 + y_2\right)(1 - y_1 - y_2)$$

$$+ \mu^2\left(1 - y_1 - y_2\right) + m^2\left(y_1 + y_2\right) - i\epsilon. \tag{6.14}$$

We rewrite Eq. (6.12) as

$$\varphi(k_E^0, |\mathbf{k}|) = \mathcal{O}^{(3+1)} \left(\int_0^{\infty} dk_E'^0 \int_0^{\infty} d|\mathbf{k'}||\mathbf{k'}|^2 \frac{\varphi(-k_E'^0, |\mathbf{k'}|)}{\left[\mathcal{A}_1(k_E'^{0\,2}, k_E^{0\,2}, \mathbf{k'}^2, \mathbf{k}^2) + \mathcal{A}_2(-k_E'^0 k_E^0) - ik_E'^0 \mathcal{C'} - ik_E^0 \mathcal{C} + \mathcal{D}\right]^2} \right.$$

$$+ \left. \int_0^{\infty} dk_E'^0 \int_0^{\infty} d|\mathbf{k'}||\mathbf{k'}|^2 \frac{\varphi(k_E'^0, |\mathbf{k'}|)}{\left[\mathcal{A}_1(k_E'^{0\,2}, k_E^{0\,2}, \mathbf{k'}^2, \mathbf{k}^2) + \mathcal{A}_2(k_E'^0 k_E^0) + ik_E'^0 \mathcal{C'} - ik_E^0 \mathcal{C} + \mathcal{D}\right]^2} \right). \tag{6.15}$$

Now using the fact that the BS amplitude must be symmetric in k_E^0, we may write

$$\varphi(k_E^0, |\mathbf{k}|) = \frac{1}{2}[\varphi(k_E^0, |\mathbf{k}|) + \varphi(-k_E^0, |\mathbf{k}|)], \tag{6.16}$$

we can write the BS equation as follows

$$\varphi(k_E^0, |\mathbf{k}|) = \frac{1}{2}\mathcal{O}^{(3+1)} \int_0^{\infty} dk_E'^0 \int_0^{\infty} |\mathbf{k'}|^2 d|\mathbf{k'}| \left(\frac{1}{\mathcal{F}_1^2} + \frac{1}{\mathcal{F}_2^2} + \frac{1}{\mathcal{F}_2^{*2}} + \frac{1}{\mathcal{F}_1^{*2}}\right) \varphi(k_E'^0, |\mathbf{k'}|)$$

$$= \mathcal{O}^{(3+1)} \int_0^{\infty} dk_E'^0 \int_0^{\infty} |\mathbf{k'}|^2 d|\mathbf{k'}| \ Re\left[\left(\frac{\mathcal{F}_1^2}{(\mathcal{F}_1 \mathcal{F}_1^*)^2} + \frac{\mathcal{F}_2^2}{(\mathcal{F}_2 \mathcal{F}_2^*)^2}\right)\right] \varphi(k_E'^0, |\mathbf{k'}|), \quad (6.17)$$

where we have used the notation

$$\mathcal{F}_1 = \mathcal{A}_1(k_E'^{0\,2}, k_E^{0\,2}, |\mathbf{k'}|^2, |\mathbf{k}|^2) + \mathcal{A}_2(-k_E'^0 k_E^0) - ik_E'^0\mathcal{C}' - ik_E^0\mathcal{C} + \mathcal{D}, \quad (6.18)$$

$$\mathcal{F}_2 = \mathcal{A}_1(k_E'^{0\,2}, k_E^{0\,2}, |\mathbf{k'}|^2, |\mathbf{k}|^2) + \mathcal{A}_2(k_E'^0 k_E^0) + ik_E'^0\mathcal{C}' - ik_E^0\mathcal{C} + \mathcal{D}. \quad (6.19)$$

The manipulation above presented enables to transform the cross-ladder Euclidean kernel in terms of real quantities. The kernel written in Eq. (6.12) depends on complex variables making its numerical treatment more difficult in that form.

The angular integration in Eq. (6.17) can be performed in order to reduce the numerical calculation: the integration in the angle ϕ is trivially done and that of θ can be achieved without any difficulty since the only dependence in θ in the kernel appears in the function $\mathcal{D}$

6.2.2 2+1 dimensions

The steps to achieve a suitable kernel in 2+1 dimensions are similar. We only have to take into account the prefactors which change owing to the dimension reduction. The cross-ladder kernel after performing the integration in the internal momentum and taking the Wick rotation reads as

$$K_{2+1}^{(CL)}(k_E^0, k_E^0{}', |\mathbf{k}|, |\mathbf{k'}|, \cos\theta) = g^4 \left(\frac{3}{32\pi}\right) \int_0^1 dy_3 \int_0^{1-y_3} dy_2 \int_0^{1-y_2-y_3} dy_1 \frac{1}{A_E'^{\frac{5}{2}}}. \quad (6.20)$$

in this case the Euclidean BS equation is

$$\varphi(k_E^0, |\mathbf{k}|) = \mathcal{O}^{(2+1)} \int_{-\infty}^{\infty} dk_E'^0 \int_0^{\infty} |\mathbf{k'}| d|\mathbf{k'}| \quad (6.21)$$

$$\times \frac{1}{\left[\mathcal{A}_1(k_E'^{0\,2}, k_E^{0\,2}, |\mathbf{k'}|^2, |\mathbf{k}|^2) + \mathcal{A}_2(k_E'^0 k_E^0) + ik_E'^0\mathcal{C}' - ik_E^0\mathcal{C} + \mathcal{D}\right]^{\frac{5}{2}}} \varphi(k_E'^0, |\mathbf{k'}|),$$

we write the operator $\mathcal{O}^{(2+1)}$ as:

$$\mathcal{O}^{(2+1)} = g^4\, G_E^{(01)} G_E^{(02)}\, \frac{3}{32\pi} \int_0^1 dy_3 \int_0^{1-y_3} dy_2 \int_0^{1-y_2-y_3} dy_1 \int_0^{2\pi} d\theta, \quad (6.22)$$

after doing the same steps as the 3+1 kernel we obtain

$$\varphi(k_E^0, |\mathbf{k}|) = \frac{1}{2} \mathcal{O}^{(2+1)} \int_0^\infty dk_E'^0 \int_0^\infty |\mathbf{k'}| d|\mathbf{k'}| \left(\frac{1}{\mathcal{F}_1^{\frac{5}{2}}} + \frac{1}{\mathcal{F}_2^{\frac{5}{2}}} + \frac{1}{\mathcal{F}_2^{*\frac{5}{2}}} + \frac{1}{\mathcal{F}_1^{*\frac{5}{2}}} \right) \varphi(k_E'^0, |\mathbf{k'}|)$$

$$= \mathcal{O}^{(2+1)} \int_0^\infty dk_E'^0 \int_0^\infty |\mathbf{k'}| d|\mathbf{k'}| \, Re \left[\left(\frac{\mathcal{F}_1^{\frac{5}{2}}}{(\mathcal{F}_1 \mathcal{F}_1^*)^{\frac{5}{2}}} + \frac{\mathcal{F}_2^{\frac{5}{2}}}{(\mathcal{F}_2 \mathcal{F}_2^*)^{\frac{5}{2}}} \right) \right] \varphi(k_E'^0, |\mathbf{k'}|). \quad (6.23)$$

Differently from the 3+1 kernel, for the 2+1 kernel the angular integration becomes the expression involved. For this reason, it is advisable to leave the integration to be done numerically. A detailed derivation of above equations in 3+1 as well as in 2+1 dimensions can be found in Ref. [60].

6.3 Euclidean Bethe-Salpeter amplitude via NIR

We take profit of this chapter where the study of the Euclidean aspects of the BS approach are analyzed to present the calculation of the Euclidean BS amplitude obtained once the Nakanishi weight-function is known. This calculation allows us to compare the Euclidean BS amplitude obtained with the NIR together with LF projection method and that obtained directly in the Euclidean without any relation with the NIR.

Consider the BS amplitude written in terms of the NIR after taking the Wick rotation $k_E^0 \to i k_E^0$

$$\varphi(k_E^0, \mathbf{k}) = -i \int_{-1}^1 dz' \int_0^\infty d\gamma' \frac{g(z', \gamma')}{\left[\gamma' + m^2 - \frac{M^2}{4} + k_E^2 - iMk_E^0 z' \right]^{n+2}}, \quad (6.24)$$

with $k_E^2 = (k_E^0)^2 + \mathbf{k}^2$. Now, we use the fact that the Nakanishi weight-function should be symmetric in z, which is required to preserve the symmetry property of the BS amplitude for two-scalar boson system. In Eq. (6.24) by exchanging the two particles the term $iMk_E^0 z'$ changes of sign. For recovering the symmetry of the BS amplitude the Nakanishi weight-function should be even in z. This fact leads to

$$\varphi(k_E^0, \mathbf{k}) = -i \int_{-1}^1 dz' \int_0^\infty d\gamma' g(z', \gamma') \, \mathcal{R} \left\{ \frac{1}{\left[\gamma' + m^2 - \frac{M^2}{4} + k_E^2 - iMk_E^0 z' \right]^{n+2}} \right\}. \quad (6.25)$$

Therefore, once known the Nakanishi weight-function we can evaluate the Euclidean BS amplitude obtained by means of Eq. (6.25).

Chapter 7

Results for 2+1 dimensions

7.1 Numerical method

As an introduction of this chapter, we present the numerical method which we will use to solve the integral equation for the Nakanishi weight-function throughout this thesis. Adopting this method, we display the numerical results of solving the BS equation in Minkowski space in 2+1 dimensions, taking into account the ladder and cross-ladder kernel for the interaction. We focus on the bound state problem in 2+1 dimensions since that this subject has not been explored in detail.

The numerical problem which we must solve is the generalized integral equation for the Nakanishi weight-function Eq. (5.15) derived previously

$$\int_0^\infty d\gamma' \frac{g(\gamma', z)}{[\gamma' + \gamma + z^2 m^2 + (1 - z^2)\kappa^2]^2} = \int_{-1}^1 dz' \int_0^\infty d\gamma' \ V(\gamma, z, \gamma', z') g(\gamma', z'),$$

or symbolically it can be written as

$$\mathcal{B}(M) \ g = \mathcal{A}(\alpha, M) \ g, \tag{7.1}$$

where α is the coupling constant of the theory and M is the mass of the bound state. To solve the eigenvalue problem Eq. (7.1), we follow the numerical method used in Ref. [12], which was successfully used to solve the bound state problem in 3+1 dimensions. We have adopted a proper basis, that allows us to expand the non-singular Nakanishi weight-function by taking into account the symmetry of $g(\gamma, z)$ with respect to z, the constraint $g(\gamma, z = \pm 1) = 0$ and the asymptotic fall-off in γ. In particular, Gegenbauer polynomials with proper indexes have been

chosen for describing the z-dependence, while Laguerre polynomials have been adopted for the γ-dependence. In this basis the Nakanishi weight-function is expanded as follows:

$$g(\gamma, z) = \sum_{l=0}^{N_z} \sum_{j=0}^{N_g} A_{lj} G_l(z) \mathcal{L}_j(\gamma), \tag{7.2}$$

the coefficients A_{lj} are obtained after the numerical diagonalization of the eigenvalue problem. The functions $G_l(z)$ are given in terms of even Gegenbauer polynomials $C_{2l}^{(5/2)}(z)$,

$$G_l(z) = 4(1 - z^2)\Gamma\left(\frac{5}{2}\right)\sqrt{\frac{(2l + 5/2)(2l)!}{\pi\Gamma(2l + 5)}}C_{2l}^{(5/2)}(z), \tag{7.3}$$

and the functions $\mathcal{L}_j(\gamma)$ written in terms of the Laguerre polynomials $L_j(a\gamma)$

$$\mathcal{L}_j(\gamma) = \sqrt{a}\ L_j(a\gamma)e^{-a\gamma/2}, \tag{7.4}$$

with the following orthogonality conditions fulfilled

$$\int_{-1}^{1} dz\ G_l(z)G_m(z) = \delta_{lm}$$
$$\int_{0}^{\infty} d\gamma\ \mathcal{L}_j(\gamma)\mathcal{L}_l(\gamma) = a\int_{0}^{\infty} d\gamma\ e^{-a\gamma}L_j(a\gamma)L_l(a\gamma) = \delta_{jl}, \tag{7.5}$$

the parameter a in the Laguerre polynomials is added in order to speed up the convergence of the numerical solution. Also, the γ variable has been rescaled according to $\gamma \to 2\gamma/a_0$. These two parameters control the range of relevance of the Laguerre polynomials. Their exact values will be specified for each problem in question.

By using the expansion of the Nakanishi weight-function Eq. (7.2) into the integral equation Eq. (5.15), the integration over the variable z is performed by using the a Gauss-Legendre quadrature rule, and the integration in the variable γ using the Gauss-Laguerre quadrature. This leads to eigenvalue problem Eq. (7.1), where the matrix dimension depends on the basis expansion used to get stability in the numerical solution.

The possibility to reduce the eigenvalue problem Eq. (7.1), relies on the existence of the inverse of the integral operator $\mathcal{B}(M)$, and the numerical feasibility of such inversion with enough accuracy. To solve Eq. (7.1), it is important to point out that the discretized integral operator $\mathcal{B}$ has small eigenvalues, but they are unphysical and make unstable the solutions. For achieving

good stability we follow the idea presented in Ref. [8]: a small parameter (here $\epsilon = 10^{-6}$) is added to the integral operator $\mathcal{B}(M)$, namely $\mathcal{B}_{ij} \to \mathcal{B}_{ij} + \epsilon\delta_{ij}$. This procedure allows to obtain stable eigenvalues with an accuracy of the same order than ϵ. This parameter regularize the matrix $\mathcal{B}(M)$ and we can obtain good stability in the calculated eigenvalues.

Once the operator $\mathcal{B}$ is inverted, the eigenvalue problem reduce to

$$\lambda\ g = \mathcal{B}^{-1}(M)\mathcal{A}(\alpha, M)\ g, \tag{7.6}$$

the dependence of the binding energy in Eq. (7.6) is given by

$$B = 2m - M, \tag{7.7}$$

which constrains the range of B/m to the interval $0 \leq M/m \leq 2$, avoiding in this way the well-known instability of the ϕ^3 model (see Ref. [56]). In the general way to get the eigenvalues, we assign values to m, μ, B and we look for the value of α such that $\lambda=1$. However, for the ladder kernel, α plays the role of eigenvalue since it appears linearly in $\mathcal{A}$, viz

$$\frac{1}{\alpha}\ g^{(L)} = \mathcal{B}^{-1}(M)\mathcal{A}(M)g^{(L)}. \tag{7.8}$$

It is important noticing that the eigenvalue equation Eq. (7.8), the involved matrices are real but not symmetric, therefore pairs of complex eigenvalues can appear. However, these eigenvalues are unphysical and can be discarded, only considering real eigenvalues.

7.2   2+1 dimensions ladder kernel

We begin by analyzing results obtained for the Yukawa model composed by two scalars particles of mass m exchanging another scalar particle of mass μ in 2+1 dimensions. The corresponding study of this model in 3+1 dimensions has been previously investigated in detail, see Ref. [8, 12].

We recall the expression for the ladder 2+1 dimensions kernel developed previously Eq. (5.51)

$$V_{2+1}^{(L)}(\gamma, z; \gamma', z') = \frac{g^2}{16\pi^{\frac{3}{2}}} \, \Gamma\left(\frac{5}{2}\right) \, \frac{1}{[\gamma + (1 - z^2)\kappa^2 + z^2 m^2]}$$

$$\times \int_0^1 dv \, v^2 \left[\frac{(1 + z)^{\frac{5}{2}} \theta(z' - z)}{[v(1 - v)(1 + z')]^{\frac{5}{2}} [\gamma + m^2 z^2 + \kappa^2(1 - z^2) + \Gamma(v, z, z', \gamma)]^{\frac{5}{2}}} \right.$$

$$\left. + \frac{(1 - z)^{\frac{5}{2}} \theta(z - z')}{[v(1 - v)(1 - z')]^{\frac{5}{2}} [\gamma + m^2 z^2 + \kappa^2(1 - z^2) + \Gamma(v, -z, -z', \gamma)]^{\frac{5}{2}}} \right].$$

In order to decrease the numerical computation, we perform analytically the integration upon v in $V_{2+1}^{(L)}(\gamma, z; \gamma', z')$,

$$
\begin{aligned}
V_{2+1}^{(L)}(\gamma, z; \gamma', z') &= \frac{3}{64} \frac{g^2}{\pi} \frac{1}{[\gamma + (1 - z^2)\kappa^2 + z^2 m^2]} \left[\left(\frac{1 + z}{1 + z'}\right)^{\frac{5}{2}} \theta(z' - z) F(z, z', \gamma, \gamma') + \right. \\
&\quad + \left. \left(\frac{1 - z}{1 - z'}\right)^{\frac{5}{2}} \theta(z - z') F(-z, -z', \gamma, \gamma') \right],
\end{aligned}
$$

(7.9)

with

$$F(z, z', \gamma, \gamma') = \frac{2 \left(8a^2 b + 4a \left(3b^2 + 3bc + 2c^2\right) + b^2(3b + 2c)\right)}{3(a + b + c)^{3/2} (b^2 - 4ac)^2} - \frac{16\sqrt{ab}}{3 (b^2 - 4ac)^2},$$

(7.10)

where

$$
\begin{aligned}
a &= \frac{1 + z}{1 + z'} \mu^2; \qquad b = \gamma + m^2 z^2 + \kappa^2(1 - z^2) + \frac{1 + z}{1 + z'}[\gamma' - \mu^2]; \\
c &= \left(z'^2 \frac{M^2}{4} + \kappa^2\right) - (\gamma + m^2 z^2 + \kappa^2(1 - z^2)).
\end{aligned}
$$

(7.11)

For the solution of Eq. (7.9) we used for both, z and γ integrals, 36 Gaussian points and extended the basis up to $N_z = 18$ and $N_g = 32$ for some values of μ/m and B/m, in order to test the stability of the solutions. In this calculation the stability of the eigenvalues is tested by changing the values of N_z and N_g, starting with small values until to reach a upper limit established. One checks for the lowest eigenvalue for each diagonalization and after increasing the dimension of the basis function the convergence of the eigenvalues can be observed. In this form we have achieved good convergence for the eigenvalues; unfortunately, the same convergence it is not possible for the eigenvectors (the Nakanishi weight-function). In general, the stability of the eigenvalues is

reached faster than the convergence of the eigenvectors. However, the corresponding LFWF, obtained by introducing $g(\gamma, z)$ into the integrals Eq. (5.12), show the same stability as the eigenvalues. We recall the expression for the LFWF:

$$\psi(z, \gamma) = \frac{(1 - z^2)}{4\sqrt{2}} \int_0^\infty d\gamma' \frac{g(\gamma', z)}{[\gamma' + \gamma + z^2 m^2 + (1 - z^2)\kappa^2]^2}.$$

A successful comparison can be done with the results obtained in the Minkowski space by using the NIR and those obtained by solving the Euclidean BS equation Eq. (6.9):

$$\varphi(k_E^0, |\mathbf{k}|) = \frac{1}{[(-(k_E^0)^2 - |\mathbf{k}|^2 + M^2/4 - m^2)^2 + (k_E^0)^2 M^2]}$$
$$\times g^2 \int \frac{dk_E'^0}{(2\pi)^2} \int_0^\infty |\mathbf{k'}| d|\mathbf{k'}| \frac{1}{\left\{[(k_E^0 - k_E'^0)^2 + |\mathbf{k}|^2 + |\mathbf{k'}|^2 + \mu^2]^2 - 4|\mathbf{k}||\mathbf{k'}|\right\}^{\frac{1}{2}}} \varphi(k_E'^0, |\mathbf{k'}|).$$

The Euclidean eigenvalue equation is solved numerically by the *Nystrom method*, which requires the choice of a quadrature

$$\int_a^b f(s) ds = \sum_{j=1}^N w_j f(s_j), \tag{7.12}$$

with w_j the set of weights of the quadrature rule and s_j the abscissas. In particular for solving the Euclidean BS equation Eq. (6.9) a conventional Gaussian-Legendre quadrature to discretize the integrals is employed, for details about the numerical techniques see Ref. [67]. We use up to 40 Gauss points for both variables k_0 and $|\mathbf{k}|$, what guarantees that the integrals are converged. As solution of this equation we obtain the set of eigenvalues $1/g^2$ and the Nakanishi weight-function, for given μ and B.

In Table. 7.2, we display a comparison between the eigenvalues obtained using the NIR with the LF projection and the standard Wick rotation method. From the table, where the comparison is done by using two decimal digits, one can observe a good agreement between the eigenvalues obtained by both methods.

Now, we show the Euclidean BS amplitude and LFWF. In Figs. 7.1 and 7.2, we show the Euclidean BS amplitude as function of k_0 and k, respectively. In the figures we use $k_0 \equiv k_E^0$ for shorthand notation. In Figs. 7.3 and 7.4 the LFWF as function of z and γ respectively is shown. Finally, in Fig. 7.5 a three-dimensional plot of the Euclidean BS amplitude is provided.

Table 7.1: Values of g^2/m^3 calculated by two methods, the Nakanishi integral representation (NIR) and Euclidean (EUCL), for different binding energies B/m; with exchange boson mass $\mu = 0.1\,m$ in the first columns and $\mu = 0.5\,m$ in the last two columns.

| | $\mu = 0.1\,m$ | | $\mu = 0.5\,m$ | |
B/m	**NIR**	**EUCL**	**NIR**	**EUCL**
0.01	0.812	0.793	5.341	5.316
0.1	4.269	4.268	14.877	14.878
0.2	8.068	8.067	22.671	22.670
0.5	19.516	19.515	42.336	42.336
1.0	36.048	36.042	67.391	67.393
1.5	46.830	46.825	82.793	82.833
1.9	50.406	50.394	87.799	87.844
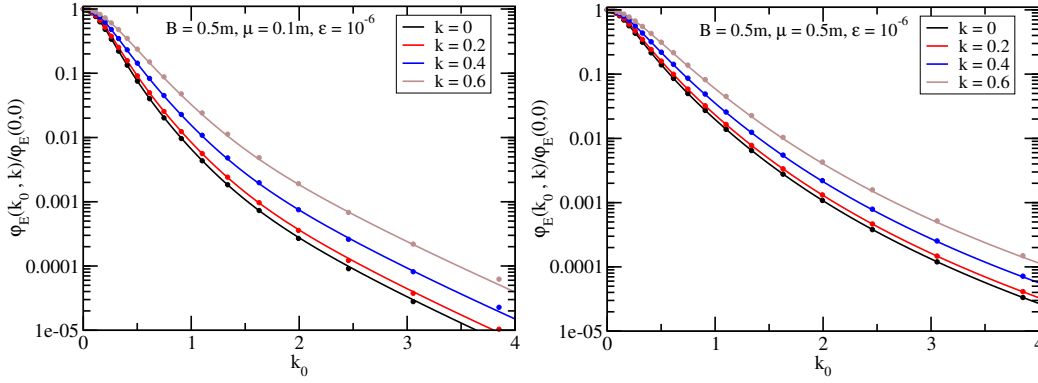
Figure 7.1: $\varphi_E(k_0, k)$ vs k_0 with the arbitrary normalization $\varphi_E(0,0)=1$ for $B = 0.5\,m$ with $\mu = 0.1\,m$ left-panel and $\mu = 0.5\,m$ right-panel. **Solid line**: results from the Nakanishi integral equation with the kernel Eq. (5.51), and then computing the Euclidean BS amplitude with Eq. (6.25). **Full circles**: results from the solution of the BS equation in the Euclidean space Eq. (6.9).

As we can see in the figures, the Euclidean BS amplitudes computed by both methods as function of k and k_0 agree in ranges where the BS amplitude varies several orders of magnitude. Small differences between the results of the two methods start to appear for $k > 3$ in the case $\mu = 0.1\,m$ since the instability of the solution when μ is small. This problem has been faced previously in the 3+1 calculation for the bound state.

In Figs. 7.3 and 7.4, the LFWF show the expected shape since it does not present zeros, corresponding to the valence LFWF for the ground state of two interacting boson system. From the figures of the LFWF as function of γ/m^2, one can appreciate that the corresponding to $\mu = 0.5\,m$ is more spread in the momentum space, since that the interaction in this case is more
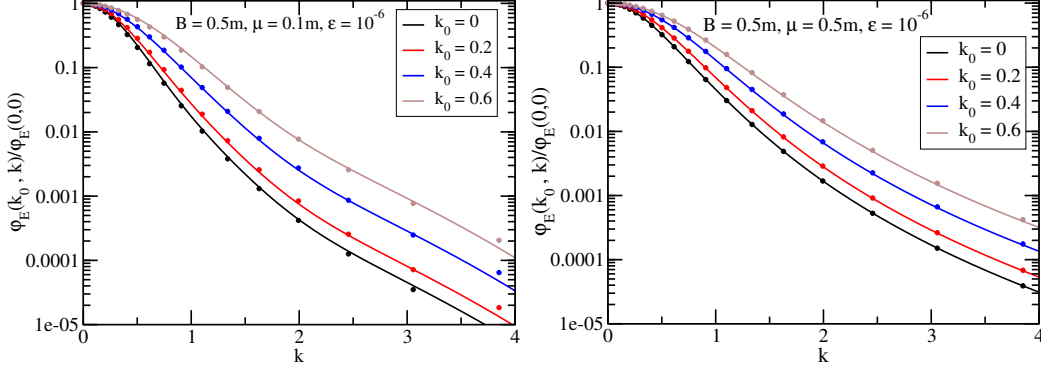
Figure 7.2: $\varphi_E(k_0, k)$ vs k for $B = 0.5\,m$ with $\mu = 0.1\,m$ left-panel and $\mu = 0.5\,m$ right-panel. The same convention as in Fig. 7.1 is used.

attractive owing to the larger mass of the exchanged boson.
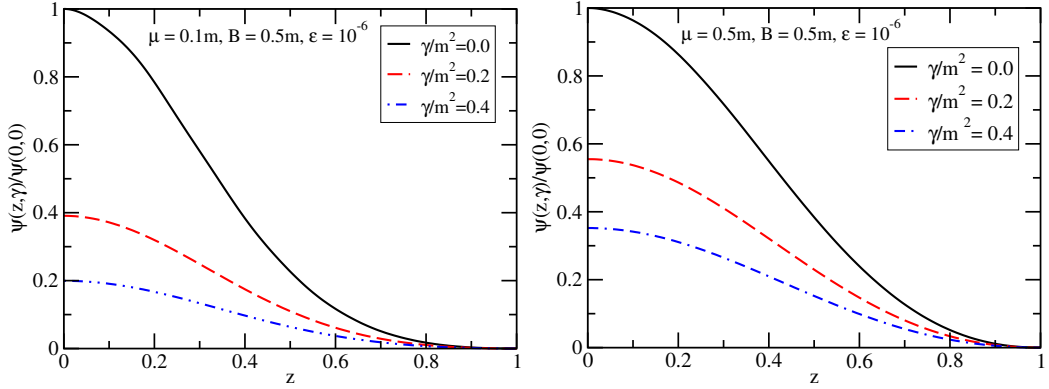
Figure 7.3: LFWF $\psi(\gamma, z)$ vs z for values $B = 0.5\,m$ with $\mu = 0.1\,m$ left-panel and $\mu = 0.5\,m$ right-panel with the normalization $\psi(0,0)=1$. The fixed values $\gamma/m^2=0$, 0.2, 0.4 were used.

As mentioned before with the dimension used for the basis functions the Nakanishi weight-function does not present convergence. However, from the plots is clear that the Euclidean BS amplitude and the LFWF are converged. We will show the numerical calculation of the Nakanishi weight-function in the next section when studying the effect of adding the cross-ladder kernel.

Fig. 7.5 shows a three-dimensional plot of the Euclidean BS amplitude. To compare clearer the results, we have added a plot with the ratio between the Euclidean BS amplitudes φ_E^n/φ_E^W obtained with the two methods. The ratio is calculated for a wide range of k and k_0 showing a impressive result of the Euclidean solution found with great accuracy from the Wick rotation of the Minkowski solution. Thus, the feasibility of the developed method was tested with success,

Figure 7.4: LFWF $\psi(\gamma, z)$ vs γ for values $B = 0.5\,m$ with $\mu = 0.1\,m$ left-panel and $\mu = 0.5\,m$ right-panel with the normalization $\psi(0,0)=1$. The fixed values $z=0$, 0.2, 0.4 were used

what encourages us to extend the method to more interesting problems.

7.3   2+1 dimensions Cross-ladder kernel

In this section, we focus on studying the effects of the Cross-ladder (CL) kernel in the eigenvalues (binding energies), the BS amplitude and LFWF, which are computed by means of the Nakanishi weight-function (eigenvectors). We consider the following kernel

$$V_{2+1}(z, z', \gamma, \gamma') = V_{2+1}^{(L)}(z, z', \gamma, \gamma') + V_{2+1}^{(CL)}(z, z', \gamma, \gamma'), \tag{7.13}$$

and we introduce it in the integral equation for the Nakanishi weight-function, then we compare the results obtained with the kernel Eq. (7.13) and those obtained with only the ladder kernel. The explicit expression of the Nakanishi kernel $V_{2+1}^{(CL)}$ is given in Eqs. (5.78), (5.79). Also, the comparison with the results obtained through Eq. (6.23), i.e, pure Euclidean calculation, is provided to verify the validity of the method by considering kernels beyond of ladder.

Below, we show in Table. 7.2 the eigenvalues corresponding to the L+CL kernel, comparing the result of the two approaches. From Table. 7.2 we see the agreement obtained between both approaches. As in the ladder case, the method is successfully extended for kernels beyond of ladder one without difficulty. We have concentrated in two values of μ, which from the numerical point view has good stability, however the calculation may be extended for other values. It is also important to point out that the time calculation for the L+CL kernel has increased respect to the ladder kernel, due to the integration in the internal momentum, which, in the numerical
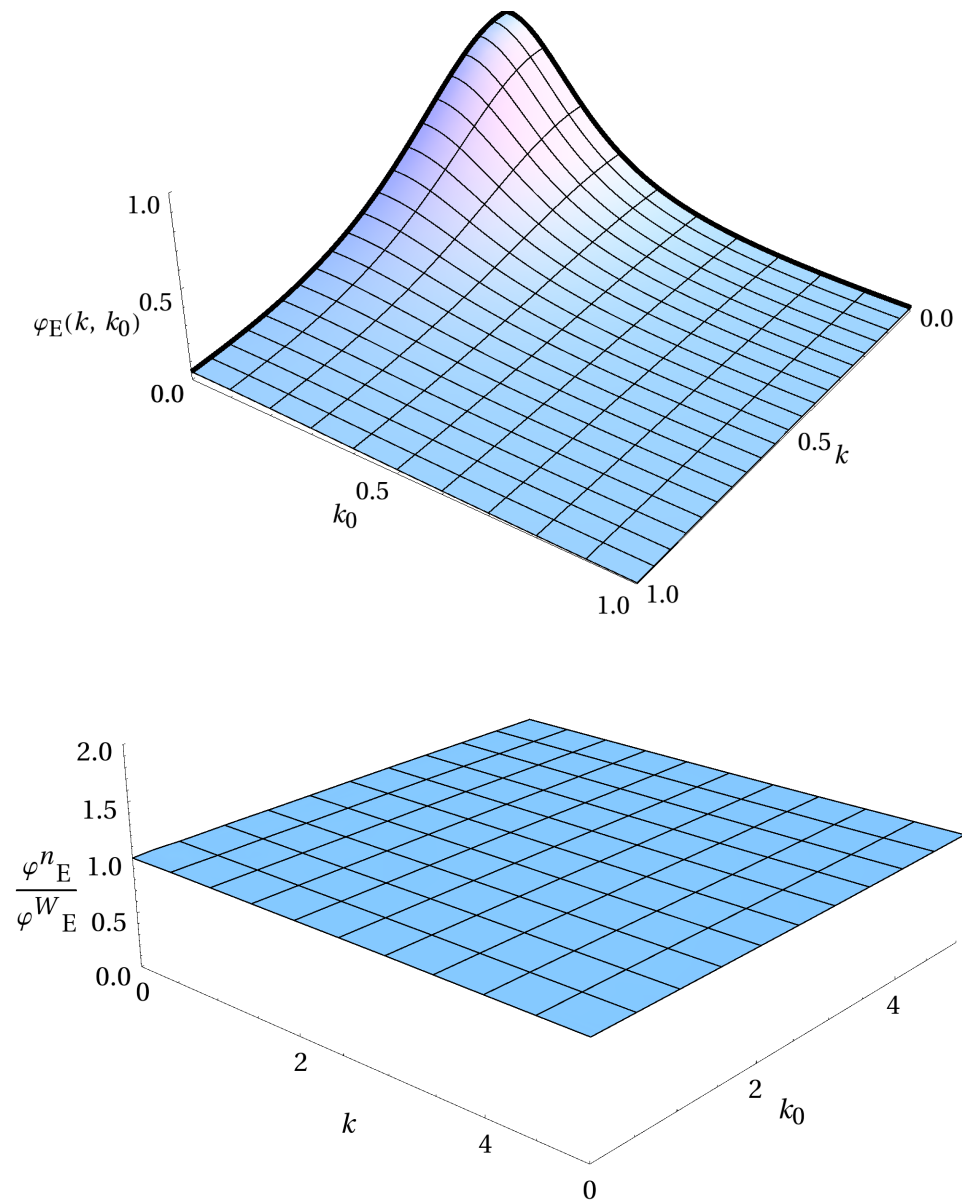
Figure 7.5: **Upper panel:** Euclidean BS amplitude calculated by means of Eqs. (6.9). **Lower panel:** Ratio between the Euclidean BS amplitude computed with the NIR method, $\varphi_E^n(k_0, k)$, and the Euclidean one computed with the standard Wick rotation, $\varphi_E^W(k_0, k)$. The parameters used for the calculations are $\mu = 0.5\,m$ and $B = 0.5\,m$

calculation is reflected in an integration upon four Feynman parameters.

Table 7.2: Comparison between the values of g^2/m^3 calculated by means of the BS equation with the NIR approach for the L+CL kernel and the calculation in Euclidean space, using only the rotation of Wick. Different binding energies B/m and two masses of the exchanged boson $\mu = 0.1\,m, 0.5\,m$ have been used.

	$\mu = 0.1$m		$\mu = 0.5$m	
B/m	**NIR**	**EUCL**	**NIR**	**EUCL**
0.01	0.730	0.72	4.832	4.82
0.1	3.273	3.27	11.984	11.98
0.2	5.832	5.825	17.261	17.26
0.5	13.177	13.17	29.720	29.71
1.0	23.396	23.36	44.818	44.80

For solving the Euclidean BS equation we have used 40 gauss points in both variables, k and k_0. For the calculation in the Minkowski space the basis expansion has been extended up to N_z=10 and N_g=25, for checking the stability of the results. In general, as in the ladder case, a larger Laguerre polynomials expansion than Gegenbauer polynomials expansion is required to get stability in the eigenvalues.

Now, we provide a comparison between the ladder and L+CL eigenvalues in 2+1 dimensions in Table. 7.3. From the table one realizes the non-negligible effect of the CL contribution in the eigenvalues. The coupling constant of the L+CL kernel has decreased with respect to the ladder one and this effect is more notable for states with high binding energy. Additionally, the effect of the CL contribution turns out in a more attractive interaction respect to the ladder one, since the CL kernel contains the exchange of two particles. To understand better this statement, consider fixed values of μ/m and B/m. The corresponding coupling constant is smaller for the L+CL kernel than for the ladder one. It means that with the L+CL kernel one can have a bound state with the same binding energy that the ladder kernel using a smaller coupling constant.

After showing the eigenvalues, we will display the effect of the CL contribution in the Euclidean BS amplitude and the LFWF. Before to discuss the physical effect of the CL contribution, we show the behavior of the Nakanishi weight-function. As mentioned in previous section, the convergence of the Nakanishi weight-function is difficult to obtain with the parameters that we used in this calculation. However, the relevant quantities computed through the Nakanishi weight-function as the LFWFs and the Euclidean BS amplitudes have the same convergence as

Table 7.3: Comparison L vs L+CL in 2+1 dimensions. Values of g^2/m^3 calculated with the BS equation in the NIR, for different binding energies B/m and masses of the exchanged boson μ/m.

B/m	$\mu = 0.1$m		$\mu = 0.5$m	
	L	**L+CL**	**L**	**L+CL**
0.01	0.812	0.730	5.341	4.832
0.1	4.269	3.273	14.877	11.984
0.2	8.068	5.832	22.671	17.261
0.5	19.516	13.177	42.336	29.720
1.0	36.048	23.396	67.391	44.818
1.5	46.830	29.937	82.793	53.904
1.9	50.406	32.087	87.799	56.795

the eigenvalues. In Figs. 7.6 and 7.7 the Nakanishi weight-function is shown for a fixed value of $N_z = 10$ and changing N_g. We appreciate that for N_z=25 the Nakanishi weight-function is different from that corresponding to N_z=10, 20, showing in this form the lack of convergence for this quantity. Instead the LFWF computed by means of this Nakanishi weight-function is quite converged as we appreciate in Figs. 7.8 and 7.9. This situation holds for ladder as well as CL kernel. The same behavior is encountered for the Euclidean BS amplitude. It is important to point out that this situation has been already found in the analysis performed in Ref. [8], for two-boson ground state in 3+1 dimensions. In that calculation a different numerical method to solve the integral equation for the Nakanishi weight-function was employed. Hence, this fact discards the possibility of this feature be associated with the numerical method employed here.
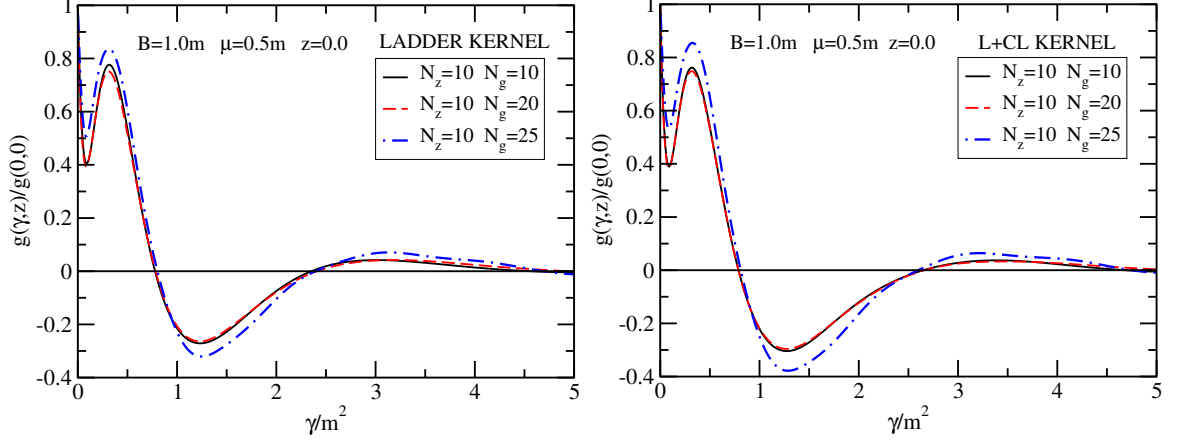
Figure 7.6: Nakanishi weight-function vs γ/m^2 for a fixed value z=0.0 with the parameters $B = 1.0\,m$ and $\mu = 0.5\,m$. Some values of the basis expansion N_g are used and N_z is fixed. **Left panel**: ladder kernel and **Right panel**: ladder + cross-ladder kernel.
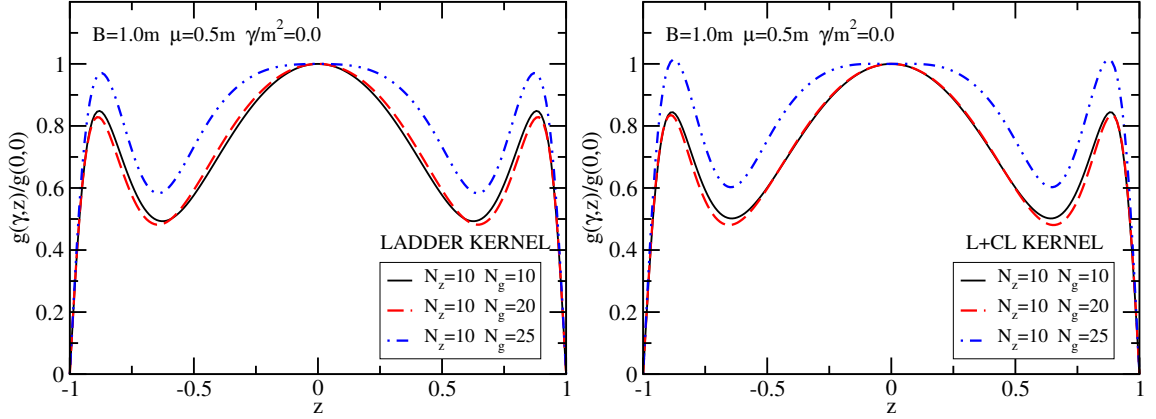
Figure 7.7: Nakanishi weight-function vs z for a fixed value γ/m^2=0.0 with the parameters $B = 1.0\,m$ and $\mu = 0.5\,m$. The same conventions of Fig. 7.6 are used.

After this remark, we analyze the Euclidean BS amplitude. As it can be seen from Fig. 7.10, the Euclidean amplitudes computed with the two methods, as in the ladder kernel, are in agreement. Besides, we see the effect of the CL contribution in the Euclidean BS amplitudes, which, differently from the eigenvalues, is very small. In fact, we have plotted Euclidean BS amplitude using logarithmic scale to recognize the CL effect. The arbitrary normalization $\varphi_E(k_0 = 0, k = 0)$=1 is adopted.
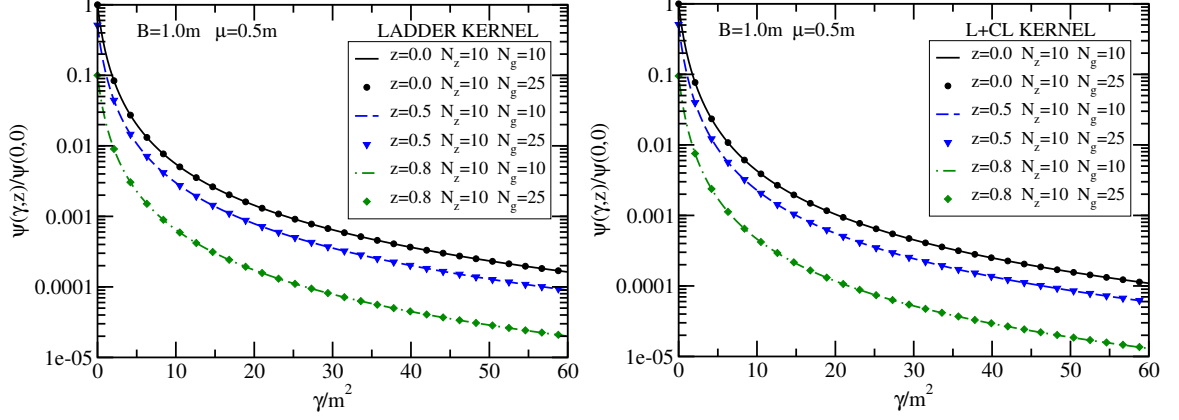
Figure 7.8: LFWF vs γ/m^2 for the parameters $B = 1.0\,m$ and $\mu = 0.5\,m$ for three values of z. The value of N_z is fixed and N_g is changing. **Left panel**: Ladder kernel and **Right panel**: L+CL kernel.
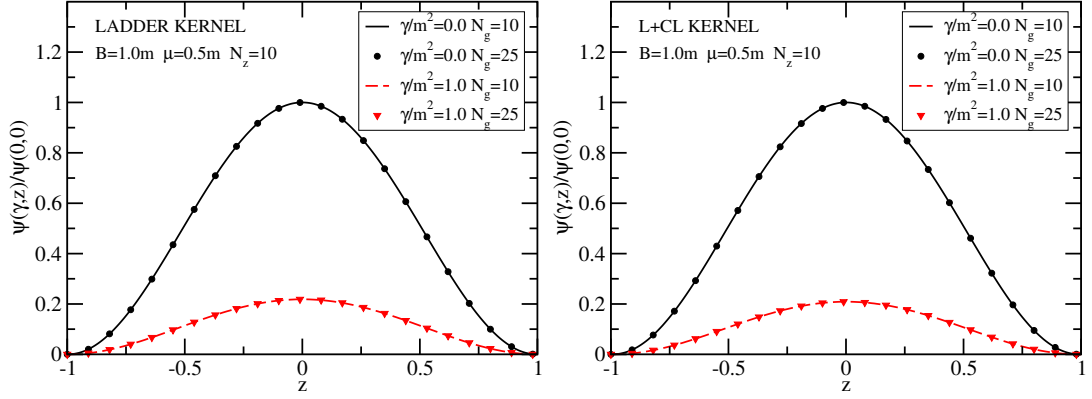
Figure 7.9: LFWF vs z for the parameters $B = 1.0\,m$ and $\mu = 0.5\,m$ for two values of γ/m^2. The other conventions are the same as in Fig. 7.8.

Now, let us to investigate the CL effects in the LFWF. In the Figs. 7.11 and 7.12 we display the behavior of the LFWF as function of γ/m^2 and z, respectively. We have plotted the LFWF for some values of the mass of the exchanged boson μ. Furthermore, we show the asymptotic behavior of the LFWF, i.e, $\gamma/m^2 \to \infty$ in Fig. 7.13. Again, the arbitrary normalization $\psi(\gamma = 0, z = 0) = 1$ is used.

Contrary to the eigenvalues, in the LFWF the CL effect is rather small as one can see from Fig. 7.11, therefore the dominant effect is given by the ladder contribution in the interaction kernel. After using the normalization $\psi(0,0) = 1$ and fixing the binding energy, one sees that in the low momentum region the LFWF is the same independently of the interaction kernel and the effect of the CL kernel, which changes the coupling constant, is manifested in the region of
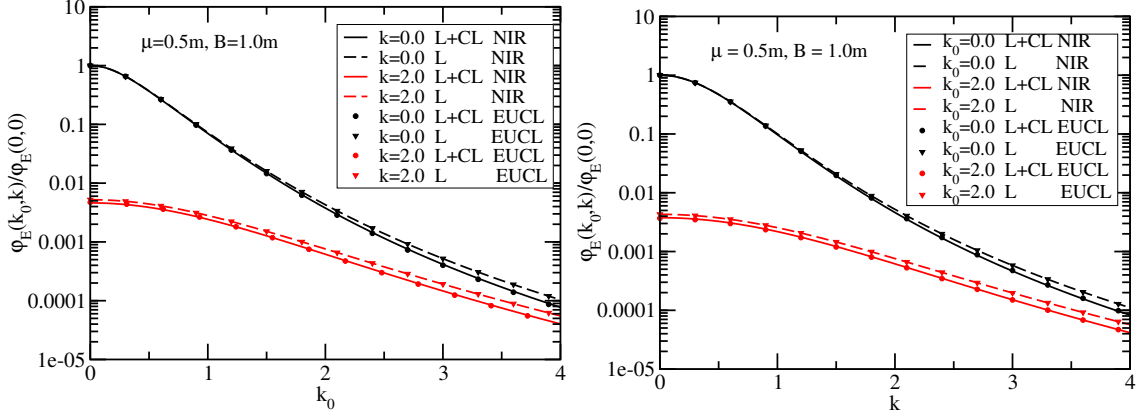
Figure 7.10: Comparison of the Euclidean BS amplitude for ladder (L) and ladder plus cross-ladder (L+CL) kernel calculated for two methods. **Left panel**: Euclidean BS amplitude vs k_0 for some fixed values of k. **Right panel**: Euclidean BS amplitude vs k for fixed values of k_0.
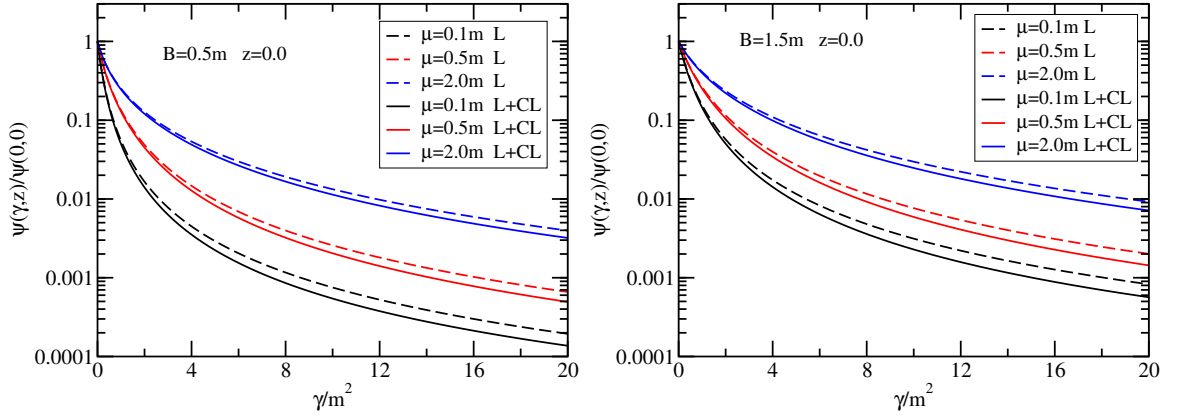
Figure 7.11: $\psi(\gamma, z)$ vs γ/m^2 for fixed value of the binding energy and changing the values of μ/m. **Left panel**: $B/m = 0.5\,m$. **Right panel**: $B/m = 1.5\,m$

high momentum, by scaling the tail of the wave function. We also appreciate from the same figure that wave function for L+CL kernel falls faster than the ladder one. This is expected since that for a given binding energy $\alpha_L > \alpha_{L+CL}$, therefore the LFWF for the ladder kernel is more concentrated towards the origin, what is consistence with the behavior in the momentum space shows in Fig. 7.11.

Exploring the asymptotic limit in Fig. 7.13, it enables us to conclude that in this limit the LFWF behaves as $1/\gamma^2$ independently of the value of μ, reproducing in this way another feature of the wave function in LF dynamics, see Ref. [11]. Furthermore, from Fig. 7.12, we appreciate the expected symmetry $z \to -z$ of the LFWF obtained through the Nakanishi weight-function.
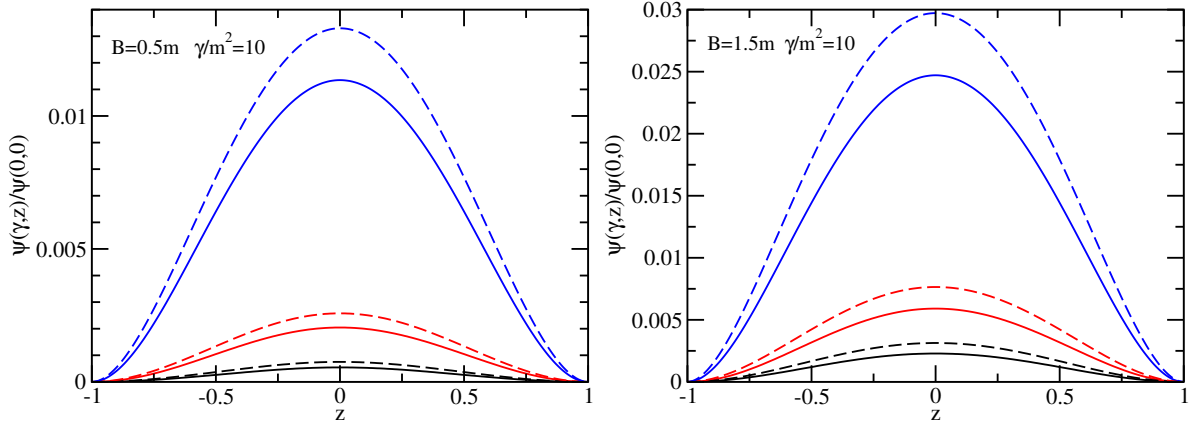
Figure 7.12: $\psi(\gamma, z)$ vs z for fixed value $\gamma/m^2{=}10$ and varying the value of the exchanged boson mass μ/m. The same conventions as in Fig. 7.11 are used. Note that the choice $\gamma/m^2{=}10$ is arbitrary and it is only a value that enables us to appreciate the difference between L and L+CL.
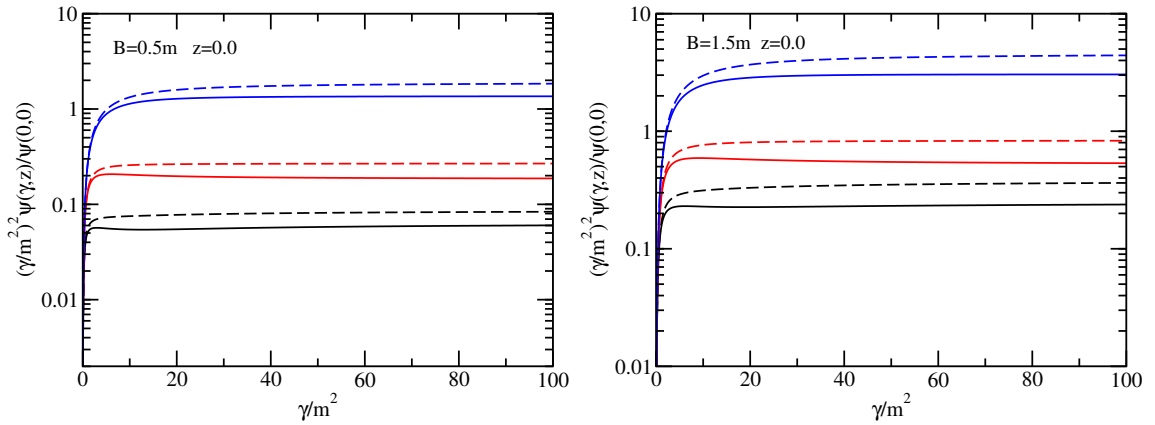
Figure 7.13: Asymptotic behavior of the LFWF for fixed value the binding energy and changing the values of μ/m. **Left panel:** $B = 0.5\,m$. **Right panel:** $B = 1.5\,m$. The same conventions as in Fig. 7.11 are used.

Chapter 8

Spectrum of the Bethe-Salpeter equation

In this chapter we focus on the study of the spectrum of the excited states of the scalar BS equation, in ladder approximation. This analysis is carried out for the Yukawa theory of an interacting system composed by two massive bosons exchanging a massive scalar, by adopting the NIR of the BS amplitude and the formal exact projection onto the null plane. Since the study of the spectrum is done for first time, we restrict the calculation to 3+1 dimensions.

We start by recalling the expression for the ladder kernel used in this analysis

$$i\,K^{(L)}(k,k') = \frac{i\,(-i\,g)^2}{(k-k')^2 - \mu^2 + i\,\epsilon} = -i\,\frac{\alpha\,(16\pi m^2)}{(k-k')^2 - \mu^2 + i\,\epsilon}\,, \tag{8.1}$$

where $\alpha = g^2/(16\pi m^2)$ is the standard coupling constant used in 3+1 dimensions. Now, we explain in shortly the method to get the spectrum in this approach. After introducing the basis function expansion and the ladder approximation Eq. (8.1), into the Nakanishi integral equation, it turns into the matrix form of a generalized eigenvalue problem, presented previously Eq. (7.8)

$$\frac{1}{\alpha}\,g^{(L)} = \mathcal{B}(M)^{-1}\mathcal{A}(M)g^{(L)}.$$

We recall that $B = 2m - M$. We start by doing an inspection of this equation to study the spectrum of excited states. We choose three values for masses of exchanged boson, then we compute the coupling constant for the ground, first- and second-excited states, covering the full range of binding energy allowed for this model. Our numerical results are summarized in Fig. 8.1
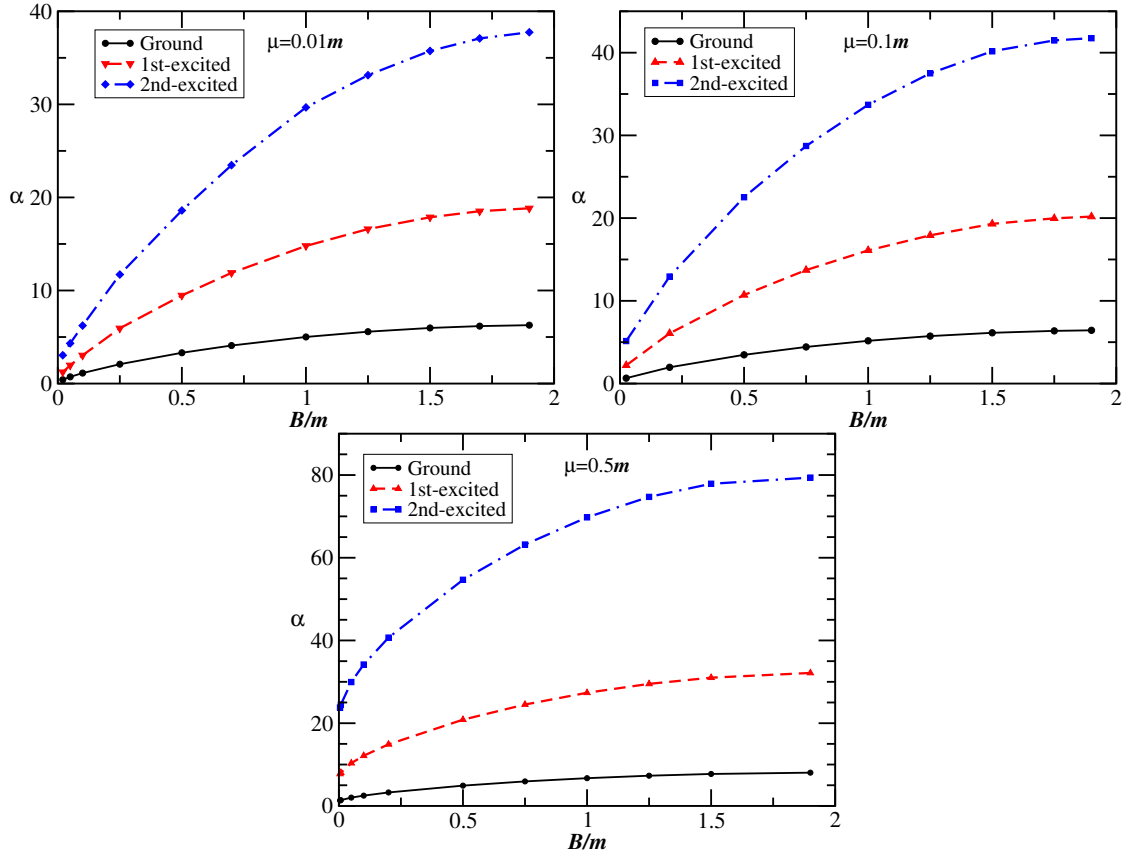
Figure 8.1: Behavior of the coupling constant as function of the binding energy for the ground (black-full line), first-excited (red-dashed) and second-excited (blue-dotted-dashed line) states. The mass of the exchanged boson is fixed in each plot.

To construct the above curves of the excited states, one uses the fact that for the eigenvalue equation with the ladder kernel, the coupling constant plays the role of eigenvalue. In the numerical diagonalization process one obtains a set of eigenvalues, where the first eigenvalue represents the coupling constant of the ground state, the second eigenvalue that of the first-excited state and so on. The interpretation of the spectrum of excited states given from Fig. 8.1 is as follows: take a value of the coupling constant and then draw a line parallel to the x-axis. This line should cut the curves of the ground and excited states in the values corresponding to the binding energies, therefore one has $B(0)/m > B(1)/m > B(2)/m$ where $B(n)$ stands for the binding energy of the ground and excited states with $n = 0, 1, 2, 3..$ and $B(0) = B_{gr}$. However, there exist an ambiguity in this interpretation, since one can choose values of coupling constants which only cut the lines of the excited states, leading to a disagreement in the identification

of the ground state. In order to avoid this ambiguity, we only consider values of coupling constant which always cut the curve of the ground state. This restriction is justified because if we compute the LFWF with the corresponding eigenvector $g(\gamma, z)$ associated to the ground and excited states, one obtains a well known feature of the excited states: the presence of nodes in the LFWF for excited states. This is consistence with what one expects from the non-relativistic counterparts.

Hence, within the NIR studies of the ladder BS equation, Eq. (7.8) has a pivotal role. First, after fixing m, μ and B_{gr}, it yields the coupling constant of the ground state, i.e. the smallest value of the coupling constant that we call α_{gr}; secondly it allows one to calculate the spectrum. Indeed, once we have found the coupling constant from the ground state α_{gr}, one can find the excited state respect to B_{gr} by slightly changing Eq. (7.8), as follows

$$\lambda \, g^{(L)} = \alpha_{gr} \, \mathcal{B}(M)^{-1} \mathcal{A}(M) g^{(L)} \quad . \tag{8.2}$$

In other words, after fixing m, μ and α_{gr}, we search for values $M = 2m - B > M_{gr}$ that produce eigenvalues $\lambda = 1$ (as trivially seen, for $M = M_{gr}$ one has $\lambda = 1$).

We close this section mentioning the similarity of the relativistic spectrum with the non-relativistic Yukawa potential, namely the existence of a finite number of excited states for $\mu/m > 0$ [48]. By observing Fig. 8.1 one realizes that the cases $\mu/m = 0.01$ and $\mu/m = 0.1$ produce two excited states for almost whole range of binding energy of the ground state. Instead, in the case $\mu/m = 0.5$ hardly appears one excited state for large binding energy of the ground state.

8.1 Comparing Minkowski and Euclidean eigenvalues

In order to verify the reliability of the computed masses for the excited states, we provide a comparison between the results of our calculations, obtained in the Minkowski space within the NIR, with those one can evaluate in the Euclidean space. To obtain the spectrum of the Euclidean BS equation we follow a similar procedure, in this case one has

$$\lambda \, \varphi_E = \alpha_{gr} \, \mathcal{A}(M) \, \varphi_E, \tag{8.3}$$

where φ_E is the Euclidean BS amplitude. In Table. 8.1, we show the binding energies, in

unit of the constituent mass m, for the first, $B(1)/m$, and the second, $B(2)/m$, excited states, corresponding to a ground state $B(0)/m = 1.9$ and different values of μ/m. The choice of such a large binding energy is motivated by the fact that strongly-bound states should be affected by large relativistic effects.

Table 8.1: Comparison of the spectra obtained in the Euclidean space and in the Minkowski one, by varying μ/m and, consequently, α_{gr}, but taken fixed the value of the ground-state binding energy to $B(0)/m = 1.9$.

$(\mu/m, \alpha_{gr})$		**Euclidean**	**Minkowski**
(0.05, 6.324)	$B(1)/m$	0.258	0.259
	$B(2)/m$	0.090	0.089
(0.1, 6.437)	$B(1)/m$	0.220	0.221
	$B(2)/m$	0.051	0.050
(0.5, 8.047)	$B(1)/m$	0.0082	0.0082

We verified from the table that the values of α_{gr} for the binding energy of the ground state of $B(0)/m = 1.9$, obtained with Euclidean- and Minkowski-space calculations are the same within our numerical accuracy. Then, we have computed the excited state energies given in Table. 8.1, achieving a very satisfactory agreement between the results evaluated in the two spaces. As a remark on the numerical procedure, it should be pointed out that for values of μ/m smaller than 0.05 or $B/m < 0.01$ the convergence is quite slow, and it is needed an extrapolation of the results with respect to N_g, in order to accurately determine the eigenvalues. The details of the extrapolation procedure are shown in Appendix.A.

It is also important to show the behavior of energy ratios, $B(n)/B(0)$ with $n \geq 0$, for small B/m and $\mu \to 0$, where one expects to obtain the non-relativistic limit. For a bound state composed for two spinless bosons exchanging a massless scalar boson, the corresponding relativistic expression in lower orders of α, as derived in Ref. [50], is

$$B(n) = \frac{m}{4} \frac{\alpha^2}{(n+1)^2} \left[1 + \frac{4\alpha}{\pi} \ln \alpha \right] + ... \quad (n \geq 0). \tag{8.4}$$

The first term is the non-relativistic limit. As verified in Fig. 8.2, for two values of $B(0)/m$: 0.5, 0.3, where $B(1)/B(0)$ and $B(2)/B(0)$ are shown for small values of μ/m, the energy ratios are consistent with the non-relativistic limit.
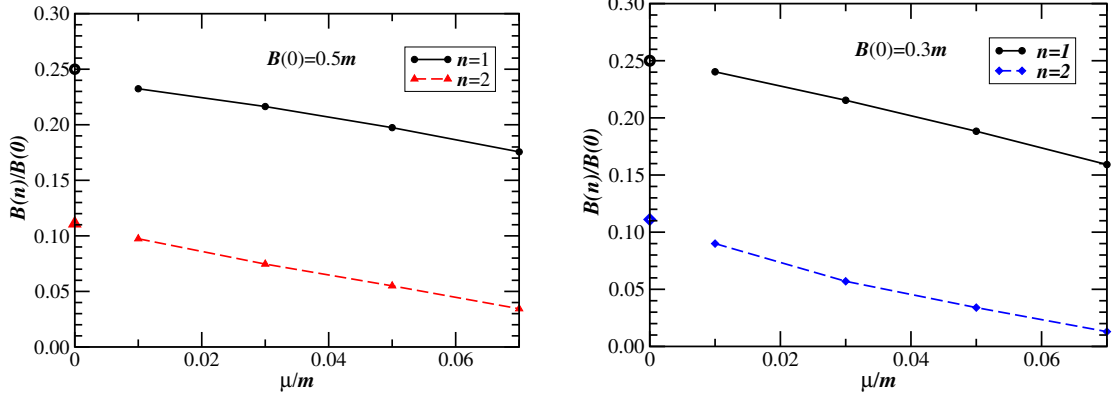
Figure 8.2: Energy ratios $B(n)/B(0)$ vs μ/m for the first (solid line with bullets) and second (dashed line with triangles) excited states. The symbols on the lines are the values obtained through Eq. (7.8), while the circle ($n = 1$) and the triangle ($n = 2$), at the origin, represent the corresponding non-relativistic limits, given by Eq. (8.4) with $B_{nr}(0)/m = 0.25\alpha^2$.

Table 8.2: Comparison between the binding energy of the ground state obtained with the NIR method and that obtained analytically in the Euclidean space Eq. (8.4) .

α_{gr}	$B(0)/m$ [NIR]	$B(0)/m$ [Eq. 8.4]
0.272	0.010	0.010
0.344	0.015	0.015
0.401	0.020	0.021
0.460	0.025	0.028
0.519	0.030	0.038
0.621	0.040	0.060

Moreover, the agreement for $\mu \to 0$ between the relativistic and non-relativistic eigenvalues is observed only for small values of $B(0)/m$ as showed in Table. 8.2. We display a set of binding energies to verify the range where the Eq. (8.4) holds. One sees that for $B(0)/m < 0.2$, our calculation agrees with the spectrum formula obtained analytically. This result is expected since Eq. (8.4) was obtained performing a standard perturbation expansion in α_{gr}, hence for small values of α_{gr} the first two terms are the most relevant.

8.2 Valence light-front wave function and momentum distributions

It is attractive to perform numerical comparisons of dynamical quantities that in perspective could be useful for an experimental investigation of actual interacting systems. In view of this, for the valence LFWF introduced in the Sec. 3.3 we have defined the normalization of the valence component in Eq. (3.35) in the following form

$$P_{val} = \frac{1}{(2\pi)^3} \int_0^1 \frac{d\xi}{2\xi(1-\xi)} \int d^2\mathbf{k}_\perp \left[\psi(\xi, \mathbf{k}_\perp)\right]^2, \qquad (8.5)$$

with $P_{val} \equiv N_2$ defined in Eq. (3.35) and $d^2\mathbf{k}_\perp = d\gamma \, d\theta/2$, $\gamma = \mathbf{k}_\perp^2$. Note that we have changed the dependence of z to ξ in LFWF by means of the relation $\xi = (1-z)/2$, because ξ will be more convenient for the forthcoming analysis. One can define both the probability distribution to find a constituent with LF longitudinal fraction $\xi = p_i^+/P^+$, given by

$$\varphi(\xi) = \frac{1}{2(2\pi)^3} \frac{1}{\xi(1-\xi)} \int d^2\mathbf{k}_\perp \left[\psi(\xi, \mathbf{k}_\perp)\right]^2, \qquad (8.6)$$

and the probability distribution to find a constituent with LF transverse momentum $k_\perp = |\mathbf{k}_\perp|$, that reads

$$\mathcal{P}(k_\perp) = \frac{1}{4(2\pi)^3} \int_0^1 \frac{d\xi}{\xi(1-\xi)} \int_0^{2\pi} d\theta \left[\psi(\xi, \mathbf{k}_\perp)\right]^2. \qquad (8.7)$$

Both LF distributions are normalized to the probability of the valence component, once the BS amplitude itself is properly normalized (see Ref. [39] for a general discussion and Ref. [12] for the application within the NIR). Such a probability yields the probability to find the valence contribution in the LF Fock expansion of the interacting two-scalar state (see, e.g., Ref. [9, 11]). In fact, one has

$$P_{val} = \int_0^1 d\xi \, \varphi(\xi) = \int_0^\infty dk_\perp \, \mathcal{P}(k_\perp). \qquad (8.8)$$

Notice that $\mathbf{k}_\perp$ can be associated with the intrinsic transverse momentum, in the frame where $\mathbf{p}_\perp = 0$, which is allowed by the covariance of our description.

Although we have discussed the issue of the proper normalization of the valence state, in what follows we are interested on the overall 3D structure of the valence wave function, and

therefore we have simply adopted an arbitrary normalization.

8.3 Momentum space valence light-front wave function for excited states

In Figs. 8.3 and 8.4, we present the LFWF of the first (left panels) and second (right panels) excited states, corresponding to the case μ/m=0.1, α_{gr}=6.437, $B(1)/m$=0.22 and $B(2)/m$=0.05 (see Table. 8.1). As clearly shown, the wave function displays the typical feature of the first- and second-excited states, i.e. one and two *nodes*, respectively.

By a direct inspection of the corresponding panels for the first-excited state in Fig. 8.3 and for the second excited state in Fig. 8.4, one observes that, in the plane $(\xi, k_\perp/m)$, the node structure is present for $(k_\perp/m)^2 < 1$ and $\xi < 0.75$, and it is symmetric with respect to $\xi = 1/2$. In particular, the node structure moves toward $\xi = 1/2$ as $k_\perp$ increases. Such a behavior can be naively expected when Cartesian three-momenta are related with the LF components

$$\left[\sqrt{\mathbf{p}_1^2 + m^2} + \sqrt{\mathbf{p}_1^2 + m^2}\right]^2 - (\mathbf{p}_1 + \mathbf{p}_2)^2 = p^+ \left[\frac{m^2 + \mathbf{p}_1^{\perp 2}}{p_1^+} + \frac{m^2 + \mathbf{p}_2^{\perp 2}}{p_2^+}\right] - \mathbf{p}_\perp^2, \qquad (8.9)$$

in the rest frame, $\mathbf{p}_1 + \mathbf{p}_2$=0, and introducing the relative coordinates we obtain the relation

$$\mathbf{k}^2 = \frac{k_\perp^2 + m^2}{4\xi(1 - \xi)} - m^2. \qquad (8.10)$$

If we assume a dependence upon $\mathbf{k}^2$ for the excited-state valence wave function (instead of the actual dependence upon ξ and $k_\perp$, separately), i.e. the same dependence found in phenomenological valence wave functions widely adopted for describing ground states (as the one exploited in the discussion of the nucleon form factors in Ref. [11]), then the behaviors shown in Figs. 8.3 and 8.4, for the node structures and asymptotic behaviors of the states, become quite reasonable. Indeed, the assumed excited-state valence wave functions have to display a node at a fixed value for $\mathbf{k}^2$, and therefore according to Fig. 8.3, for increasing $k_\perp$ the variable ξ is constrained to approach 1/2 (i.e. the maximal value of $\xi(1 - \xi)$), in order to take (almost) constant $\mathbf{k}^2$. In conclusion, the correlation between the LF components, ξ and $k_\perp$, in determining the node position can be largely explained by the rotational invariance of the phenomenological wave functions, if they depend upon $\mathbf{k}^2$. Notably, our calculations, genuinely in Minkowski space, actually confirm the overall expectation, based on a simple phenomenological *ansatz*, that takes

into account the rotational invariance. It should be reminded that, within a LF framework, the rotational invariance can be fully recovered only if the whole Fock expansion is considered [11]. We just add that the second node present in the right panel of Fig. 8.3.
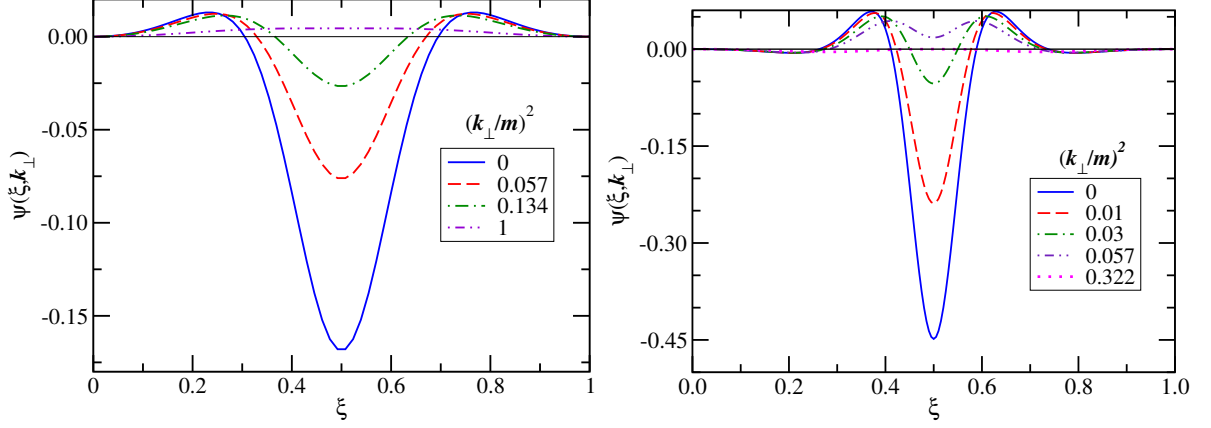
Figure 8.3: The valence wave functions vs ξ with fixed values of $(k_\perp/m)^2$, for the first (left panel) and second (right panel) excited states, with $B(1)/m = 0.22$ and $B(2)/m = 0.05$, respectively, obtained from Eq. (7.8) with $\mu/m = 0.1$ and $\alpha_{gr}=6.437$.

According to Eq. (5.12), the LFWF in terms of $\mathbf{k}_\perp$ and ξ reads as

$$\psi(\xi, \mathbf{k}_\perp) = \frac{1}{\sqrt{2}}\xi(1-\xi) \int_0^\infty d\gamma' \frac{g(\gamma', 1-2\xi)}{\left[\gamma' + k_\perp^2 + \kappa^2 + (1-2\xi)^2 \frac{M^2}{4}\right]^2}, \tag{8.11}$$

hence, one can obtain the asymptotic behaviors, $k_\perp \to \infty$, of the valence LFWF for bound states, which are given by

$$\psi(\xi, \mathbf{k}_\perp) \to k_\perp^{-4}\, C(\xi)\,. \tag{8.12}$$

Such behavior is explicitly shown in Fig. 8.5 for the first two excited states (for ground-state, see Ref. [12]). For the second-excited state the range of $(k_\perp/m)^2$ is extended up to 400 to appreciate the asymptotic of the LFWF. It should be emphasized that independently of the value of ξ the wave function is damped as $\sim k_\perp^4$.
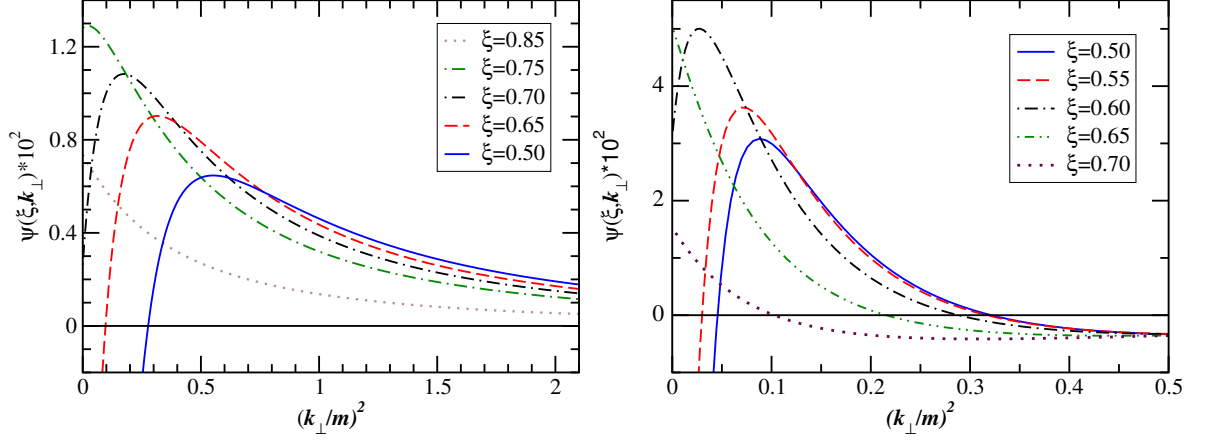
Figure 8.4: The valence wave functions vs $(k_\perp/m)^2$ with fixed values of ξ, for the first (left panel) and second (right panel) excited states, with $B(1)/m = 0.22$ and $B(2)/m = 0.05$, respectively, obtained from Eq. (7.8) with $\mu/m = 0.1$ and $\alpha_{gr} = 6.437$.

8.4 Transverse-momentum amplitudes

In this subsection we discuss the equivalence of the transverse-momentum amplitudes in Minkowski and Euclidean spaces [45], respectively defined as

$$\phi_M^T(\mathbf{k}_\perp) \equiv \int dk^0 \ dk^3 \varphi(k,p) = \frac{1}{2} \int dk^+ \ dk^- \varphi(k,p) \qquad (8.13)$$

$$\phi_E^T(\mathbf{k}_\perp) \equiv i \int dk_E^0 \ dk^3 \varphi_E(k_E,p), \qquad (8.14)$$

where $\varphi_E(k_E,p)$ is obtained from $\varphi(k,p)$ after applying the Wick rotation with $k^0 \to ik_E^0$. We explore the equivalence of these two amplitudes in this section.

One can easily prove within the NIR that $\phi_M^T(\mathbf{k}_\perp) = \phi_E^T(\mathbf{k}_\perp)$, since one can exploit the explicit expression of the analytic dependence of the BS amplitude, given by

$$\varphi(k,p) = -i \int_{-1}^{1} dz' \int_0^\infty \frac{g(\gamma',z')}{[\gamma' + \kappa^2 - k^2 - p \cdot k z' - i\epsilon]^3}. \qquad (8.15)$$

In fact, choosing the rest frame, $p = (M, \mathbf{0})$, one can straightforwardly see that the zeros of the Nakanishi denominator in the complex plane of k_0 are given by:

$$k_0 = -\frac{M z'}{2} \pm \sqrt{\frac{M^2 z'^2}{4} + \gamma' + \kappa^2 + k_3^2 + k_\perp^2 - i\epsilon}, \qquad (8.16)$$
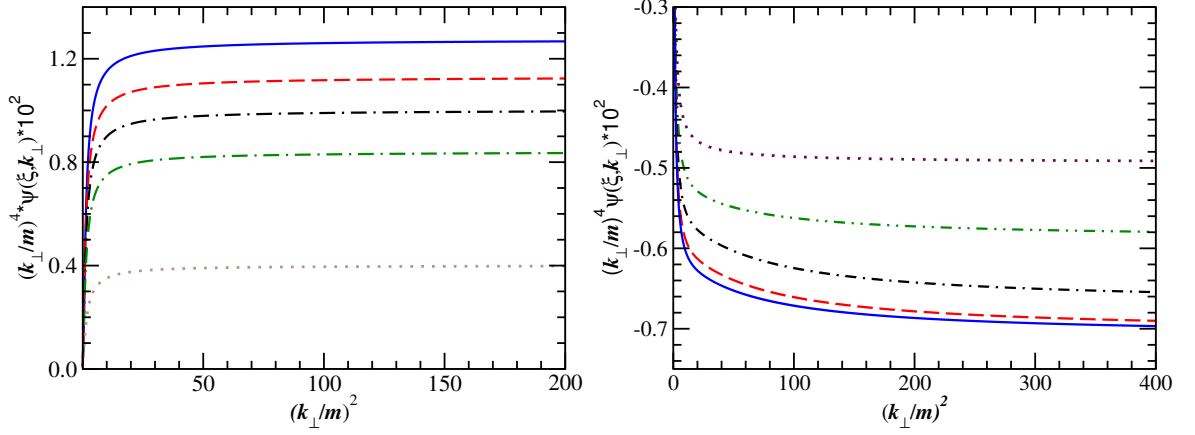
Figure 8.5: The asymptotic $k_\perp$ behaviors of the first (left panel) and second (right panel) excited states are shown, using the same label convention as given in Fig. 8.4.

with $z' \in [-1, 1]$ and $\gamma' \in [0, \infty]$. Therefore, Eq. (8.15), as a function of complex k_0, has two cuts, with branch-points at

$$k_{0\pm}^b = \pm \left(\frac{M}{2} - \sqrt{\frac{M^2}{4} + \kappa^2} + i\epsilon \right) , \tag{8.17}$$

with $k_\perp^2 = k_3^2 = 0$ as minimal values and recalling that κ^2 is positive for bound states. We can appreciate the branch cuts in Fig. 8.6. The branch-point k_{0+}^b a cut starts in the upper half-plane for $\mathrm{Re}\,k_0 < 0$, while at the branch-point k_{0-}^b the cut is placed in the lower half-plane for positive values of $\mathrm{Re}\,k_0$, as shown in Fig. 8.6.
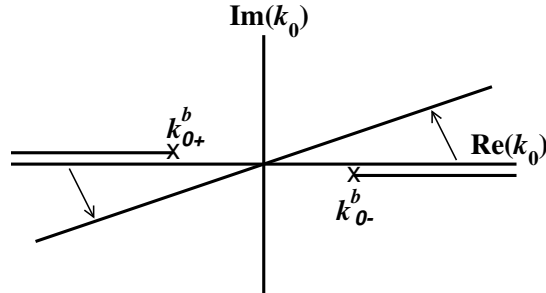
Figure 8.6: Analytic structure of the BS amplitude in the complex plane of k_0, showing the left- and right-hand cuts with the corresponding branch points $k_{0\pm}^b$. The rotation path of the k_0-integration contour is also shown for the transverse amplitude Eq. (8.13).

Adopting the Minkowski BS amplitude in Eq. (8.14), the position of the cuts enables to

rotate the integration variable k_0 to the complex values, i.e. $k_0 = |k_0|e^{i\theta}$, and the angle θ rotates up to 90°, without cross singularities. Furthermore, assuming that the BS amplitude drops out fast enough for large complex $|k_0|$, the Cauchy theorem holds and the Wick rotation [3] can be applied for computing the transverse amplitude. Namely, one can adopt a new integration path, along a purely imaginary k_0, without dealing with any singular integrals. Consequently, the Minkowski and Euclidean transverse amplitudes, given by Eqs. (8.13) and (8.14) are formally equivalent. It should be pointed out that this analytic behavior is also obtained when studying the analytical properties of the BS amplitude without knowledge of the NIR, as presented in Sec.2.2. The equivalence Eq. (8.13) gives an additional confidence in NIR, since allows to compare the transverse amplitudes obtained by two methods. Differently from the Euclidean BS amplitude evaluated previously, where the NIR together with the Wick rotation must be adopted, the transverse amplitudes are evaluated independently by using the NIR and the Wick rotation.

The quantitative comparison for the cases μ/m=0.1 and 0.5, with α_{gr} taken from Table. 8.1 (recall that one has always $B(0)/m = 1.9$), is presented in Fig. 8.7, showing an impressive agreement between the transverse amplitudes, within the accuracy of our numerical approaches. Therefore the comparison in Fig. 8.7 should be considered as a further check of the reliability of the NIR itself, at least at the ladder level, besides the passed tests for both eigenvalues [6, 7, 8, 12] and scattering lengths [16]. Moreover, Fig. 8.7 illustrates nice and general features of the transverse amplitudes, that appear when the binding energies change. For instance, the position of the node in the first excited state moves toward smaller values of $k_\perp$ as the binding energies decreases, i.e. from the left panel ($B(1)/m = 0.22$) to the right panel ($B(1)/m = 0.0082$). Analogously, the amplitudes themselves decrease more quickly in momentum space. Both features can be explained by the increase of size of the bound state when the binding energy decreases.

8.5 Valence light-front wave function in the impact-parameter space

In addition to the spectrum of the excited states obtained previously using the NIR, we explore the three-dimensional structure of the ground and excited states. The structure is analyzed
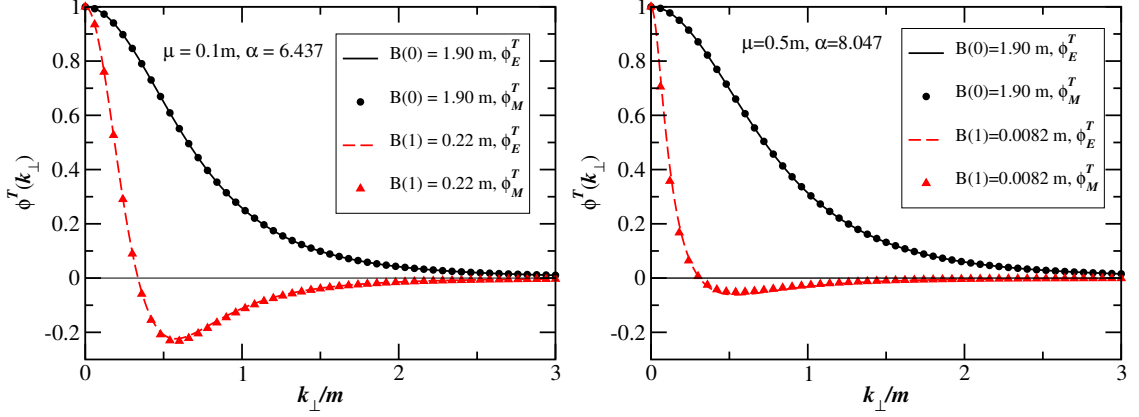
Figure 8.7: Transverse momentum amplitudes $s-$wave states, in Euclidean and Minkowski spaces, vs $k_\perp$, for both ground- and first-excited states, and two values of μ/m and α_{gr} (as indicated in the insets). The amplitudes ϕ_E^T and ϕ_M^T, arbitrarily normalized to 1 at the origin, are not easily distinguishable.

by means of the three-dimensional representation of the valence component of the LFWF. A convenient and useful form to study the valence amplitude is by considering the impact parameter (IP) space (see, e.g., Ref. [27]), in connection with the Generalized Parton Distributions (GPD), by keeping the longitudinal momentum and performing the Fourier transform over the transverse momentum. This mixed representation shows the correlation between the momentum fraction carried by the constituent and its probability distribution in the transverse plane. It is particularly interesting for the analysis of fermionic systems carrying both angular momentum and spin, with a distribution correlated to the longitudinal momentum, as a reflection of the internal dynamics.

The concept of transverse charge densities have been thoroughly discussed by Miller in Ref. [62], in close relation to the elastic electromagnetic form factor. Indeed, the transverse charge density enables one to properly generalize the well-known non-relativistic relation between form factor and density to a relativistic framework. In fact, it turns out that for a composite bosonic state, the form factor $F(Q^2 = -q^2)$ can be written as

$$F(Q^2) = \int d^2\mathbf{b}\ \rho(\mathbf{b})\ e^{-i\mathbf{b}\cdot\mathbf{q}_\perp}, \qquad (8.18)$$

where (i) the momentum transfer q^μ is evaluated in the Breit frame with $q^+ = 0$, (ii) $Q^2 = \mathbf{q}_\perp^2$, (iii) $\mathbf{b}$ belongs to the transverse plane or IP-space, and (iv) $\rho(\mathbf{b})$ is the IP density. The impact

parameter density is a sum of the contributions from all Fock components of the LF wave function,

$$\rho(\mathbf{b}) = \rho_{\text{val}}(\mathbf{b}) + \text{ higher Fock states densities} \cdots . \tag{8.19}$$

The valence term is defined through the valence wave function in the IP space, $\phi(\xi, \mathbf{b})$, as follows

$$\rho_{\text{val}}(\mathbf{b}) = \frac{1}{4\pi} \int_0^1 \frac{d\xi}{\xi(1-\xi)^3} \, |\phi(\xi, \mathbf{b}/(1-\xi))|^2 \tag{8.20}$$

with normalization (cf. Eq. (8.8))

$$\int d^2\mathbf{b} \, \rho_{\text{val}}(\mathbf{b}) = P_{val}. \tag{8.21}$$

In Eq. (8.20), the IP-space valence wave function is the 2D Fourier transform of $\psi(\xi, \mathbf{k}_\perp)$, given by

$$\phi(\xi, \mathbf{b}) = \int \frac{d^2\mathbf{k}_\perp}{(2\pi)^2} \, \psi(\xi, \mathbf{k}_\perp) e^{i\mathbf{k}_\perp \cdot \mathbf{b}}, \tag{8.22}$$

where $\phi(\xi, \mathbf{b})$ results to be symmetric with respect to $1 - 2\xi$, as a consequence of the already discussed symmetry of $g(\gamma, z)$ under the transformation $z \to -z$. Moreover, one can deduce the general behavior for large transverse separations, $b = |\mathbf{b}|$, as illustrated in what follows. By performing the 2D Fourier transformation, the IP-space valence wave function can be written within NIR for the s-wave state as follows

$$\phi(\xi, \mathbf{b}) = \frac{\xi(1-\xi)}{4\pi\sqrt{2}} F(\xi, b), \tag{8.23}$$

where

$$F(\xi, b) = \int_0^\infty d\gamma \, J_0(b\sqrt{\gamma}) \int_0^\infty d\gamma' \, \frac{g(\gamma', 1 - 2\xi)}{[\gamma + \gamma' + \kappa^2 + (1/2 - \xi)^2 M^2]^2} \,, \tag{8.24}$$

with $J_n(x)$ the integer-order Bessel function for $n = 0$. The integration over γ can also be analytically carried out, leading to

$$F(\xi, b) = b \int_0^\infty d\gamma \, g(\gamma, 1 - 2\xi) \frac{K_1\left(b\sqrt{\gamma + \kappa^2 + (1/2 - \xi)^2 M^2}\right)}{\sqrt{\gamma + \kappa^2 + (1/2 - \xi)^2 M^2}}, \tag{8.25}$$

where $K_1(x)$ is the modified Bessel function of the second kind. The function $F(\xi, b)$ exponentially drops out for $b \to \infty$. It is pointed out that the evaluation of $F(\xi, b)$ in terms of $K_1(x)$ represents a numerical advantage, because of the fall-off behavior for large b, avoiding in this form the integration of Bessel function in Eq. (8.24), which due to its oscillating nature is more difficult to integrate.

The structure of the excited state in the IP-space is further explored in Fig. 8.8 with the binding energy $B(1)/m$=0.22 obtained for μ/m=0.1 and α_{gr}=6.437. In the figure, we provide the sections of $F(\xi, b)$ for ξ constant (left panel) and for b constant (right panel). The moving position of the node in the (ξ, b) plane, can be appreciated in both panels of the figure. As a general remark, the position of the node increases with b for ξ approaching the end-points and tends to be suppressed close to such boundaries, this is the counterpart of the previous observation done in momentum space. In addition in the right panel of the figure, one can verify the fast fall-off of the wave function for large values of b. Such decrease is indeed exponential, as we detail below.
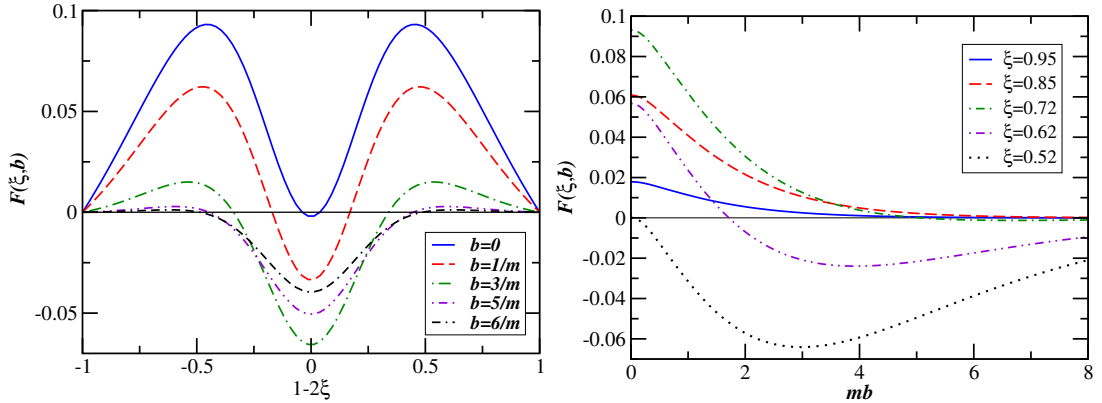
Figure 8.8: The first-excited state function $F(\xi, b)$, given by Eq. (8.25), for $B(1)/m$=0.22 with μ/m=0.1 and α_{gr}=6.437, is shown as function of ξ (left panel), for some fixed values of $b\,m$; and, as function of $b\,m$ (right panel), for some fixed values of ξ. In view of the symmetry, we should also add that all the plots for fixed ξ are exactly the same for $1 - \xi$. As evidenced in both the panels, the existence of zeros for $F(\xi, b)$ occurs only for values of b not larger than $\sim 7/m$.

The exponentially drops out behavior in $F(\xi, b)$ can be understood by a close analysis of Eq. (8.25). First, from the physically-motivated request Ref. [62] that $\phi(\xi, b)$ is finite for $b \to 0$ (see also Ref. [12]), such that

$$\phi(\xi, b=0) = \frac{\xi\,(1-\xi)}{4\pi\sqrt{2}} \int_0^\infty d\gamma\,\frac{g(\gamma, 1-2\xi)}{\gamma + \kappa^2 + (1/2-\xi)^2 M^2} < \infty \quad, \tag{8.26}$$

one can deduce that $g(\gamma, 1-2\xi)$ must vanish for $\gamma \to \infty$. Therefore, the relevant interval of γ in the integral Eq. (8.25) can be taken effectively finite. Exploiting such an observation, one can extract the driving exponential fall-off of $F(\xi, b)$ in the asymptotic limit $b \to \infty$. In this limit $K_1(x)$ reads:

$$K_1(x)|_{x\to\infty} \to \left(\frac{\pi}{2x}\right)^{\frac{1}{2}} e^{-x}. \tag{8.27}$$

Because $b \to \infty$, the leading exponential behavior in the integral Eq. (8.25) comes from values of $e^{-b\sqrt{\gamma+\kappa^2+(\xi-1/2)^2 M^2}}$ with γ close to 0. Therefore,

$$F(\xi, b)|_{b\to\infty} \to e^{-b\sqrt{\kappa^2+(\xi-1/2)^2 M^2}}\, f(\xi, b), \tag{8.28}$$

where the exponential fall-off is singled out and the reduced function $f(\xi, b)$ should decrease more smoothly for large values of b. The above feature has been investigated by actually calculating $F(\xi, b)$, and in turn $f(\xi, b)$, for both ground and first-excited states.
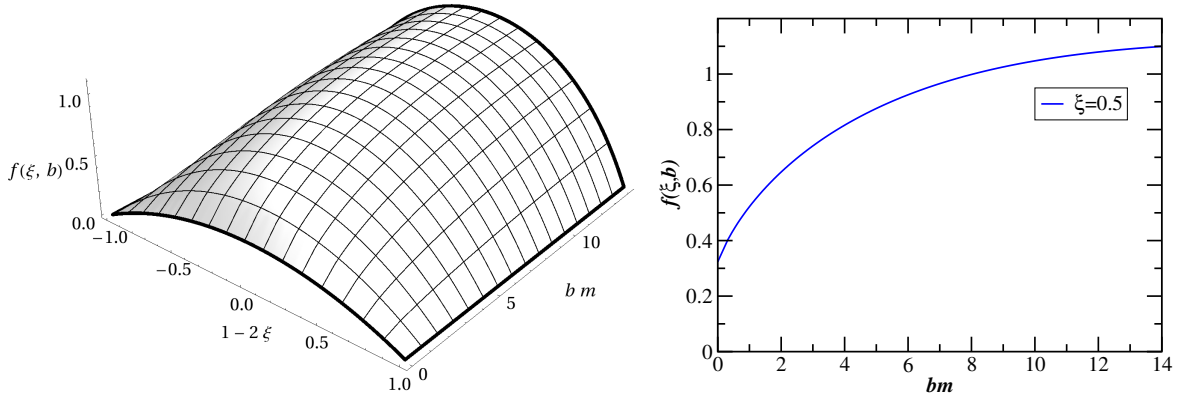
Figure 8.9: Corresponding to Eq. (8.28), we show $f(\xi, b)$ for the ground state obtained with $B(0)/m = 1.9$, $\mu/m = 0.1$ and $\alpha_{gr}=6.437$. In the left-panel, it is given as a function of b and ξ; and, in the right-panel, as a function of b, for a fixed ξ.

In Fig. 8.9, $f(\xi, b)$ is presented for the ground state with $B(0)/m = 1.9$, $\mu/m = 0.1$ and $\alpha_{gr}=6.437$. In the left panel we display a 3D plot, showing the correlation between ξ and b.
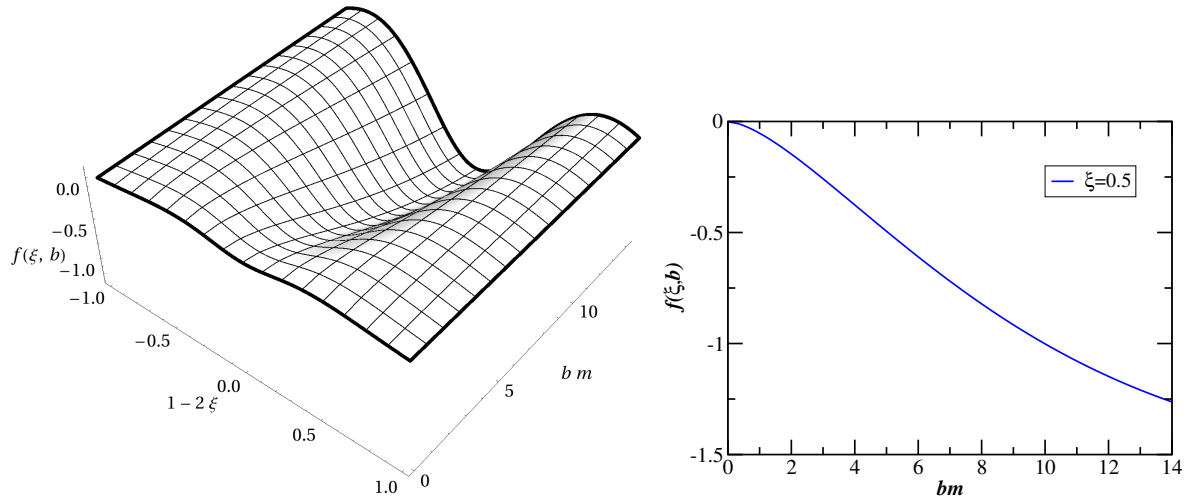
Figure 8.10: $f(\xi, b)$ for the excited state obtained with $B(1)/m = 0.221$, $\mu/m = 0.1$ and $\alpha_{gr}=6.437$. In the left-panel, it is given as a function of b and ξ; and, in the right-panel, as a function of b, for a fixed ξ.

In the right panel $f(\xi, b)$ is plotted as function of bm for a fixed value ξ=0.5. This plot puts in evidence that the steep fall-off of the valence wave function is largely taken into account by the leading exponential term, included in the definition Eq. (8.28). This suggests at most a polynomial behavior in $f(\xi, b)$, which is clearly seen in the figure for $b < 15/m$.

The same analysis is performed in Fig. 8.10 but for the first-excited state with $B(0)/m = 0.221$, $\mu/m = 0.1$ and $\alpha_{gr}=6.437$. Similar features are encountered for the excited state, from the right panel, $f(\xi, b)$ shows an almost linear increase in its absolute value, in agreement with the previous discussion, because the exponential leading behavior has been singled out.

Chapter 9

Electromagnetic properties

Scattering processes has played an important role to investigate the internal structure of composite systems. Since the early days of electron scattering processes on nucleus, which revels the internal structure of nucleus until the high energy deep inelastic scattering putting in evidence the existence of quarks as fundamental particles making up hadrons, scattering processes have provided important physical information to understand the dynamics and structure of composite systems. These processes are mostly dominated by the electromagnetic interaction and allow to access to different physical regions depending on the energy scale used for the incident particle. In particular, in low energy elastic scattering, *form factors* (FFs) are the relevant physical quantities, since that provides information about the charge and magnetization distribution in the composite system. FFs are functions depending on the transfer momentum in the process and can be extracted from the experimental data. In order to predict that dependence, a microscopic model in terms of fundamental constituents, quarks for the case of hadrons, must be proposed. Thus, the accuracy in describing the electromagnetic FFs depend highly on the model proposed.

In the realm of the non-perturbative hadron physics to study bound states, in particular for systems composed of light quarks, the relativistic effects are quite relevant for the consistence description of hadrons. Therefore, the description by means of the BS approach is quite desired because it provides a relativistic scheme to study the bound sates as we have stressed through of this thesis.

Within the BS framework, FFs are computed by using the BS amplitude of the bound state. As explained before and verified numerically, the Euclidean BS equation provides the same binging energies as the Minkowski BS equation. But if one is interested not only in the binding

energies but also in the FFs, the Euclidean solution is not enough.

In this chapter we present the calculation of FFs considering two kind of contributions: the impulse approximation (IA) widely used in many calculations and the next leading order, which we call two-body current (TBC) contribution. We analyze the effect of these contributions in the FFs.

9.1 Impulse approximation

In practice, for the calculation of the FF in the impulse approximation, we consider the electromagnetic vertex depicted in Fig. 9.1
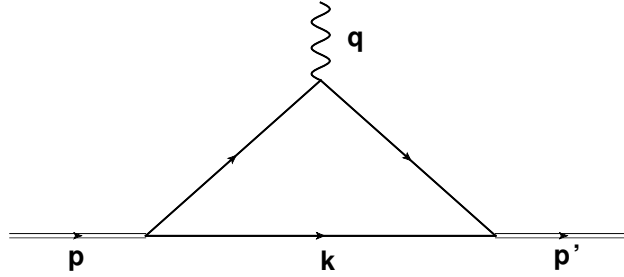
Figure 9.1: Feynman diagram for the electromagnetic FF in the impulse approximation

In this approximation, the interaction of the virtual photon with the composite system is through one of the constituents of the bound state and the another particle plays the role of spectator in this approximation. By applying the Feynman rules to this diagram, we obtain

$$
\begin{aligned}
-i(p+p')^\nu F_I(Q^2) = \int \frac{d^4k}{(2\pi)^4}(-i)\ (p+p'-2k)^\nu \frac{i}{k^2-m^2+i\epsilon}\frac{i}{(p-k)^2-m^2+i\epsilon} \\
\times \frac{i}{(p'-k)^2-m^2+i\epsilon}\Gamma\left(\frac{p}{2}-k,p\right)\Gamma\left(\frac{p'}{2}-k,p'\right),
\end{aligned}
\tag{9.1}
$$

where the vertex scalar-photon $-i(p+p')$ was used, and $\Gamma(k,p)$ is the vertex function related with the BS amplitude

$$
\varphi(k,p) = \frac{i}{[(\frac{p}{2}+k)^2-m^2+i\epsilon]}i\ \Gamma(k,p)\frac{i}{[(\frac{p}{2}-k)^2-m^2+i\epsilon]},
\tag{9.2}
$$

according to the definition given in Eq. (4.41). Writing in terms of the BS amplitude, the FF reads as

$$(p + p')^\nu F_I(Q^2) = \int \frac{d^4k}{(2\pi)^4} i \, \varphi\left(\frac{p}{2} - k, p\right) \varphi\left(\frac{p'}{2} - k, p'\right)(k^2 - m^2)(p + p' - 2k)^\nu. \tag{9.3}$$

To compute the FF using the Euclidean BS amplitude, the Wick rotation in the variable k_0 must be performed in Eq. (9.3). Now, we show that the Wick rotation cannot be done without crossing singularities in the integral Eq. (9.3). This statement is illustrated by the simple case with $\Gamma(k, p) = 1$, $p' = p = (M, \mathbf{0})$ and $\nu = 0$. For this case the propagators have the following form

$$\begin{aligned} \frac{i}{(p - k)^2 - m^2 + i\epsilon} &\to \frac{i}{(M - k_0)^2 - \mathbf{k}^2 - m^2 + i\epsilon} \\ \frac{i}{(p' - k)^2 - m^2 + i\epsilon} &\to \frac{i}{(M - k_0)^2 - \mathbf{k}^2 - m^2 + i\epsilon} \\ (p + p' - 2k)^\nu &\to (2M - 2k^0), \end{aligned} \tag{9.4}$$

and the integral for the FF reads as

$$I = i \int \frac{d^3k}{(2\pi)^3} \int \frac{dk^0}{(2\pi)} \frac{(2M - 2k_0)}{(k^2 - m^2 + i\epsilon)\left[(p - k)^2 - m^2 + i\epsilon\right]^2}. \tag{9.5}$$

The singularities from the first denominator are at $k_0 = \pm\sqrt{\mathbf{k}^2 + m^2} \mp i\epsilon$, therefore these singularities do not produce difficulties to perform the Wick rotation. For the second denominator the poles are

$$k_0 = M \mp \sqrt{\mathbf{k}^2 + m^2} \pm i\epsilon, \tag{9.6}$$

if $M < \sqrt{\mathbf{k}^2 + m^2}$ these poles neither represent a problem, but in the case $M > \sqrt{\mathbf{k}^2 + m^2}$ both poles are in the right hand side of the complex plane, what prevents to carry out the Wick rotation without cross these singularities. One can omit the contribution of this pole and perform the Wick rotation but in this case the result becomes approximated. This situation is the same for non-trivial $\Gamma(k, p)$ and non-zero Q^2.

In addition, there exist another reason that does not allow to compute the electromagnetic FF by using the Euclidean BS amplitude. To illustrate it, let us to recall the Euclidean BS equation

$$\varphi(k_E^0, \mathbf{k}) = \frac{1}{\left[(-(k_E^0)^2 - \mathbf{k}^2 + M^2/4 - m^2)^2 + (k_E^0)^2 M^2\right]} \int \frac{dk_E'^0 \, d\mathbf{k'}}{(2\pi)^4} K(k_E^0, \mathbf{k}; k_E'^0, \mathbf{k'}) \varphi(k_E'^0, \mathbf{k'}),$$

(9.7)

written for any irreducible interaction kernel. The Euclidean BS amplitude is obtained by solving Eq. (9.7) in the rest frame $\mathbf{p}=0$, what is enough to compute eigenvalues, but in the calculation of the FF Eq. (9.1), it is needed to know the BS amplitude for the total initial momentum $\mathbf{p}$ and the final total momentum $\mathbf{p}'$. These momentums in the initial and final state are different due to the recoil of the system in the scattering process. This problem could be avoided if one solves the Euclidean BS equation for non-zero $\mathbf{p}$ as done in Ref. [55], however given the difficulty of crossing singularities when performing the Wick rotation the evaluation of the FF is still approximate. For a detailed analysis of approximated results obtained by computing FFs dealing with the Euclidean BS amplitude, see Ref. [29].

The above problems disappear if one solves the BS equation directly in the Minkowski space and obtain the Minkowski BS amplitude, since no Wick rotation is needed in the integral Eq. (9.1) and the BS amplitude is obtained for arbitrary total momenta $\mathbf{p}$. The calculation of FF is one of the important motivations to carry out this calculation in the Minkowski space.

We illustrate in shortly the calculation of the FF directly in the Minkowski space using the Nakanishi approach within the IA. Consider Eq. (9.3), in this expression we introduce the NIR

$$\varphi(k, p) = -i \int_{-1}^{1} dz' \int_0^\infty d\gamma' \frac{g(\gamma', z')}{[\gamma' + m^2 - \frac{M^2}{4} - k^2 - (p \cdot k)z' - i\epsilon]^3},$$

(9.8)

we obtain

$$(p + p')^2 F_I(Q^2) = \int \frac{d^4 k}{(2\pi)^4} i \int dz \, dz' \, d\gamma \, d\gamma' g(\gamma, z) g(\gamma', z')(m^2 - k^2)[(p + p')^2 - 2k \cdot (p + p')]$$

$$\times \frac{1}{\left[\gamma' + m^2 - \frac{M^2}{4} - (\frac{p'}{2} - k)^2 - (\frac{p'}{2} - k) \cdot kz' - i\epsilon\right]^3} \frac{1}{\left[\gamma + m^2 - \frac{M^2}{4} - (\frac{p}{2} - k)^2 - (\frac{p}{2} - k) \cdot kz - i\epsilon\right]^3}$$

(9.9)

we have also multiplied by $(p + p)^\nu$ to both sides, in order to isolated $F_I(Q^2)$. The integration in k can be done analytically, this is achieved by putting together the denominators with aid of the well known Feynman parameterization

$$\frac{1}{a^3 b^3} = \int_0^1 du \frac{30 u^2 (1-u)^2}{(au + b(1-u))^6}. \tag{9.10}$$

By shifting the variable k as usual, namely

$$k \rightarrow k + \frac{1}{2}(1+z)u\, p + \frac{1}{2}(1+z')(1-u)p', \tag{9.11}$$

one can perform the integration in the internal momentum by using the formula

$$\int \frac{d^4 k}{(2\pi)^4} \frac{1}{(k^2 - M + i\epsilon)^\alpha} = \frac{i}{(4\pi)^2} \frac{\Gamma(\alpha - 2)}{\Gamma(\alpha)} \frac{(-1)^\alpha}{(M - i\epsilon)^{\alpha - 2}}, \tag{9.12}$$

where M is independent of k. The procedure to compute this integral is standard, obtained by performing the Wick rotation, but we show explicitly the calculation. The integral Eq. (9.12) is written as

$$\int d^3\mathbf{k} \int_{-\infty}^{\infty} dk_0 \frac{1}{[k_0^2 - \mathbf{k}^2 - M + i\epsilon]^6}, \tag{9.13}$$

therefore the poles of are placed at $k_0 = \pm\sqrt{\mathbf{k}^2 + M} \mp i\epsilon$. Thus, when performing the Wick rotation $k_0 \rightarrow ik_0$, the rotate contour does not cross singularities, contrary what happens when using the Euclidean BS amplitude, as explained before.

To complete the calculation, we analyze the term in the numerator: $[(p + p')^2 - 2k \cdot (p + p')](m^2 - k^2)$. After performing the shift Eq. (9.11), the terms with odd exponent in k vanish. The integral with quadratic term is done with the formula

$$\int \frac{d^4 k}{(2\pi)^4} \frac{k^2}{(k^2 - M + i\epsilon)^\alpha} = i(-1)^{\alpha+1} \frac{1}{(4\pi)^2} \frac{4}{2} \frac{\Gamma(\alpha - 3)}{\Gamma(\alpha)} \frac{1}{(M - i\epsilon)^{\alpha - 3}}. \tag{9.14}$$

Putting all together the FF reads as

$$F_I(Q^2) = \frac{1}{2^7 \pi^3 N} \int_0^\infty d\gamma \int_{-1}^1 dz\, g(\gamma, z) \int_0^\infty d\gamma' \int_{-1}^1 dz'\, g(\gamma', z') \int_0^1 du\, u^2 (1-u)^2 \frac{f_{num}}{f_{den}^4}, \tag{9.15}$$

where

$$f_{num} = (6C - 5)m^2 + [\gamma'(1 - u) + \gamma u](3C - 2) + 2M^2 C(1 - C) + \frac{1}{4}Q^2(1 - u)u(1 + z)(1 + z'),$$

$$f_{den} = m^2 + \gamma'(1 - u) + \gamma u - M^2(1 - C)C + \frac{1}{4}Q^2(1 - u)u(1 + z)(1 + z'),$$

$$C = \frac{1}{2}(1 + z)u + \frac{1}{2}(1 + z')(1 - u),$$

$$(9.16)$$

as usual $Q^2 = -(p - p')^2 > 0$ and the factor N is obtained from the normalization condition $F_I(0) = 1$.

9.2 Higher-order contributions in the form factor

We have presented the calculation of the electromagnetic FF taking into account the conventional IA diagram. In order to go beyond of this approximation and to take profit of our approach we add the next contribution to the FF, i.e, the TBC contribution. The corresponding Feynman diagram for this contribution is depicted in Fig. 9.2
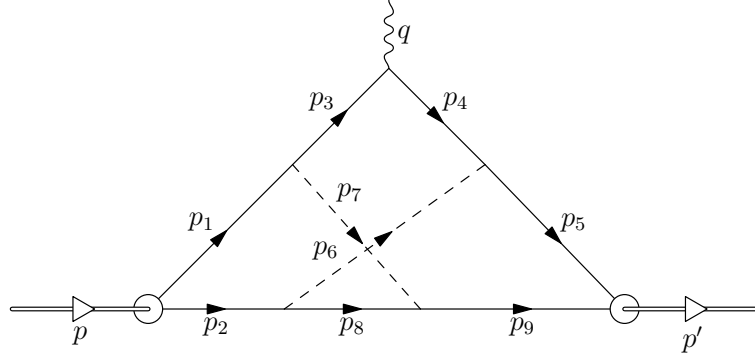
Figure 9.2: Feynman diagram of the electromagnetic FF for the two-body current contribution.

The steps to compute this kind of diagram are quite similar what we have done for the IA, however the calculation of this diagram requires more algebraic steps. From the momentum

conservation in each vertex, we have the following relations between the momentums in Fig. 9.2

$$p_1 = p - p_2$$

$$p_3 = p - p_2 - p_9 + p_8$$

$$p_4 = p - p_2 - p_9 + p_8 + q = p' - p_2 - p_9 + p_8$$

$$p_5 = p - p_9 + q$$

$$p_6 = p_2 - p_8$$

$$p_7 = p_9 - p_8.$$

(9.17)

Therefore all momentums in the diagram may be expressed in terms of three internal momentums, namely p_2, p_8 and p_9, which are chosen arbitrary and should be integrated. After applying the Feynman rules the expression for this diagram reads as:

$$
\begin{aligned}
(p+p')^\mu F_X(Q^2) &= -ig^4 (2\pi)^{-12} \int d^4 p_2 \, d^4 p_8 \, d^4 p_9 \\
&\times \varphi(p'-p_2-q,p_2,p)\varphi(p'-p_9,p_9,p')(2p'-2p_9-2p_2+2p_8-q)^\mu \\
&\times \frac{1}{[(p'-p_9-p_2-q+p_8)^2 - m^2 + i\epsilon]}\frac{1}{[(p'-p_9-p_2+p_8)^2-m^2+i\epsilon]} \\
&\times \frac{1}{[(p_9-p_8)^2-\mu^2+i\epsilon]}\frac{1}{[p_8^2-m^2+i\epsilon]}\frac{1}{[(p_2-p_8)^2-\mu^2+i\epsilon]},
\end{aligned}
$$

(9.18)

where we have used the relation between the vertex function and the BS amplitude Eq. (9.2). The BS amplitude in terms of the NIR is written as

$$
\varphi(p'-p_9,p_9) = -i\int_{-1}^1 dz' \int_0^\infty d\gamma' \frac{g(z',\gamma')}{[\gamma'+m^2-\frac{M^2}{4}-(p_9-\frac{p'}{2})^2-(p_9-\frac{p'}{2}).p'z'-i\epsilon]^3},
$$

$$
\varphi(p'-p_2-q,p_2) = -i\int_{-1}^1 dz \int_0^\infty d\gamma \frac{g(z,\gamma)}{[\gamma+m^2-\frac{M^2}{4}-(\frac{p'}{2}-\frac{q}{2}-p_2)^2-(\frac{p'}{2}-\frac{q}{2}-p_2).(p'-q)z-i\epsilon]^3},
$$

(9.19)

by introducing the BS amplitude in terms of the NIR in Eq. (9.18), one has

$$
(p'+p)^2 F_X(Q^2) = \frac{-ig^4}{(2\pi)^{12}} \int d\gamma \, d\gamma' \, dz \, dz' \int d^4 p_2 \, d^4 p_8 \, d^4 p_9 [(p'+p)^2 - 2(p+p')_\mu (p_9+p_2-p_8)^\mu]
$$

$$
\frac{g(z',\gamma')}{[\gamma'+m^2-\frac{M^2}{4}-(p_9-\frac{p'}{2})^2-(p_9-\frac{p'}{2}).p'z']^3} \frac{g(z,\gamma)}{[\gamma+m^2-\frac{M^2}{4}-(\frac{p'}{2}-\frac{q}{2}-p_2)^2-(\frac{p'}{2}-\frac{q}{2}-p_2).(p'-q)z]^3}
$$

$$
\frac{1}{[(p'-p_9-p_2-q+p_8)^2-m^2]}\frac{1}{[(p'-p_9-p_2+p_8)^2-m^2]}
$$

$$
\frac{1}{[(p_9-p_8)^2-\mu^2]}\frac{1}{[p_8^2-m^2]}\frac{1}{[(p_2-p_8)^2-\mu^2]}.
$$

(9.20)

For shorthand notation the term $i\epsilon$ has been omitted in all denominators. The steps to compute Eq. (9.20) are as follows: (i) one performs the integration in the three internal momentums and

(ii) take into account the shift in the integration, which brings some constant terms in the numerator of Eq. (9.20), these do not vanish when the integration is carried out. The remaining integrals are computed numerically. The details of this calculation are presented in Appendix. B. After the tedious steps have been performed, the TBC contribution reads as

$$F_X(Q^2) = \frac{-3g^4}{(2)^{11}\pi^6} \int d\gamma \, d\gamma' \, dz \, dz' g(z,\gamma) g(z',\gamma') \int [dy_i](1-y_5)^2 y_5^2 (1-y_6)^2 \, y_6^3 \, \tilde{g}^2 s^3 \frac{f_{\text{numer}}}{(M_3)^5}, \quad (9.21)$$

where M_3 is given by

$$M_3 = \text{constr } s - M^2 \frac{w_{p'}^2}{4} + Q^2 \frac{w_q(w_{p'} + w_q)}{4}$$

$$\text{constr} = -Q^2 \, \text{constr1} + M^2 \, \text{constr2} + \text{constr3}, \quad (9.22)$$

f_{numer} has the following form

$$f_{\text{numer}} = \frac{4f_{p'}s + 2b_{p9}f_{p'}s + 8\tilde{g}s - 4b_{p'}\tilde{g}s - 2f_{p2}w_{p'} - b_{p9}f_{p2}w_{p'} + 4w_{p'}\tilde{g} + 2b_{p2}w_{p'}\tilde{g}}{8\tilde{g}s}, \quad (9.23)$$

and we have used the compact notation for the integrals in the Feynman parameters

$$\int [dy_i] = \int_0^1 dy_4 \int_0^{1-y_4} dy_3 \int_0^{1-y_3-y_4} dy_2 \int_0^{1-y_2-y_3-y_4} dy_1 \int_0^1 dy_5 \int_0^1 dy_6. \quad (9.24)$$

The explicit expression of the coefficients are given in Appendix. B.

We have derived an expression for the FF considering two contributions. Now, our objective is to analyze how the higher contribution affects the FF in low a large momentum transfered. Before showing the numerical results, we mentioned that a test to verify the correctness of the expression for the two-body current contribution was performed, since the lengthy expression obtained we cannot trust in this expression without a test. This kind of test is presented in Appendix. C.

9.3 Numerical results for the impulse and two-body current form factors

We start by discussing the issue of the current conservation for the elastic FF considering two contributions:

$$F(Q^2) = F_I(Q^2) + F_X(Q^2). \quad (9.25)$$

As explained in Ref. [54], given the gauge invariance, in the calculation of the FF there must exist a consistency between the BS amplitudes in the initial and final states and the current operator. Namely, if the TBC contribution of Fig. 9.2 is considered in the current operator, one has also to consider the cross-ladder contribution in the BS amplitudes or in our case the corresponding Nakanishi weight-function. This consistency has been tested numerically to satisfy the current conservation for the process bound state $\rightarrow$ scattering state, in Ref. [53].

In principle, the strong test of the current conservation should work in the present calculation. However, in the calculation of the elastic FF this requirement is trivially fulfilled. To understand better this statement, let us to consider the two contributions of the FF, in Eqs. (9.9) and (9.18). By looking inside of these expressions one realizes of the symmetry for the replacement $p' \rightarrow p$. Therefore, when contracting with q^μ, an antisymmetric tensor, it gives zero for *any* Nakanishi-weight function. Thus, the test of consistency for the elastic FF is meaningless, since the current conservation is fulfilled trivially for each contribution of the FF independently of the BS amplitudes.

Now, we present some plots of the FF showing both contributions independently, namely, impulse approximation (IA) and two-body current (TBC). In Fig. 9.3, we show four cases with representative binding energies $B/m = 1.5$ and $B/m = 0.1$ and masses of exchanged bosons μ/m=0.15 and μ/m=0.5. The range of transfer momentum considered is: $0 < (Q/m)^2 < 50$. The FF has been calculated with the Nakanishi weigh-function corresponding to the L+CL kernel and the sum of the two contributions, $F_I + F_X$, is normalized to 1 at $(Q/m)^2 = 0$.
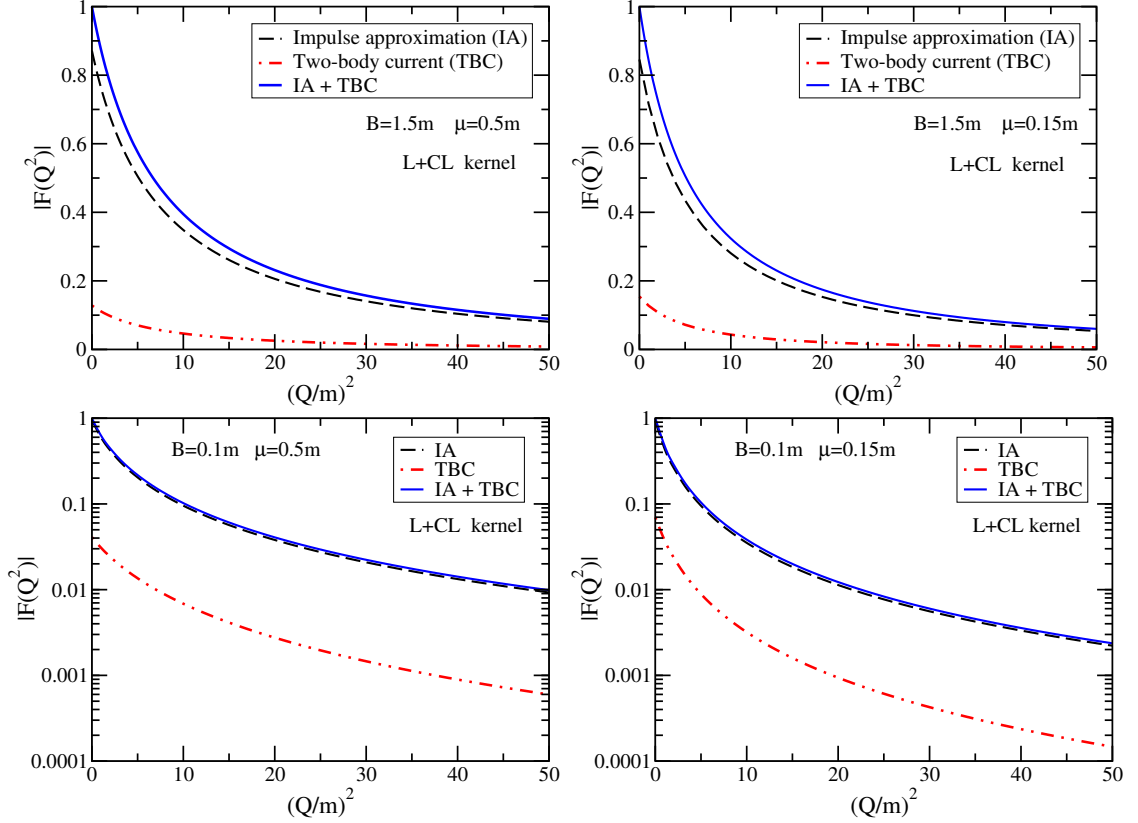
Figure 9.3: Electromagnetic FF computed with the IA + TBC contributions, using the ladder plus cross-ladder (L+CL) amplitudes. Contributions to the FF are shown separately IA (back-dashed line) and TBC (dotted-dashed-red line). The sum of the two contributions is represented by the solid-blue line. The binding energy of the ground state is fixed at B/m=1.5 (upper panels) and B/m=0.1 (lower panels). Two values of the exchanged boson mass are considered μ/m=0.5 (left panels) and μ/m=0.15 (right panels).

As we may appreciate from Fig. 9.3, the IA is the dominant contribution for the FF. Looking carefully the curves one realizes that the effect of the TBC contribution is larger for μ small, as one can appreciate when μ changes from $0.5\,m$ to $0.15\,m$. Also, it is clear that the TBC contribution increases for large binding energy.

Additionally, we provide a comparison between the electromagnetic FF in Fig. 9.4 obtained in the IA with the Nakanishi-weight function corresponding to the ladder and ladder + cross-ladder kernel to analyze the sensibility of the FF to the dynamics. Also the FF with the full current computed with the ladder + cross-ladder kernel is displayed. The binding energy is fixed at $B/m = 1.5$ and the three curves are normalized at 1 in $Q^2/m^2 = 0$.
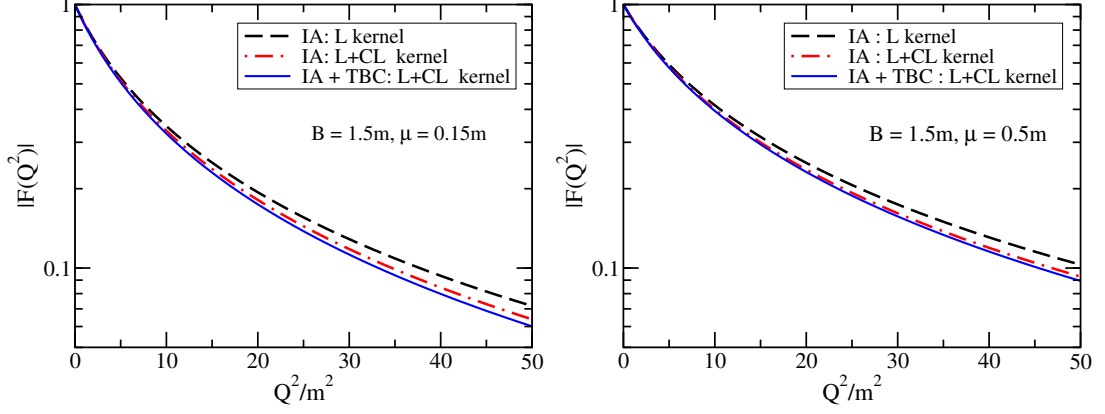
Figure 9.4: FF as a function of Q^2 . The dashed curve is the impulse approximation (IA) for the FF calculated with the BS amplitude found for ladder (L) kernel. The dot-dashed curve is the IA to the form factor computed with the BS amplitude obtained with the ladder plus cross-ladder (L + CL) kernel. The solid curve is the full form factor obtained from the BS amplitude calculated with L + CL kernel. The binding energy is $B/m = 1.5$, with the mass of the exchanged boson $\mu/m = 0.15$ (left-panel) and $\mu/m = 0.5$ (right-panel). All curves are normalized to 1 at $Q^2 = 0$.

We observe at low momentum, below m, very similar slopes, that reflects close charge radius and the bound state size, which is determined by the same binding energy. This finding is independent on the mass of the exchanged boson, as one can verify by inspecting the left and right panels of Fig. 9.4. From this figure it is also clear the dominance of the IA in the FF behavior for large momentum. This dominance makes us conclude that the TBC contribution decays much faster than the IA. In fact, in the next section when exploring the asymptotic behavior of each contribution, it will be clear that each contribution has different fall-off.

9.4 Asymptotic behavior of the form factor

It is important to study the behavior of the electromagnetic FF in the region of high momentum transfer to understand better the fact of the dominance of the IA in the FF. To this purpose we recall the expression for F_I, Eq. (9.9):

$$
\begin{aligned}
F_I(Q^2) &= \int \frac{i d^4 k}{(2\pi)^4} \int dz\, dz'\, d\gamma\, d\gamma' \frac{g(\gamma, z) g(\gamma', z')(m^2 - k^2)\left[1 - \frac{2k\cdot(p+p')}{(p+p')^2}\right]}{\left[\gamma' + m^2 - \frac{M^2}{4} - (\frac{p'}{2} - k)^2 - (\frac{p'}{2} - k)\cdot kz' - i\epsilon\right]^3} \\
&\quad \times \frac{1}{\left[\gamma + m^2 - \frac{M^2}{4} - (\frac{p}{2} - k)^2 - (\frac{p}{2} - k)\cdot kz - i\epsilon\right]^3}.
\end{aligned}
$$

In the asymptotic limit*, i.e, $Q^2 \to \infty$ and adopting the Breit-frame where $\vec{p} = -\vec{p'}$, $Q^2 = -(p'-p)^2 = 4p^2$ and $p_0 = p_0' = \sqrt{M^2 + Q^2/4}$, Eq. (9.9) can be written as

$$F_I(Q^2) = \frac{i}{(2\pi)^4} \int d\gamma dz d\gamma' dz' g(\gamma, z) g(\gamma', z') \frac{(m^2 - k^2)}{\mathcal{D}^3 \mathcal{D}'^3}, \tag{9.26}$$

where

$$\mathcal{D} \propto (1+z)Q + \delta(\gamma, z) \qquad\qquad \mathcal{D}' \propto (1+z')Q + \delta'(\gamma', z'). \tag{9.27}$$

δ and δ' are two functions which do not have dependence in Q and their explicit form can be omitted in the asymptotic limit. Thus, the FF in the IA can be written as

$$\begin{aligned}
F_I(Q^2) &\propto \int_{-1}^{1} \frac{g(z)\, dz}{[(1+z)Q + \delta]^3} \int_{-1}^{1} \frac{g(z')\, dz'}{[(1+z')Q + \delta']^3}, \\
&= \frac{1}{Q^6} \int_{-1}^{1} \frac{g(z)\, dz}{\left[1 + z + \frac{\delta}{Q}\right]^3} \int_{-1}^{1} \frac{g(z')\, dz'}{\left[1 + z' + \frac{\delta'}{Q}\right]^3}.
\end{aligned} \tag{9.28}$$

The other integrations have been omitted since that give finite corrections and do not affect the asymptotic limit. By analyzing Eq. (9.28), one realizes that in the asymptotic limit the integral is divergent at the point $z = -1$. However, one can analyze the behavior of $g(z)$ as $z \to -1$. The behavior of $g(z)$ is linear in this region: $g(z) \sim (1+z)$. Thus, one obtains

$$\int_{-1}^{1} \frac{(1+z)\, dz}{\left(1 + z + \frac{\delta}{Q}\right)^2} \sim \frac{Q}{\delta}, \tag{9.29}$$

therefore, one can conclude

$$F_I(Q^2) \longrightarrow \frac{1}{Q^4}. \tag{9.30}$$

Following the same steps one can obtain the asymptotic behavior of the TBC Eq. (9.20):

---

*The study of the asymptotic behavior of the FF was based on the notes developed by Prof. V.A. Karmanov. *Asymptotic of EM form factor for triangle and cross-ladder contributions.*

$$(p'+p)^2 F_X(Q^2) = \frac{-ig^4}{(2\pi)^{12}} \int d\gamma \ d\gamma' \ dz \ dz' \int d^4p_2 \ d^4p_8 \ d^4p_9 [(p'+p)^2 - 2(p+p')_\mu (p_9 + p_2 - p_8)^\mu]$$

$$\frac{g(z',\gamma')}{[\gamma' + m^2 - \frac{M^2}{4} - (p_9 - \frac{p'}{2})^2 - (p_9 - \frac{p'}{2}).p'z']^3} \frac{g(z,\gamma)}{[\gamma + m^2 - \frac{M^2}{4} - (\frac{p'}{2} - \frac{q}{2} - p_2)^2 - (\frac{p'}{2} - \frac{q}{2} - p_2).(p'-q)z]^3}$$

$$\frac{1}{[(p' - p_9 - p_2 - q + p_8)^2 - m^2]} \frac{1}{[(p' - p_9 - p_2 + p_8)^2 - m^2]}$$

$$\frac{1}{[(p_9 - p_8)^2 - \mu^2]} \frac{1}{[p_8^2 - m^2]} \frac{1}{[(p_2 - p_8)^2 - \mu^2]}.$$

In this case we have seven denominators. However, we can find easily the contribution of each denominator using the result of the FF in IA. As before in the asymptotic limit, we can cancel $(p'+p)^2$ from the both sides of Eq. (9.20). Therefore the last three propagators which depends upon p_8, p_9 and p_2 can be omitted in this limit. The denominators $1/[\ ]^3$ in Eq. (9.20) have the same structure of cubic denominators in Eq. (9.9), therefore they contribute in the same form than before, namely $\frac{1}{Q^4}$. Finally, we consider the contribution of the other two propagators. Performing the same process that before, i.e, taking the Breit-frame one obtains

$$\frac{1}{[(p' - p_2 - p_9 + p_8)^2 - m^2]} \longrightarrow \frac{1}{[\mathcal{C} + \mathcal{B}Q]}, \tag{9.31}$$

$\mathcal{C}$ and $\mathcal{B}$ depend on the internal momentums. Adding the contribution of these two denominators one finds the asymptotic behavior for TBC as

$$F_X(Q^2) \longrightarrow \frac{1}{Q^6}. \tag{9.32}$$

Now we must verify this prediction in the numerical results. We consider the case $B/m = 0.1$ and $\mu/m = 0.15$. In the figures presented before, we show the behavior of the FF considering $0 \leq (Q/m)^2 \leq 50$, but for this range of momentum transfer the FF still does not reach the asymptotic limit. Indeed, we have to go to larger values of $(Q/m)^2$ to observe the behavior predicted before in Eqs. (9.32) and (9.30). The two contributions of the FF are shown in the left-panel of Fig. 9.5.

In order to verify the asymptotic behavior we have multiplied the curves of the FF by Q^4 and Q^6 in the IA and TBC contribution, respectively, which can be appreciated by the corresponding curves in the right-panel of Fig. 9.5. From this right-panel one can realize the correct asymptotic behavior of the FF in the IA, which does not seem enough in the case of TBC. However, as
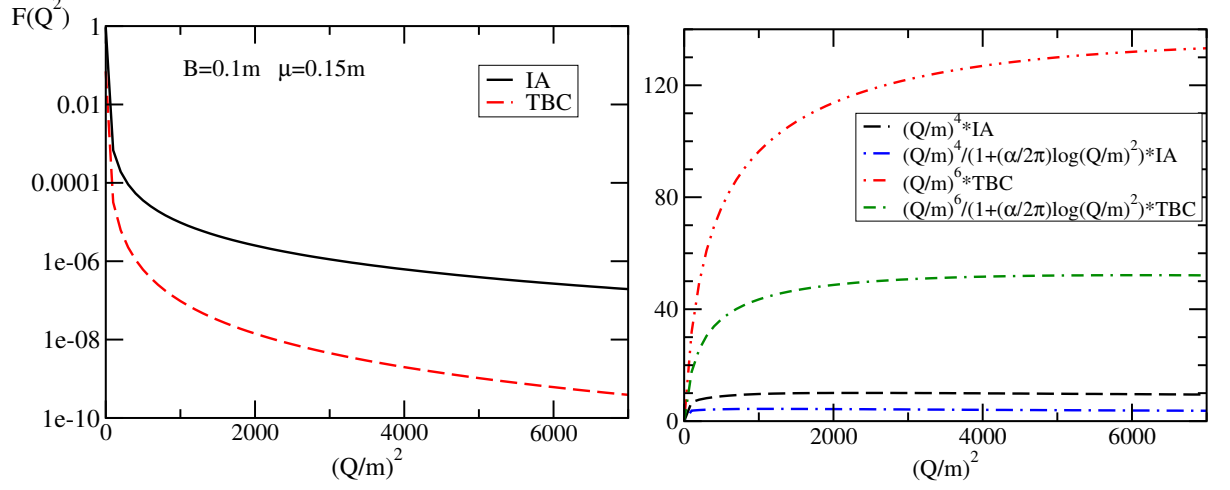
Figure 9.5: Electromagnetic FF for the case μ/m=0.15 and B/m=0.1. In the left-panel the two contributions of the FF is shown for large values of (Q^2/m). In the right-panel the asymptotic behavior of the corresponding contributions are analyzed.

explained in Ref. [51], where the asymptotic limit of the FF for the Wick-Cutkosky model($\mu = 0$) and small binding energy is studied, the asymptotic limit has logarithmic corrections:

$$F(Q^2) \sim \frac{16\alpha^2 m^2}{Q^4} \left[1 + \frac{\alpha}{2\pi} \log \left(\frac{Q^2}{m^2} \right) \right]. \tag{9.33}$$

Therefore, one can include these corrections to improve the results, since we are using small binding energy and small mass of the exchanged boson, namely μ/m=0.15 and $B/m = 0.1$. The result is presented in the right-panel of Fig. (9.5). It is clear that the logarithmic corrections are important to find the correct asymptotic behavior of the TBC contribution.

The analysis of the electromagnetic FF including higher order contributions in the current operator makes part of a study of the bound state structure in Minkowski space considering contributions beyond of the ladder kernel [61].

Chapter 10

Conclusions

In this thesis we presented results of an approach exploring bound-state solutions of the Bethe-Salpeter equation in Minkowski space, using the Nakanishi integral representation. By continuing some previous related studies, we extend the approach to excited states, lower dimensional systems and kernels beyond ladder considering the non-perturbative regime. The initial investigations performed by Kusaka and Williams Refs. [6, 7] gave the first clues about the validity of the Nakanishi representation in the non-perturbative regime. Then, in a series of works, Karmanov and Carbonell [8, 15, 18] have followed this idea, putting together the Nakanishi integral representation with the light-front projection to easily handle the singularities. This method is valid for any irreducible kernel in the Bethe-Salpeter equation. This really represents a step forward in the study of the bound state within a relativistic field theory framework, since several structure properties can be accessed directly in Minkowski space, differently from the usual Euclidean approach to the solution of the Bethe-Salpeter equation. Afterwards, Frederico, Salmè and Michele have formally investigated the Nakanishi integral representation to extend it for scattering states [9], by exploring the uniqueness of the Nakanishi weight-function. The quantitative studies were presented in Refs. [12, 16].

The previous successful studies have greatly encouraged us to explore the technique to lower dimensions, in particular for (2+1) dimensions in view of the promising applications in condensed-matter physics. We have restricted to the Yukawa model of two spinless bosons interacting by exchanging of another scalar boson in ladder approximation. Although, this model is not applicable to real systems, this allows us to access the main difficulties faced when implemented the Nakanishi integral representation to real systems. As a result of our calculations,

the extension of the Nakanishi integral representation to (2+1) dimensions was found satisfactory. In order to verify the feasibility of the method, we have calculated the eigenvalues in the Minkowski and Euclidean space and the Euclidean Bethe-Salpeter amplitude by means of two methods: (i) by using the Nakanishi integral representation together with the light-front projection and then performing Wick rotation; (ii) the Euclidean Bethe-Salpeter amplitude obtained directly in the Euclidean space. The light-front wave function which is available in light-front dynamics is also presented, showing the expected shape for the *s*-wave state. This calculation has been performed considered the ladder and cross-ladder contributions for the interaction kernel. The effect of the cross-ladder contribution in the eigenvalues is remarkable, hence the contribution of this kernel is relevant to study masses of relativistic bound states. On the other hand, the cross-ladder effect in the light-front wave function appears in the asymptotic limit, i.e, in the large momentum region as a scaling in the tail of the wave function with the dominance of the ladder kernel. In the region of low momentum the wave function is independent of the inclusion of the ladder or cross-ladder kernel, once the wave function has been arbitrarily normalized.

As a natural extension of the previous analysis, we have investigated the spectrum of excited states of the Bethe-Salpeter equation in the Yukawa model in (3+1) dimensions, considering the *s*-wave state in the ladder approximation. We have found a finite number of excited states for non-zero exchanged-scalar mass, and we have successfully compared our results with the corresponding ones obtained in the Euclidean space, where obviously the Nakanishi integral representation is not assumed. The method has allowed us to obtain up to three excited states $B(n)(n = 1, 2...)$ for large enough ground state binding energy $B(0)$ and small mass of the exchanged boson. The calculation was limited for very small $B(0)$ and small mass of exchanged boson due to instabilities of the integral equation in this case. In order to verify the non-relativistic limit when the mass of the exchanged boson is approaching to zero and small $B(0)$, the ratios $B(n)/B(0)$ obtained through the Bethe-Salpeter approach are in agreement with those of the well known non-relativistic calculation. To compute these ratios an extrapolation was performed due to the numerical problem mentioned above. A detailed study of the valence wave function has shown the expected node structure of the first- and second-excited states. Additionally, our investigation, both analytic and quantitative, of the transverse-momentum amplitude has allowed us to remarkably show the equivalence of this quantity evaluated both in

Euclidean and Minkowski spaces. This shows the reliability of the approach based on Nakanishi integral representation for solving the Bethe-Salpeter equation, already applied to ground state considering scalar and fermionic systems [8, 18] and in the zero-energy scattering case [16]. We also explored the asymptotic properties of the impact parameter space valence wave function for large transverse distances, where an exponential fall-off was singled out and quantitatively tested for the excited states.

Finally, in this thesis we have studied the electromagnetic properties of the composite systems, i.e, the response of the composite system when an incident particle is scattered-off, process which are mediated by the electromagnetic interaction. The relevant quantities are the electromagnetic form factors, which can be computed within the Bethe-Salpeter approach. Aware that the correct calculation of form factors must be performed directly in the Minkowski space, we have taken profit of the Nakanishi integral representation method to compute the form factors. We have computed the leading contribution of the elastic form factor known as the impulse approximation and in addition the next contribution, that we have called two-body current. By virtue of the current conservation, (see Ref. [53, 54]), in addition to the ladder kernel one must introduce the cross-ladder one for the Bethe-Salpeter amplitudes needed to compute the form factor if the two-body current is considered in the operator of the electromagnetic current. Although, the current conservation provides a strong test for the consistency of the current operator associated with a given kernel of the Bethe-Salpeter equation, we have found that for the calculation of the elastic form factor, each contribution, namely impulse approximation and two-body current, independent of the BS amplitudes conserves electromagnetic current in view of the symmetry of the integrals. The test of the current conservation is expected to be performed successfully for the inelastic form factor, which will be investigated elsewhere. Nevertheless, we have analyzed the form factor taking into account these contributions. As a result we have found the dominance of the impulse approximation in the electromagnetic form factor. In particular, the effect of the two-body current decreases for small binding energies. As main features of the analysis, we may conclude that in the region of low momentum transfered, the slopes of the form factor are independent of the contribution in the current operator and the interaction kernel, which shows a similar charge radius of the bound state once the binding energy is fixed. In the region of large momentum transfered the dominance of the impulse approximation is evidenced, which can be understood by the faster decay of the two-body current contribution

in the asymptotic limit. This fact was proved analytically and verified numerically. They presented the asymptotic behaviors $1/Q^4$ for the impulse approximation and $1/Q^6$ for the two-body current. This result agrees with the previous analyzes. The results of the electromagnetic form factors make part of the survey in current investigation about the Minkowski space structure of the bound state considering cross-ladder effects.

Bibliography

[1] D.J. Gross and F. Wilczek, Phys. Rev. Lett. **30**, 1343 (1973); H.D. Politzer, Phys. Rev. Lett. **30**, 1346 (1973).

[2] E.E. Salpeter, H.A. Bethe, Phys. Rev. **84**, 1232 (1951).

[3] G. C. Wick, Phys. Rev. **96**, 1124 (1954).

[4] C.D Roberts and A.G Williams, Dyson-Schwinger Equations and their Application to Hadronic Physics, in Progress in Particle and Nuclear Physics Vol. 33(Pergamon, Oxford, 1994), p.477.

[5] N. Nakanishi, Phys. Rev. **130**, 1230 (1963); Graphy Theory and Feynman Integrals (Gordon and Breach, New York, 1971).

[6] K. Kusaka and A. G. Williams, Phys. Rev. D **51**, 7026 (1995).

[7] K. Kusaka, K. Simpson and A. G. Williams, Phys. Rev. D **56**, 5071 (1997).

[8] V. A. Karmanov and J. Carbonell, Eur. Phys. J. A **27**, 1 (2006).

[9] T. Frederico, G. Salmè and M. Viviani, Phys. Rev. D **85**, 036009 (2012).

[10] J. Carbonell, B. Desplanques, V.A. Karmanov and J.F. Mathiot, Phys. Reports, **300**, 215 (1998).

[11] S. J. Brodsky, H. C. Pauli and S. S. Pinsky, Phys. Rep. **301**, 299 (1998).

[12] T. Frederico, G. Salmè and M. Viviani, Phy. Rev. D **89**, 016010 (2014).

[13] V. Sauli and J. Adam, Phys. Rev. D **67**, 085007 (2003).

[14] V. Sauli, J. Phys. G **35**, 035005 (2008); Few-Body Syst. **39**, 45 (2006).

[15] J. Carbonell and V. A. Karmanov, Eur. Phys. J. A **27**, 11 (2006).

[16] T. Frederico, G. Salmè and M. Viviani, Eur. Phys. J. C **75**, 398 (2015).

[17] J. Carbonell, V.A. Karmanov, Bethe–Salpeter scattering state equation in Minkowski space. Phys. Rev. D **90**, 056002 (2014).

[18] J. Carbonell, V. A. Karmanov, Eur. Phys. J. A **46**, 387 (2010).

[19] W. de Paula, T. Frederico, G. Salmè and M. Viviani, arXiv:1609.00868 (2016).

[20] A. Castro, et al, Rev. Mod. Phys. **81**, 109 (2009).

[21] N. M. R. Peres, Rev. Mod. Phys. **82**, 2673 (2010).

[22] R. Jackiw and S.Y. Pi, Phys. Rev. Lett. **98**, 266402 (2007).

[23] C. E. Cordeiro, A. Delfino, W. de Paula, T. Frederico, Phys. Rev. B **83**, 155419 (2011).

[24] V. Gigante, T. Frederico, C. Gutierrez, L. Tomio, Few-Body Syst. **56**, 375 (2015).

[25] C. Gutierrez, V. Gigante, T. Frederico, G. Salmè, M. Viviani, L. Tomio, Phys. Lett. B **759**, 131 (2016).

[26] M. Burkardt, Int. J. Mod. Phys. A **18**, 173 (2003).

[27] M. Diehl, Phys. Rep. **388**, 41 (2003).

[28] V. Barone, A. Drago, and P. G. Ratcliffe, Phys. Rep. **359**, 1 (2002).

[29] J. Carbonell, V. A. Karmanov and M. Mangin-Brinet, Eur. Phys. J. A **39**, 53 (2009).

[30] Murray Gell-Mann and Francis Low, Phys. Rev. **84**, 350-354 (1951).

[31] J. Schwinger: *On the Green's functions of quantized fields. 1*, Proc. Nat. Acad. Sci. **37**, 452-455 (1951).

[32] J. Schwinger: *On the Green's functions of quantized fields. 2*, Proc. Nat. Acad. Sci. **37**, 455-459 (1951).

[33] N. Nakanishi, Prog. Theor. Phys. Suppl. **43**, 1 (1969).

[34] K. Nishijima, Prog. Theoret. Phys **10**, 549 (1953); **12**, 279 (1954); and **13**, 305 (1955).

[35] S. Mandelstam, Proc. Roy. Soc. **A233** 248 (1955).

[36] A. Klein and C. Zemach, Phys. Rev. **108**, 126 (1957).

[37] G. R. Allcock and D. J. Hooten, Nuovo Cimento **8**, 590 (1958).

[38] R. E. Cutkosky and M. Leon, Phys. Rev. **135**, B1445 (1964).

[39] D. Lurie, A. J. Macfarlane and Y. Takahashi, Phys. Rev **140**, B1091 (1965).

[40] P.A.M. Dirac, Rev. of Mod. Phys. **21**, 392 (1949).

[41] P. Ramond, *Field Theory: A Modern Primer*, Westview Press, Mineola (NY) (2005).

[42] S.N. Sokolov and A. N. Shatnii, *Theoretical and Mathematical Physics* **37**, 1029 (1978).

[43] Bernard L.G. Bakker: Forms of Relativistic Dynamics, Lecture Notes in Physics, Volume 571, (2001).

[44] B.D. Keister, W.N. Polyzou, Adv. Nucl. Phys. **20**, 225-479 (1991).

[45] J. H. O. Sales, T. Frederico, B. V. Carlson, and P. U. Sauer, Phys. Rev. C **61**, 044003 (2000).

[46] T. Frederico and G. Salmè, Few Body Syst. **49**, 163 (2011).

[47] J. H. O. Sales, T. Frederico, B. V. Carlson, and P. U. Sauer, Phys. Rev. C **63**, 064003 (2001).

[48] Edward R. Vrscay, Phys. Rev. A **33**, 2 (1986).

[49] F. Gross, Phys. Rev. C **26**, 2203 (1982).

[50] G. Feldman, T. Fulton and J. Townsend, Phys. Rev. D **7**, 1814 (1973).

[51] Dae Sung Hwang and V. A. Karmanov, Nucl. Phys. **696**, 413 (2004).

[52] L. Theuβl and B. Desplanques, Few-Body Systems. **30**, 5-19 (2001).

[53] J. Carbonell, V. A. Karmanov, Phys. Rev. D **91**, 076010 (2015).

[54] J. Adam, Jr, J.W. Van Orden, Franz Gross, Nuclear Physics A **640**, 391-434 (1998).

[55] Nuclear Physics B (Proc. Suppl.) **161**, 136–152 (2006).

[56] G. Baym, Phys. Rev. **117**, 886 (1959).

[57] F. Gross, Ç. Şavkli, and J. Tjon, Phys. Rev. D **64**, 076008 (2001).

[58] T. Nieuwenhuis and J. A. Tjon, Phys. Rev. Lett. **77**, 814 (1996).

[59] E. zur Linden and H. Mitter, Nuovo Cimento **61B**, 389 (1969).

[60] V. Gigante, et al., Notes: *Cross-ladder effects in the Bethe-Salpeter equation in 2+1 dimensions in Minkowski space*, (2016).

[61] V. Gigante, J. H. Alvarenga Nogueira, E. Ydrefors, C. Gutierrez, V.A. Karmanov, T. Frederico, *Bound state structure and electromagnetic form factor beyond the ladder approximation*, arXiv:1611.03773 (2016).

[62] G. A. Miller, Annu. Rev. Nucl. Part. Sci. **60**, 25 (2010).

[63] C. Itzykson, J.B. Zuber, *Quantum Field Theory*, Dover Publications (2006).

[64] F. Gross: *Relativistic Quantum Mechanics and Field Theory*, Wiley Interscience, 1993.

[65] P. Roman, *Introduction to Quantum Field Theory*, John Wiley & Sons Inc, 1969.

[66] J. D. Bjorken and S.D. Drell, *Relativistic Quantum Fields* (McGraw-Hill, New York, 1965).

[67] W H. Press, S A. Teukolsky, W T. Vetterling, B P. Flannery, *Numerical Recipes in Fortran 77*, Cambridge University Press, 1986.3

[68] F. E. Close: *An Introduction to Quarks and Partons*, Academic Press, 1979.

[69] V. Gigante, *Equação de Bethe-Salpeter em 2+1 dimensões para estado ligado de duas partículas no espaço de Minkowski*. PhD Thesis — Instituto Tecnológico de Aeronáutica, São José dos Campos, Brasil, 2014.

[70] A. Iannone, *The Homogeneous Bethe-Salpeter Equation and the Nakanishi Integral Representation.* Tesi Magistrale-Università degli Studi di Roma "La Sapienza", Roma, Italy, 2013.

Appendices

Appendix A

Improving the accuracy for the excited states

As we mentioned, one has numerical difficulties for obtaining binding energies of excited states. Unlike the ground state where the stability is reached with small matrix dimension, for excited states it is needed to use a larger matrix dimension, which is not desirable from the numerical point of view. In addition, differently from the ground state with the ladder kernel where by assigning values of μ/m and B/m one obtains directly the coupling constant α_{gr}, for excited states one has to find the precise value of B/m corresponding to $\lambda{=}1$ once μ/m and α_{gr} have been fixed. Therefore, to avoid the long time numerical calculation and also to improve the accuracy of binding energy values of the spectrum, we adopt an *extrapolation trick*. This procedure is divided in two steps as explained below:

First step: From the numerical analysis one realizes that stability of the eigenvalues with N_z is achieved quickly, while to reach stability in N_g, it is needed to increase the number of terms in the basis expansion. Therefore, one may keep constant N_z and varying N_g to study that behavior. In this calculation we use $N_z{=}10$ since it is enough to get the convergence. By choosing a value of B/m and changing N_g, recalling that μ/m and α_{gr} are fixed, we obtain a set of λ values. This enables to extrapolate the behavior of λ for large values of N_g. In this form, we obtain the asymptotic value $\lambda^{\mathbf{asy}}$ for the corresponding B/m. This plot is displayed in Fig. A.1, where we show the behavior of the λ for the second- and third-excited state for the case $\mu/m = 0.05$, $B(0)/m = 1.9$ and $\alpha_{gr}{=}6.324$. Actually, we have plotted λ^{-1} as function of N_g because with this quantity is easier to perform the extrapolation process, but this will not

produce a relevant change in our calculation since that always we are interested in the B/m values corresponding to $\lambda=1$. We have not presented the behavior for the first-excited state because for this case the stability is easily achieved.
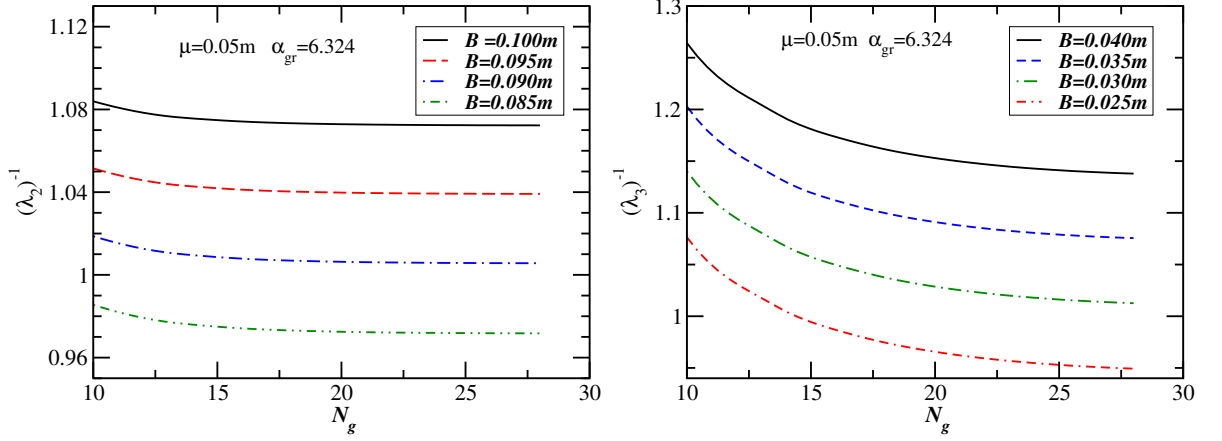
Figure A.1: Asymptotic behavior of eigenvalues $(\lambda_2)^{-1}$ and $(\lambda_3)^{-1}$ as function of N_g.

Second step: From the asymptotic values of λ^{-1} obtained from Fig. A.1, one may plot $(\lambda^{\text{asy}})^{-1}$ as a function of B/m and by performing the fit one can obtain the exact value of B/m corresponding to $(\lambda^{\text{asy}})^{-1}=1$. We show this kind plot in Fig. A.2
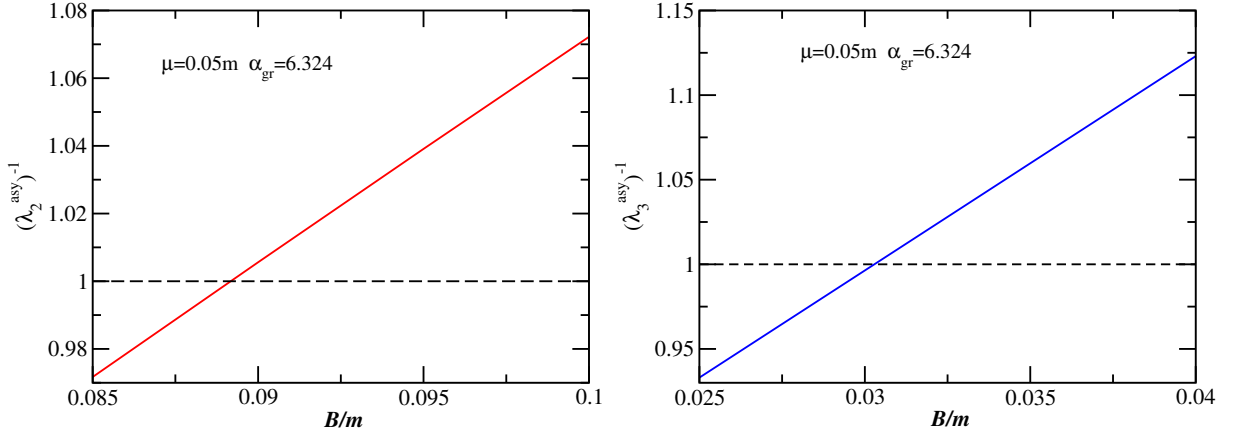
Figure A.2: Asymptotic values $(\lambda_2^{\text{asy}})^{-1}$ and $(\lambda_3^{\text{asy}})^{-1}$ as function of the binding energy B/m

As we can see fortunately the relationship is a simple linear one and easily we obtain the value of B/m corresponding to $\lambda^{\text{asy}}=1$. This linear relation have been tested for other excited states and different values of μ/m.

This trick has been useful to obtain the binding energies of excited states, in particular for the states with small binding energies where the convergence is more difficult. After performing the two-steps process for four values of μ/m: 0.01, 0.05, 0.1 and 0.5, the spectrum of excited states is shown in the Table. A.1. Note that the case μ/m=0.5 only one excited state appears by virtue of the large value of μ/m, in agreement with the previous results.

μ/m	0.01	0.05	0.1	0.5
α_{gr}	6.274	6.324	6.437	8.047
B_{gr}/m	1.9	1.9	1.9	1.9
$B(1)/m$	0.281	0.259	0.221	0.0082
$B(2)/m$	0.117	0.089	0.050	——
$B(3)/m$	0.054	0.030	0.005	——

Table A.1: Spectrum of the excited states for some values of μ for the case B_{gr}/m=1.9

Appendix B

Computation of the two-body current contribution

This Appendix is devoted to calculate explicitly the TBC expression Eq. (9.20) derived in Sec.9.2. We recall the expression

$$(p'+p)^2 F_X(Q^2) = \frac{-ig^4}{(2\pi)^{12}} \int d\gamma \ d\gamma' \ dz \ dz' \int d^4 p_2 \ d^4 p_8 \ d^4 p_9 [(p'+p)^2 - 2(p+p')_\mu (p_9+p_2-p_8)^\mu]$$

$$\frac{g(z',\gamma')}{[\gamma' + m^2 - \frac{M^2}{4} - (p_9 - \frac{p'}{2})^2 - (p_9 - \frac{p'}{2}).p'z']^3} \frac{g(z,\gamma)}{[\gamma + m^2 - \frac{M^2}{4} - (\frac{p'}{2} - \frac{q}{2} - p_2)^2 - (\frac{p'}{2} - \frac{q}{2} - p_2).(p'-q)z]^3}$$

$$\frac{1}{[(p'-p_9-p_2-q+p_8)^2 - m^2]} \frac{1}{[(p'-p_9-p_2+p_8)^2 - m^2]}$$

$$\frac{1}{[(p_9-p_8)^2 - \mu^2]} \frac{1}{[p_8^2 - m^2]} \frac{1}{[(p_2-p_8)^2 - \mu^2]}.$$

(B.1)

Looking in Eq. (B.1), one realizes that the Nakanishi's denominators are independent of the momentum p_8, therefore we can start with the integration in p_8, putting together the five denominators with the Feynman parametrization,

$$\int \frac{d^4 p_8}{ABCDE} = 24 \int_0^1 dy_4 \int_0^{1-y_4} dy_3 \int_0^{1-y_3-y_4} dy_2 \int_0^{1-y_2-y_3-y_4} dy_1$$

$$\times \int \frac{d^4 p_8}{[Ay_1 + By_2 + Cy_3 + Dy_4 + E(1-y_1-y_2-y_3-y_4)]^5}.$$

After joining the five denominators, the result denominator can be written as

$$\text{denom} = a(p_8)^2 + b(p_8) + c_1, \tag{B.2}$$

and as usual, the linear dependence is removed by applying the shift: $p_8 \to p_8 - \frac{b}{2a}$. This leads to:

$$\text{denomshift} = a(p_8)^2 + M_1, \tag{B.3}$$

139

in this particular case $a=1$. The integration is done by using the formula Eq. (9.12), we get

$$\int \frac{d^4p_8}{ABCDE} = 2i\pi^2 \int_0^1 dy_4 \int_0^{1-y_4} dy_3 \int_0^{1-y_3-y_4} dy_2 \int_0^{1-y_2-y_3-y_4} dy_1 \frac{1}{(M_1)^3}. \qquad (B.4)$$

In Eq. (B.1) there are linear terms in the numerator, which vanish when performing the integration. However, each shift brings some additional constant terms in the numerator, which must be taken into account in the final expression. For the moment, we only deal with the terms in the denominator and at the end of the calculation we show the result of the numerator after taking into account the shift in the three momentums.

Now, we continue with the integration in p_9, adding one of the Nakanishi's denominators

$$L = \gamma' + m^2 - \frac{M^2}{4} - \left(p_9 - \frac{p'}{2}\right)^2 - \left(p_9 - \frac{p'}{2}\right) \cdot p'z'$$

$$\int \frac{d^4p_9}{M_1^3 L^3} = 30 \int_0^1 dy_5 \, (1-y_5)^2 \, y_5^2 \int \frac{d^4p_9}{[(1-y_5)L + y_5 M_1]^6} \qquad (B.5)$$

$$= 30 \int_0^1 dy_5 \, (1-y_5)^2 \, y_5^2 \int \frac{d^4p_9}{[\tilde{g}p_9^2 + fp_9 + c_2]^6},$$

after applying the shift and integrating with the formula Eq. (9.12), we obtain

$$\int \frac{d^4p_9}{(M_1)^3 L^3} = \frac{3}{2} i\pi^2 \int_0^1 dy_5 (1-y_5)^2 y_5^2 \frac{g^2}{(M_2)^4} \qquad (B.6)$$

Finally, we add the other Nakanishi's denominator and carry out the integration in p_2

$$H = \gamma + m^2 - \frac{M^2}{4} - \left(\frac{p'}{2} - \frac{q}{2} - p_2\right)^2 - \left(\frac{p'}{2} - \frac{q}{2} - p_2\right) \cdot (p' - q)z$$

$$\int \frac{d^4p_2}{(M_2)^4 H^3} = 60 \int_0^1 dy_6 \, y_6^3 (1-y_6)^2 \int \frac{d^4p_2}{[y_6 M_2 + (1-y_6)H]^7}$$

$$= 60 \int_0^1 dy_6 \, y_6^3 (1-y_6)^2 \int \frac{d^4p_2}{[s(p_2)^2 + w(p_2) + c_3]^7} \qquad (B.7)$$

$$\int \frac{d^4p_9}{(M_2)^4 H^3} = 2i\pi^2 \int_0^1 dy_6 \, (1-y_6)^2 \, y_6^3 \frac{s^3}{(M_3)^5},$$

where M_3 is given by

$$M_3 = \text{constr } s - M^2 \frac{w_{p'}^2}{4} + Q^2 \frac{w_q(w_{p'} + w_q)}{4} \qquad (B.8)$$

$$\text{constr} = -Q^2 \, \text{constr1} + M^2 \, \text{constr2} + \text{constr3}.$$

We write below the explicit expressions for the coefficients

$$w_q = -1 - z + y_6(1 - 2y_1y_5(y_3 + y_4 + (y_3(-2 + y_1 + y_2 + y_3) - y_4)y_5) + z)$$

$$
\begin{aligned}
w_{p'} = {}& 1 + z + y_6(-1 - z - (y_1 + y_2)y_4(-1 + y_5)y_5(1 + z') + y_3y_5(1 + y_1 + y_2 \\
& - y_4 - y_5 - 3y_1y_5 + 2y_1^2y_5 - 3y_2y_5 + 4y_1y_2y_5 + 2y_2^2y_5 + y_4y_5 \\
& - (-1 + y_1 + y_2 + y_4)(-1 + y_5)z') + y_3^2y_5(-1 + y_5 + 2y_1y_5 + 2y_2y_5 + z' - y_5z'))
\end{aligned}
\tag{B.9}
$$

$$
\begin{aligned}
s = {}& -1 - (-1 - (-1 + y_3 + y_4)(y_3 + y_4)y_5 + (y_3(-1 + y_1^2 + y_3 + y_2(-1 + y_2 + y_3) \\
& + y_1(-1 + 2y_2 + y_3)) + (-1 + y_1^2 - y_2 + y_3 + (y_2 + y_3)^2 \\
& + y_1(-1 + 2y_2 + 2y_3))y_4 + (1 + y_1 + y_2 + y_3)y_4^2)y_5^2)y_6
\end{aligned}
$$

$$
\begin{aligned}
\text{constr1} = {}& \frac{1}{2}y_1y_5y_6(-1 + y_1 - y_2 + y_3 + y_5 - y_1y_5 + 3y_2y_5 - 2y_1y_2y_5 \\
& - 2y_2^2y_5 - y_3y_5 - 2y_2y_3y_5 + (-1 + y_1 + y_2 + y_3)(-1 + y_5)z')
\end{aligned}
$$

$$
\begin{aligned}
\text{constr2} = {}& \frac{1}{4}(-1 - 2z - y_6(-1 + y_5(y_1 - y_1^2 + y_2 - 2y_1y_2 - y_2^2 + y_3 + 2y_1y_3 + 2y_2y_3 \\
& - y_3^2 + (-y_1 + y_1^2 - y_2 + 2y_1y_2 + y_2^2 - y_3 + 2(y_1 + y_2)(-3 + 2y_1 + 2y_2)y_3 \\
& + (1 + 4y_1 + 4y_2)y_3^2)y_5) - 2z + \\
& 2(y_1 + y_2 - y_3)(-1 + y_1 + y_2 + y_3)(-1 + y_5)y_5z' + (-1 + y_5)^2z'^2))
\end{aligned}
$$

$$
\begin{aligned}
\text{constr3} = {}& \frac{1}{4}(-4\Delta_2(-1 + y_6) + 4(1 + (-1 + y_1^2 - y_2 - y_3 + (y_2 + y_3)^2 \\
& + y_1(-1 + 2y_2 + 2y_3))y_5)(-\Delta_1 + (\Delta_1 - \mu^2(-1 + y_1 + y_2 + y_4) + \mu^2(y_1 + y_2 + y_4))y_5)y_6),
\end{aligned}
\tag{B.10}
$$

with $\Delta_1 = \gamma' + m^2 - M^2/4$, $\Delta_2 = \gamma + m^2 - M^2/4$. To handle the long expressions we have done the following decomposition

$$b = b_{p_2}p_2 + b_{p_9}p_9 + b_{p'}p' + b_q q$$

$$f = qf_q + p'f_{p'} + p_2 f_{p_2} \tag{B.11}$$

$$w = p'w_{p'} + qw_q$$

Taking into account the contributions of the shifts in the numerator, we have the following expression

$$f_{\text{numer}} = \frac{4f_{p'}s + 2b_{p9}f_{p'}s + 8\tilde{g}s - 4b_{p'}\tilde{g}s - 2f_{p2}w_{p'} - b_{p9}f_{p2}w_{p'} + 4w_{p'}\tilde{g} + 2b_{p2}w_{p'}\tilde{g}}{8\tilde{g}s}. \quad \text{(B.12)}$$

Note that the dependence on the transfer momentum Q^2 only appears in the denominator through the function M_3 for the TBC, differently from the IA where the dependence appears in both in the numerator as well as in the denominator. Below we show the remaining coefficients:

$$b_{p9} = -2(y_1 + y_2 + y_3); \qquad b_{p2} = 2(-1 + y_3 + y_4); \qquad b_{p'} = 2(y_1 + y_2); \qquad b_q = -2y_1$$

$$f_q = -2y_1(-1 + y_1 + y_2 + y_3)y_5; \qquad f_{p2} = 2(y_3(-1 + y_1 + y_2 + y_3) + (y_1 + y_2 + y_3)y_4)y_5$$

$$f_{p'} = 1 - z' + y_5(-1 + 2y_1^2 + 2y_2(-1 + y_2 + y_3) + 2y_1(-1 + 2y_2 + y_3) + z')$$

$$\tilde{g} = -1 + y_5 - (-1 + y_1 + y_2 + y_3)(y_1 + y_2 + y_3)y_5.$$

$$\text{(B.13)}$$

Putting all pieces together, the expression for the TBC reads as

$$F_X(Q^2) = \frac{-3g^4}{(2)^{11}\pi^6} \int d\gamma \, d\gamma' \, dz \, dz' g(z,\gamma)g(z',\gamma') \int [dy_i](1-y_5)^2 y_5^2 (1-y_6)^2 y_6^3 \, \tilde{g}^2 \, s^3 \frac{f_{\text{numer}}}{(M_3)^5}, \quad \text{(B.14)}$$

where we have used the compact notation for the integrals in the Feynman parameters

$$\int [dy_i] = \int_0^1 dy_4 \int_0^{1-y_4} dy_3 \int_0^{1-y_3-y_4} dy_2 \int_0^{1-y_2-y_3-y_4} dy_1 \int_0^1 dy_5 \int_0^1 dy_6. \quad \text{(B.15)}$$

Appendix C

Test for the two-body current contribution

Calculating the electromagnetic FF, including the TBC contribution, we deal with rather lengthy expressions. For example, formula Eq. (9.18) contains seven propagators and three 4D integrations. These integrals are calculated using Feynman parametrization with six Feynman parameters. The expressions are rather lengthy, therefore one can easily make errors. Without a test, one can hardly trust to these calculations. Below we propose a possible test. The main point is to use another parametrization, so this calculation is completely independent.

We put in the expression Eq. (9.18) $q= 0$ and $\gamma = \gamma' =0$, $z = z = 0$, $p' = p$, (or, equivalently: $g(\gamma, z) = \delta(\gamma)\delta(z)$). We obtain

$$
\begin{aligned}
F_X(0) = &\frac{-ig^4}{4M^2} \int d^4p_2 \ d^4p_9 \ d^4p_8 \ 4[M^2 - p \cdot (p_9 + p_2 - p_8)] \\
&\times \frac{1}{\left[m^2 - \frac{M^2}{4} - \left(p_9 - \frac{p}{2}\right)^2\right]^3} \frac{1}{\left[m^2 - \frac{M^2}{4} - \left(\frac{p}{2} - p_2\right)^2\right]^3} \\
&\times \frac{1}{[(p - p_9 - p_2 + p_8)^2 - m^2]^2} \frac{1}{[(p_9 - p_8)^2 - \mu^2]} \frac{1}{[p_8^2 - m^2]} \frac{1}{[(p_2 - p_8)^2 - \mu^2]}.
\end{aligned}
\tag{C.1}
$$

Now, we use another parametrization, where the scalar free-propagator read as

$$
\frac{i}{p^2 - m^2 + i\epsilon} = \int_0^\infty d\alpha \ \exp[i\alpha(p^2 - m^2 + i\epsilon)],
\tag{C.2}
$$

with this integral parametrization, we have the following expressions for the propagators

$$\frac{1}{(p^2 - m^2 + i\epsilon)} = -i \int_0^\infty dx \frac{1}{m^2} \exp[i\frac{x}{m^2}(p^2 - m^2 + i\epsilon)]$$

$$\frac{1}{(p^2 - m^2 + i\epsilon)^2} = -\int_0^\infty dx \frac{x}{m^4} \exp[i\frac{x}{m^2}(p^2 - m^2 + i\epsilon)] \tag{C.3}$$

$$\frac{1}{(p^2 - m^2 + i\epsilon)^3} = \frac{i}{2} \int_0^\infty dx \frac{x^2}{m^6} \exp[i\frac{x}{m^2}(p^2 - m^2 + i\epsilon)].$$

Thus, the expression for Eq. (C.1) becomes

$$F_X(0) = \frac{-ig^4}{(4M^2)} \int \frac{d^4p_2}{(2\pi)^4} \frac{d^4p_9}{(2\pi)^4} \frac{d^4p_8}{(2\pi)^4} [4M^2 - 4p \cdot (p_9 + p_2 - p_8)](-1)\frac{i^5}{2^2 m^{22}}$$

$$\times \int_0^\infty dx_1 \, x_1^2 \, \exp\left[i\frac{x_1}{m^2}\left(\left(p_9 - \frac{p}{2}\right)^2 + \frac{M^4}{4} - m^2 + i\epsilon\right)\right]$$

$$\times \int_0^\infty dx_2 \, x_2^2 \, \exp\left[i\frac{x_2}{m^2}\left(\left(p_2 - \frac{p}{2}\right)^2 + \frac{M^4}{4} - m^2 + i\epsilon\right)\right]$$

$$\times \int_0^\infty dx_3 \, x_3 \, \exp\left[i\frac{x_3}{m^2}((p - p_9 - p_2 + p_8) - m^2 + i\epsilon)\right] \tag{C.4}$$

$$\times \int_0^\infty dx_4 \, \exp\left[i\frac{x_4}{m^2}((p_9 - p_8)^2 - \mu^2 + i\epsilon)\right]$$

$$\times \int_0^\infty dx_5 \, \exp\left[i\frac{x_5}{m^2}(p_8^2 - \mu^2 + i\epsilon)\right]$$

$$\times \int_0^\infty dx_6 \, \exp\left[i\frac{x_6}{m^2}((p_2 - p_8)^2 - \mu^2 + i\epsilon)\right],$$

or in a compact form

$$F_X(0) = \frac{-g^4}{4m^{22}M^2} \int_0^\infty x_1^2 \, x_2^2 \, x_3 \, dx_1 \, dx_2 \, dx_3 \, dx_4 \, dx_5 \, dx_6$$

$$\times \int \frac{d^4p_2}{(2\pi)^4} \frac{d^4p_9}{(2\pi)^4} \frac{d^4p_8}{(2\pi)^4} [M^2 - p \cdot (p_9 + p_2 - p_8)] \exp[if(p_2, p_8, p_9)]. \tag{C.5}$$

The six arguments of the exponents have been grouped as

$$\exp[if(p_2, p_8, p_9)] = \exp\left[i\frac{x_1}{m^2}\left(\left(p_9 - \frac{p}{2}\right)^2 + \frac{M^2}{4} - m^2 + i\epsilon\right) + .. + i\frac{x_6}{m^2}\left((p_2 - p_8)^2 - \mu^2 + i\epsilon\right)\right]. \tag{C.6}$$

To carry out the integration in p_2, p_9 and p_8 we use the formula

$$\int \frac{d^4p}{(2\pi)^4} \exp(i\alpha p^2) = \frac{-i}{(4\pi\alpha)^2}, \tag{C.7}$$

therefore, we must to remove the linear dependence in $f(p_2, p_8, p_9)$ by means of a shift as usual. We start with the integration in p_8 doing the shift

$$p_8 = p_8' - \frac{(2px_3 - 2(p_9(x_3 + x_4) + p_2(x_3 + x_6)))}{x_3 + x_4 + x_5 + x_6}, \tag{C.8}$$

the f function gets the following form

$$f = (x_3 + x_4 + x_5 + x_6)\frac{p_8'^2}{m^2} + ..., \tag{C.9}$$

where the terms ... does not contain any contribution in the variable p_8, it only has dependence in p_2, p_9, p. The shift in the momentum p_8 leads to the following expression in the numerator

$$M^2 - p \cdot (p_9 + p_2 - p_8) = M^2 - \frac{p \cdot (px_3 + p_2(x_4 + x_5) + p_9(x_5 + x_6))}{x_3 + x_4 + x_5 + x_6} - p_8'. \tag{C.10}$$

After the integration in p_8 we obtain

$$F_X(0) = \frac{-g^4}{4m^{18}M^2} \int_0^\infty x_1^2\, x_2^2\, x_3\, dx_1\, dx_2\, dx_3\, dx_4\, dx_5\, dx_6 \int \frac{d^4p_2}{(2\pi)^4} \frac{d^4p_9}{(2\pi)^4}$$
$$\times \left[M^2 - \frac{p \cdot (px_3 + p_2(x_4 + x_5) + p_9(x_5 + x_6))}{x_3 + x_4 + x_5 + x_6} \right] \frac{-i}{16\pi^2(x_3 + x_4 + x_5 + x_6)^2} \exp[if(p_8' = 0)]. \tag{C.11}$$

Similarly we integrate over p_2 and p_9 doing the same steps. Finally, we obtain

$$F_X(0) = \frac{-ig^4}{2^9\pi^6 m^{10}} \int_0^\infty x_1^2\, x_2^2\, x_3\, dx_1\, dx_2\, dx_3\, dx_4\, dx_5\, dx_6 \frac{f_{\text{num}}}{d^3}$$
$$\exp\left[-i(x_1 + x_2 + x_3 + x_5) - i(x_4 + x_6)\frac{\mu^2}{m^2} + i\frac{c_{M^2}}{d}\frac{M^2}{m^2} - (x_1 + x_2 + x_3 + x_4 + x_5 + x_6)\epsilon \right], \tag{C.12}$$

with

$$d = 4[x_3x_4x_5 + x_3x_4x_6 + x_3x_5x_6 + x_4x_5x_6 + x_2(x_3 + x_4)(x_5 + x_6)$$
$$+ x_1((x_4 + x_5)(x_3 + x_6) + x_2(x_3 + x_4 + x_5 + x_6))]$$

$$f_{num} = x_1x_2x_4 + x_2x_4x_5 + x_1x_2x_6 + x_1x_4x_6 + x_2x_4x_6 + x_1x_5x_6 + 2x_4x_5x_6$$

$$c_{M^2} = (2x_3x_4 + x_2(x_3 + x_4))(2x_5x_6 + x_2(x_5 + x_6)) + x_1^2((x_4 + x_5)(x_3 + x_6) + x_2(x_3 + x_4 + x_5 + x_6))$$
$$+ x_1(x_2^2(x_3 + x_4 + x_5 + x_6) + 2x_2(x_5x_6 + x_4(x_5 + x_6) + x_3(x_4 + x_5 + x_6))$$
$$+ 2(x_4x_5x_6 + x_3(x_5x_6 + x_4(x_5 + x_6)))),$$

$$\text{(C.13)}$$

The numerical calculation of the integral Eq. (C.12) seems to be easy. Therefore, to complete the test we can assign values to m, μ, M, ϵ and g^4 and obtain a numerical value from the expression Eq. (C.12). On the other hand, we use the same values in the expression obtained by means of the Feynman parametrization Eq. (9.21) and compare the result. In fact, we have obtained the same result for the two methods, within the accuracy of the calculation. Therefore, one can say that the expression for the TBC is correct, since the confidence provided from the test.

List of Figures

147

List of Tables